The Use of Soybean Peroxidase in Amperometric Biosensors

By

Neil Carolan B. Sc.

A thesis submitted for the degree of

Doctor of Philosophy

Supervised by Dr. Ciarán Ó Fágáin

School of Biotechnology

Dublin City University

July 2004

DECLARATION

I hereby certify that this material, which I now submit for assessment on the programme of study leading to the award of Doctor of Philosophy, is entirely my own work and has not been taken from the work of others, save and to the extent that such work has been cited and acknowledged within the text of my work.

Signed: Neil Carolan *ID no: 99171620*

Neil Carolan

Date: 12-Jul-04

Acknowledgements:

- To my Mam and Dad, to you I owe all, thanks for the support and help through all the years. Words can't thank you enough!

- To Sinéad and Martin, thanks for being there. Your support over the years is immeasurable! Thanks for putting up with me!

- To Alicia, Bernard, Declan, and Caithríona, You Guys are always there for me.

- To all my Relations, especially Gran and Micéal.

- To my supervisor Dr. Ciarán Ó Fágáin, for the opportunity to carry out this research. His constant support over the last few years, his being always available to talk and his knowledge of references. His sense of humour his taste in music and wine!
- To Professor Robert Forster, for the use of his lab and equipment,
- To my lab mates past and present Barry, Damien, Sandra, Deborah, and Karima in X2-65 and in the electrochemistry lab, especially Darren, Jenny, Johan, Lorraine, Mary, and Sonia.
- To my coffee buddies (Ciaran, Ger, Helen, Mairead, Jenny, Richard and the countless others), thanks for laughing at my funny jokes.
- To all the Post-grads (Aishling, Caroline, Dave, Eva, Linda, Mary L, Pam, Paraic, and Stephen) and Post-Docs (Paul, Lenny, Allan and Phil) the BRS and anyone I've forgotten, these past few years with you all was memorable!!
- To all my friends I have made in the DCU rock-climbing club: Eilís, Gary, Jonathon, Mick, Mikey, Jamie, Donal, Nicole, Dave, Sean, Stuart, Orla and anyone I've forgotten. To my many other friends I've made in DCU especially Theresa, Aoife and Tony.
- To Annette, Eoin, and Fintan your friendship means so much to me.
- Thanks to everyone past and present who helped me in one way or another to get me to where I am today.

A certain swordsman in his declining years said the following:

> In one's life, there are levels in the pursuit of study. In the lowest level, a person studies but nothing comes of it, and he feels that both he and others are unskilful. At this point he is worthless. In the middle level he is still useless but is aware of his own insufficiencies and can also see the insufficiencies of others. In a higher level he has pride concerning his own ability, rejoices in praise from others, and laments the lack of ability in his fellows. This man has nothing.
>
> These are the levels in general. But there is one transcending level, and this is the most excellent of all. This person is aware of the endlessness of entering deeply into a certain Way and never thinks of himself as having finished. He truly knows his own insufficiencies and never in his whole life thinks that he has succeeded. He has no thoughts of pride but with self-abasement knows the Way to the end. It is said Master Yagyū once remarked, "I do not know the ways to defeat others, but the way to defeat myself."
>
> Throughout your life advance daily, becoming more skilful than yesterday, more skilful than today. This is never ending.

Yamomoto Tsunetomo, (Translated by William Scott Wilson),
Hagakure. The book of the Samurai.

ABBREVIATIONS:

A	Geometric area of the microelectrode,
AADH	Adipic acid dihydrazide,
ADH	Alcohol dehydrogenase,
ABTS	2,2'-Azino-di-(3-ethyl-benzthiazoline-6-sulphonic acid),
AE	Auxiliary electrode,
AH	Deionised acid,
A_p	Area beneath the cathodic/anodic peaks.
App	Applied,
APX	Ascorbic acid peroxidase,
AOX	Adsorbable organic halogens,
ARP	Fungal peroxidase from *Arthromyces ramosus*,
BCA	Bicinchoninic acid,
Bis-TRIS	(bis[2-hydroxyethyl]iminotris[hydroxymethyl]-methane).HCl,
BSA	Bovine serum albumin,
bpy	2,2'-bipyridyl,
C*	Actual Concentration of H_2O_2 in the solution,
C	Concentration of the redox active species,
C	Capacitance ($F.cm^{-2}$),
CcP	Cytochrome C peroxidase,
CiP	*Coprinus cinereus* peroxidase,
CLECs	Cross-linked enzyme crystals,
Cpd	Compound,

CV	Cyclic voltammogram,
D	Diffusion coefficient,
DAB	3,3'-diaminobenzidine,
EC	Enzyme classification,
EDC	[1-(3-dimethylaminopropyl)-3-ethylcarbodiimide hydrochloride],
EDTA	Ethylene diamine tetraacetic acid,
$E^1/_2$	Oxidative potential,
FCA	Ferrocene carboxylic acid,
$FeCl_3.6H_2O$	Iron (III) chloride hexahydrate,
Fuc	Fucose,
GOx	Glucose oxidase,
GlcNAc	*N*-acetyl-D-glucosamine,
H	Hydrogen,
H_{ads}	Adsorbed hydrogen,
HRP-A2	Horseradish peroxidase isoenzyme A2
HRP-C	Horseradish peroxidase isoenzyme C
I	Inactive form of an enzyme,
IEF	Isoelectric focusing,
i_{max}	Maximum current,
ip	Peak current ($A.cm^{-2}$),
ip_a	Anodic peak current,
ip_c	Cathodic peak current,
iss	Steady-state current,
i-t	Current-time amperommetry,

ITO	Indium tin oxide,
k	Electron-transfer rate
k_{cat}	Turnover number of an enzyme,
k_{cat}/K_m	Catalytic efficiency,
K_m^{app}	Apparent Michaelis constant,
K_m	Michaelis constant,
kV	kilovolt,
L	Laevo rotary,
$LiClO_4$	Lithium perchlorate,
LiP	Lignin peroxidase,
M	Molar,
mA	MilliAmperes,
MALDI-TOF	Matrix-assisted laser desorption/ionisation time of flight mass spectrometry,
Man	Mannose,
MES	(2-[*N*-Morpholino] ethanesulfonic acid),
MET	Mediated electron transfer,
MnP	Manganese peroxidase,
MOPS	(3-[*N*-Morpholino] propanesulfonic acid),
mV	Millivolts (10^{-3} V),
MWCO	Molecular weight cut off,
N	Native form of an enzyme,
n	Number of electrons involved in overall electrode reaction,
$NaBr_4O_7$	Sodium tetraborate (Borax),

NC-IUBMB	Nomenclature Committee of the International Union of Biochemistry and Molecular Biology,
$(NH_4)_2S_2O_8$	Ammonium persulfate,
NHS	*N*-hydroxysuccinimide,
OPD	*o*-phenyl diamine,
$Os(bpy)Cl_2$	Osmium bipyridyl dichloride,
$[Os(bpy)_2(PVP)_{10}Cl]^+$	Osmium dibipyridyl polyvinyl pyridine chloride,
ox	Oxidation,
P^+	Localised cation on the porphyrin ring or the polypeptide chain,
PC	Personal computer,
PAH	Polycyclic aromatic hydrocarbons,
PCP	Pentachlorophenol,
PDB	Protein Data Bank,
PEG	Poly(ethylene glycol),
PEGDGE	Poly(ethylene glycol) (400) diglycidylether,
*p*I	Isoelectric point,
PNP	Peanut peroxidase,
POs-EA	$Os(bpy)_2Cl^{+/2+}$ poly(4-vinylpyridine),
PTFE	Poly tetra fluro ethylene,
PVP	Polyvinyl pyridine
PQQ	Pyrroloquinoline quinone
Pyr	pyrrolidone carboxylic acid,
r	Radius,
r^2	Correlation coefficient,

RCSB	Research Collaboratory for Structural Bioinformatics,
RE	Reference electrode,
red	Reduction,
RH	Conjugate acid,
rSBP	Recombinant soybean peroxidase,
RZ	Reinheitzahl (purity number), (A_{403}/A_{280})
S	Substrate,
SBP	Soybean Peroxidase,
SBP (Q)	SBP sourced from Quest International,
SDS-PAGE	Sodium Dodecyl Sulphate Polyacrylamide Gel Electrophoresis,
SEM	Scanning electron microscope,
TEMED	*N,N,N',N'*-Tetramethylethylenediamine,
TCA	Trichloro acetic acid,
T_m	Melting temperature,
TMB	3,3',5,5'-Tetramethyl benzidine,
TNBS	2,4,6-Trinitrobenzenesulfonic acid,
TRIS	Tris-(hydroxymethyl) aminomethane,
$t^1/_2$	Half-life of a protein and/or enzyme,
UV-VIS	Ultra violet/visible light,
V	Applied voltage,
v	Scan rate (V/s),
v/v	volume per volume,
V_{max}	Maximal velocity,

vs.	Versus,
WE	Working electrode,
w/v	Weight per volume,
WR	Working reagent,
Xyl	Xylose,
μA	Microampere,
∅	Diameter,
$-\Delta G^{\theta}_{ads}$	Free energy of adsorption,

TABLE OF CONTENTS

The use of a soybean peroxidase enzyme in a biosensor

Neil Carolan BSc.

Abstract:

Traditionally Horseradish peroxidase (HRP) the archetypal class III plant peroxidase has been investigated with respect to chemical modifications, organic solvent tolerance studies, reaction kinetics, kinetics in organic solvents, immunohistochemical and in biosensor fabrication. However HRP has many factors that prevent its use in industrial, and research areas. This is because of its inherent structure, and activity restrictions in regard to temperature, its pH range of activity, and solvents it is catalytically active in. There is another class III plant peroxidase, which has greater stability with regards to the above factors, this peroxidase is Soybean peroxidase (SBP). This is the peroxidase that is investigated in this work.

Chemical modifications historically have targeted amino acid residues in the tertiary folded active form of an enzyme. HRP and many other enzymes have been chemically modified by modifying the ε-NH_3 group of lysine (HRP has 3 lysines available for modification out of 5 lysines). SBP cannot be chemically modified in this fashion, because it has no lysines available for modification, out of 3 lysines). Therefore in order to attempt to successfully chemically modify SBP another approach needs to be studied. SBP is a glycosylated enzyme. By chemically modifying this catalytically inactive region of SBP, an increase in stability and activity can be achieved.

Three methods of chemically modifying the carbohydrate shell, these were modifying by dextran dialdehyde, adipic acid dihydrazide (AADH), and ferrocene carboxcylic acid (FeCOOH). The dextran dialdehyde modification yielded a 2-fold modification. The AADH modification yielded a three-fold modification, but problems arose with the inhibition of the enzymes active site and the cross-linking agent. The FeCOOH modification was successful adding at least 2 extra irons to the enzyme. The modified was used in conjunction with a sensor. This modification also reduces the electron transfer distance between the enzyme and the transducer. This sensor was characterised and compared to a native SBP biosensor.

Also investigated in this work was the non-heme peroxidase vanadium bromoperoxidase (VBrPO). VBrPO is a sourced enzyme, utilising vanadium at its active site. The native enzyme was characterised and the dextran dialdehyde modification was carried out on it. The modification was then characterised and compared to the native form of the enzyme.

"The ubiquitous peroxidases are among the most versatile of enzymes. Their extremely broad specificity, almost a contradiction in meaning, is both a blessing and a curse to the research worker."

H., B. Dunford.

CHAPTER 1

INTRODUCTION

1.1: Biosensors:

1.1.1: Biosensors:

A biosensor by definition is "an analytical device that brings together an immobilised biological sensing material (enzyme, antibody, cell), and a transducer to produce an electronic signal that is proportional to the concentration of the target chemical substance" (Luong, *et al.*, 1995). Many of Nature's mechanisms exploit redox chemical processes, including cellular respiration and photosynthesis. Electrochemistry is a very useful tool in measuring the electron transfer properties of these proteins, enzymes and cells (Frew and Hill, 1988). Electrocatalysis by enzymes can be referred to as "bioelectrocatalysis" (Kulys and Samalius, 1983). Many biological processes, including enzyme-catalysed ones, are redox in nature. This allows the combination of electrochemical with biological systems.

There is a need to selectively detect the presence or absence of a particular substance, at low analyte concentrations, and even in the presence of interfering substances. There are many techniques available to do this type of analysis; however, as a result of the costs involved in the purchasing and running of these instruments routine analysis can be financially expensive. The development of biosensors has provided a cheap, easy to use method, and results in a real time alternative for selective analyte analysis (Scheller and Schubert, 1992).

The field of biosensors is vast, and each year literally thousands of papers are published. These include the construction, characterisation and application of biosensors in research, clinical applications, and their industrial uses including the biotechnology, food areas and many many more.

Biosensors operate on the direct spatial coupling of an immobilised biological entity with a signal transducer connected to an electronic amplifier. The biosensor operates through a series of stages (Figure 1.1). Firstly the biological entity (can be any biological material; enzyme, antibody, receptor, cell, and even tissue slice), reacts with the analyte. Secondly when the enzyme-substrate reaction occurs, an electron is generated; this leaves the enzyme's active site and diffuses to the surface of the transducer. And thirdly the transducer detects the electron and converts it to a readable signal.

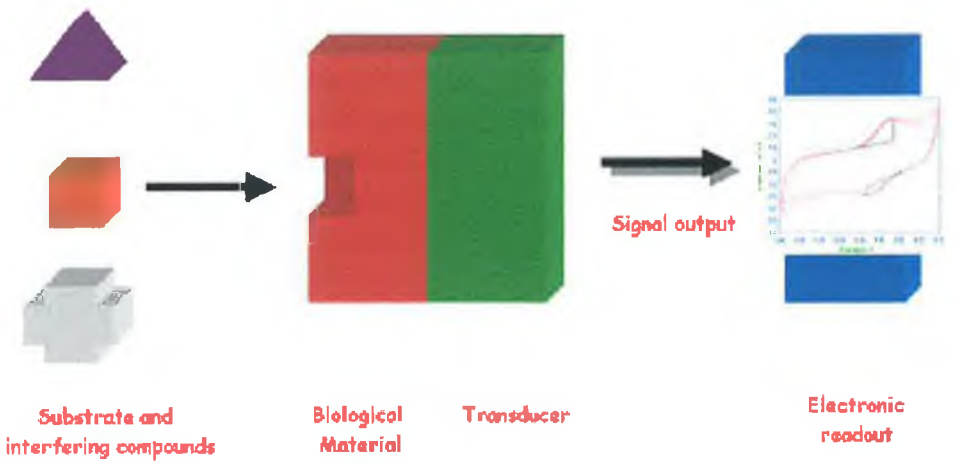

Figure 1.1: The signal process in a biosensor. The substrate enters the active site of the enzyme and generates an electron, which is detected by the transducer and an electronic signal is reported.

1.1.2: Microelectrode biosensors:

Microelectrodes are electrodes with diameters as small as 10Å. They have many advantages over the more usual macroelectrodes, including small currents, short

response times and steady state attributes. These small currents give them advantages over macroelectrodes and currents can be measured on the pico to the nanoAmp scale. Microelectrodes have many different geometries, including band, cylinder, ring and disk electrodes. Microdisk electrodes are the most common type of microelectrodes and used because of their ease of manufacture and the ability to mechanically clean the surface of the electrode (Forster, 1994; Somasundrum and Aoki, 2002).

1.2: Electron-transfer in biosensors:

Over the years since they were first devised biosensors have undergone many evolutions. The main principle for an enzyme biosensor is that the enzyme be immobilised onto the electrode such that the enzyme active site can shuttle electrons to the electrode surface. In 1962, Clark and Lyons described a glucose oxidase biosensor that could detect O_2 at an electrode surface. They immobilised glucose oxidase (GOx) onto the surface of a Clark-electrode behind a semi-permeable membrane. Consumption of the co-substrate oxygen was detected at the surface of the platinum electrode held at a potential sufficient to reduce the oxygen. This is an example of a first generation electrode biosensors (Figure 1.3) where the enzyme prosthetic group is recycled by a freely diffusing cofactor (molecular oxygen in the case of GOx). These cofactors can be oxidised or reduced at the surface of the electrode and cofactors can be used as electron-transfer shuttles. The decrease in concentration of the co-substrate (or the increase in co-product concentration) is determined by the change in current at the electrode surface, held at a suitable pre-determined working potential.

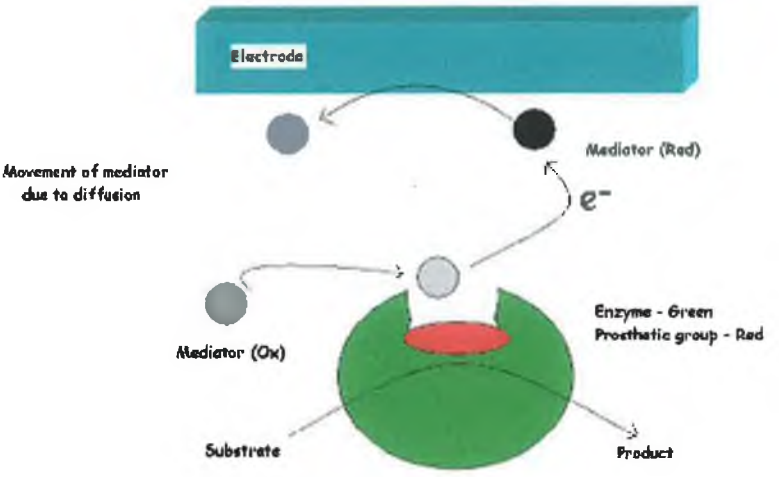

Figure 1.2.1: Electron transfer via a redox mediator used an electron-transfer shuttle. The green and red images are the enzyme, the grey, and black discs are the mediators and the blue bar represents the electrode.

The second generation of biosensors utilise an artificial mediator. Figure 1.4 shows the general method of electron hopping in a mediator-modified electrode surface. There are many different ways that mediators can be employed in a biosensor system. The easiest is to use low molecular weight redox metal complexes. By covalently attaching the redox mediator to a polymer backbone, electron-transfer from the enzyme's active site can proceed in two ways, (i) the "seaweed" mechanism or (ii) the whip mechanism (Habermüller *et al.*, 2000). In the first case, the seaweed mechanism operates where the mediator surrounding the enzyme shortens the distance from the active site to the surface of the electrode (Schuhmann, 1995). The whip mechanism operates where the mediator is attached to a long and flexible polymer chain, which can whip into the active site and whip out again transferring the electrons to the electrode surface. Both systems have advantages and disadvantages for use and the choice of mediator using these mechanisms can be chosen depending

on the needs of the experiment. A new area of mediators in biosensors is the use of carbon nanotubes to immobilise enzymes to an electrode surface, which is becoming a major area of research (Yu *et al,* 2003, Yamamoto *et al,* 2003).

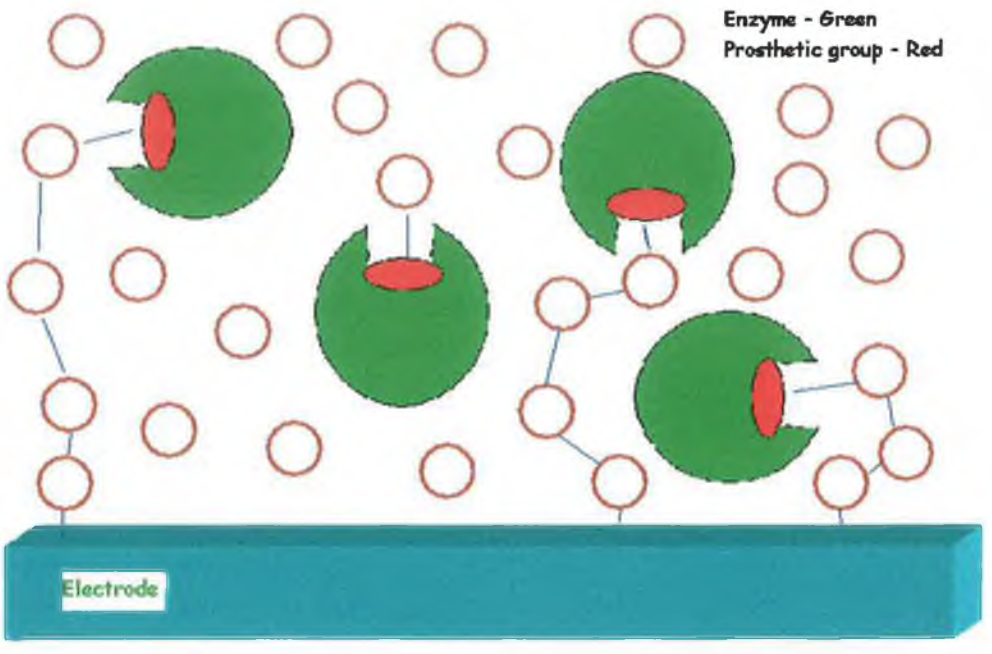

Figure 1.2.2: The general method of electron hopping in a mediator-modified electrode surface. The mediator transfers the electron from the enzyme's active site to the surface of the electrode.

The third generation of biosensors aims to have direct communication between the enzyme's active site and the electrode surface (Figure 1.5). The best system would have as little distance as possible between the active site and the transducer. With unglycosylated recombinant enzymes (from bacterial hosts) the electron-transfer distance is less; this helps optimise the system (Wong and Schwaneberg, 2003). "Ordinary" enzymes can also be used: if they can be placed as close as possible to the

surface of the electrode, direct bioelectrocatalysis can be achieved (Kulys and Schmid, 1990). The enzyme can be positioned in such a way upon immobilisation that the active site can be open to the substrate and can complete electron-transfer to the transducer.

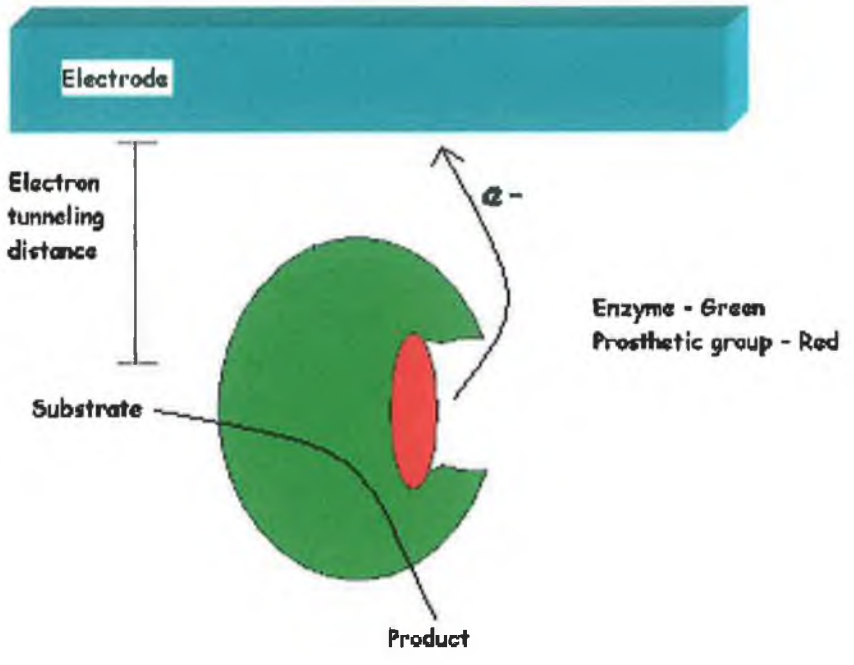

Figure 1.2.3: Direct electron-transfer between the enzyme active site and the surface of the electrode (transducer). For direct electron-transfer to occur the electron tunnelling distance has to be as small as possible.

1.3: Mediated electron transfer in biosensors:

In most cases, the redox centres of enzymes are buried within the three-dimensional structure. As a result they are electrically isolated, making direct electrical communication to the surface of a conventional electrode difficult (Boguslavsky *et al.*, 1993). This is because slow rates of diffusion give rise to low Faradaic currents

(Frew and Hill, 1988). The use of low molecular weight, well-characterised mediators has become widespread. However, some of these mediators suffer from inherent problems due to their solubility, which causes them to leach into the bulk electrolyte solution over the time course of any assay. One method to overcome this problem is to chemically attach the redox mediators to polymers such as poly(pyrrole), poly(ethylene) (Boguslavsky, *et al.,* 1993), poly(thiophene) (Pal and Sarkar, 2002), poly(vinyl imidazol), poly(dicarbazole) (Cosnier, *et al.,* 2003), and as in this work, to poly(vinyl pyridine) (PVP) (Boguslavsky, *et al.,* 1993; Kong *et al.,* 2003). This can lead to "electrical wiring" of the enzyme to the polymerised redox mediator (Boguslavsky, *et al.,* 1993). However in this potential range there is a possibility of interference by agents such as uric acid and ascorbic acid that can be easily oxidised at this potential. This can and does cause errors in the recording of clinical and *in vivo* analyses. Use of a redox mediator can lower the working potential of the sensor (Davis, 1985; Cass *et al.,* 1984). Hodgson *et al.* (1992) used additives as molecular carriers for the introduction of the enzyme into the polymer. Where neutral solutions are used, proteins do not exhibit an overall charge. They are difficult to incorporate into the polymer. Hodgson *et al.* (1992) utilised in a unique manner that surfactants through their zwiterionic properties can be used to include proteins into polymers at neutral pHs.

Transition metal complexes have proven to be suitable redox mediators in biosensors, especially enzyme biosensors (Ivanova *et al.,* 2003). Covalent binding of osmium to *N*-substituted pyrrole derivatives by long spacer chains improve the flexibility of the polymer-bound redox relays. The inclusion of the Cl^- counter ion in the osmium complex improves the solubility of the polymer in aqueous solutions. Another useful

property of this polymer is that it can be used as a form of immobiliser for the enzyme in the biosensor configuration (Schuhmann, 2002).

Direct electron tunnelling between the enzyme and electrode would seem to be the simplest form of electron transfer (Gaspar *et al,* 2000; Gaspar *et al,* 2001). Amperometric enzyme electrodes need electrical communication between the electrode and the active site (Gregg and Heller, 1990). Enzyme prosthetic groups however, tend to be buried within the protein, with access to the outside environment through an access channel. SBP, for instance has an intrinsic redox electron transfer mechanism, where electron transfer takes place within the vicinity of the prosthetic group. Electrochemical insulation of the active site by the glycoprotein architecture rules out the possibility (in most cases) of direct electron-transfer between the enzyme and the electrode (Katz, 2002). Also the distance between the site of electron transfer and the surface of the electrode can sometimes be too large for electron transfer to be achieved (Degani and Heller, 1987). According to the Marcus theory, the rate of direct electron transfer is governed by the electron distance (Marcus and Sutin, 1985). Mayo *et al.,* (1986) showed that the rate of electron transfer falls off exponentially with distance, as seen in the relationship below:

$$k \propto e^{-\alpha d}$$

Which states that the electron-transfer rate (k) decays exponentially with distance (d) between the enzyme's active site and the surface of the electrode. In some cases, when the distance from the electron donor to the acceptor is increased to

approximately 10Å, the electron transfer rate drops by a factor of 10^4 (Degani and Heller, 1987; Cassidy *et al.*, 1998).

1.4: Mediators in biosensor systems:

Properties of a good mediator include the following:

1. Reversible kinetics,
2. React readily with the reduced form of the enzyme,
3. Have a low oxidation potential and be pH independent,
4. Stable in both redox forms,
5. Easily retained at the surface of the electrode,
6. Unreactive toward oxygen, and
7. Unreactive chemically with the immobilised biological material.

The physical properties of mediators determine their usefulness in electrochemistry. The most common use of a mediator involves its immobilisation onto the electrode surface by adsorption. Foulds and Lowe (1988) developed a method, which is the basis today for mediated electron transport. They functionalised monomeric pyrrole with a ferrocene derivative. This forms an electropolymerised polymer (Cassidy *et al.,* 1998). The redox potential of the mediator, $E_m^{o'}$, should be more negative or positive than the redox potential of the enzyme's active site, $E_e^{o'}$, in the case of oxidative ($E_m^{o'} < E_e'^{o}$) and reductive ($E_m^{o'} > E_e'^{o}$) bioelectrocatalysis (Katz, 2002). The use of polymers in biosensors also prevents fouling at the electrode surface (Murray *et al.,* 1987). Polymers are of three types: conducting, nonconducting and composite. Conducting polymer mediators enhance the electron transfer from the surface of the enzyme to the electrode surface. Nonconducting films are used mainly for their permiselective characteristics, while composite polymers try to combine the positive attributes of more than one film (Pal and Sarkar, 2002). Use of an enzyme

with a mediator gives what is known as a multi-step mediated electron-transfer (MET) process, where each step transports the electron a small distance (Katz, 2002). However, the use of a mediator in conjunction with a redox enzyme can create its own problems when the mediator-enzyme film can, depending upon its thickness, obstruct the diffusion of the substrate (Sun, *et al.*, 1998).

The electrochemical reactions of the $Os(bpy)_2(PVP)_{10}$-soybean peroxidase electrode system upon addition of H_2O_2 into the bulk electrolyte are as follows (Li *et al.*, 2000).

$$H_2O_2 + 2H^+ + SBP_{red} \longrightarrow SBP_{ox} + 2H_2O \quad \text{equation 1}$$

$$SBP_{ox} + 2PVP\text{-}Os^{2+} \longrightarrow SBP_{red} + 2PVP\text{-}Os^{3+} \quad \text{equation 2}$$

$$2PVP\text{-}Os^{3+} + 2e^- \longrightarrow 2PVP\text{-}Os^{2+} \quad \text{equation 3}$$

$$H_2O_2 + 2e^- + 2H^+ \longrightarrow 2H_2O$$

Where SBP_{red} is the reduced form of SBP, SBP_{ox} its oxidised form of SBP, and PVP-Os^{2+}/PVP-Os^{3+} represents the reduced and oxidised forms of the mediator respectively. Upon addition of H_2O_2 to the supporting electrolyte the peroxide is reduced by the immobilised SBP_{red} (equation 1). Next the oxidised SBP produced oxidises the mediator PVP-Os^{2+} to PVP-Os^{3+} (equation 2). The PVP-Os^{2+} is then electrochemically reduced when the applied potential becomes more negative than the E_{pc} of the PVP-Os^{2+}/PVP-Os^{3+} redox couple (equation 3).

Chemical modification of redox enzymes with an electron relay moiety can increase multi-step mediated electron-transfer by decreasing the electron transfer distance.

This leads to improved electrical communications between the enzyme's redox centre and its external environment (Katz, 2002); (See also Chapters 5 and 6).

1.5: Biosensor kinetics:

In the production of enzyme biosensors, enzymes are immobilised onto an electrode surface, sometimes with an electron transfer mediator (Horvath and Engasser, 1974). Immobilisation has been defined in the literature as "the process whereby the movement of the enzyme in space is highly restricted due to its entrapment in a distinct phase" (Vishwanath, *et al.,* 1995). Through its immobilisation (Section 1.15) on the surface of the electrode, the kinetic properties of the enzyme are altered. These alterations have been characterised by Goldstein (1976):

1. Conformational and steric effects;
2. Partitioning effects;
3. Microenvironmetal effects; and
4. Diffusional and mass transfer effects;

Conformational and steric effects are where the immobilised enzyme may present itself in a differently from when it is free in a buffer. Partitioning effects are the manner of how the substrate reaches equilibrium in concentration between the aqueous and immobilised regions (Goldstein, 1976). Microenvironmental effects are associated with the intrinsic enzyme catalytic parameters, i.e.: the effects of immobilisation on the enzyme-substrate reaction and how the substrate binds/dissociates in the microenvironment of the immobilised enzyme system (Bartlett and Pratt, 1995; Goldstein, 1976).

Diffusion can be defined as "the movement of a species down a concentration gradient, and it must occur whenever there is a chemical change at a surface" (Southampton Research Group, 2001). This is important because, at the electrode surface, SBP, the peroxidase enzyme is oxidising hydrogen peroxide and there is, therefore, a changing concentration gradient of both substrate and product at the electrode surface. This zone where the substrate and product concentrations are different from those in the bulk solution is termed as the diffusion layer. With microelectrodes, diffusional mass transport is extremely efficient and is comparable to that of an electrode rotating at several thousand revolutions per minute (Forster, 1998).

A low K_m (Michaelis-Menten constant) value reflects a high affinity of the enzyme for its substrate. At low substrate (S) concentrations ($S << K_m$) the reaction rate is directly proportional to the substrate concentration (a first order reaction). At high substrate concentrations ($S >> K_m$) the reaction becomes zero order reaction and no longer depends on the substrate concentration, only on the activity of the enzyme (Scheller and Schubert, 1992). The reaction area of the enzyme (concentration of the enzyme at the surface of the electrode) can influence the K_m^{app} (the apparent Michaelis-Menten constant) and this information can be used to measure the extent of diffusional limitations of the enzyme in the support (Miyakawa, *et al.*, 1999b).

The kinetics of an enzyme embedded in a porous material are controlled by two diffusional resistances to the migration of substrate from bulk solution to the active site. These are: external diffusional resistance, where the substrate has to migrate from bulk solution to the enzyme across a liquid boundary layer, and internal

diffusion, where there is resistance to the substrate movement inside the porous medium (Limoges and Savéant, 2003).

Kamin and Wilson (1980) described biosensor kinetics using the Eadie-Hofstee plot. The equation has been modified (Csöregi *et al. 1993*) to appear as follows:

$$I_{ss} = i_{max} - K_m^{app}(i_{ss}/C^*)$$

Where I_{ss} is the experimentally obtained peak current, C^* is the actual solution concentration of H_2O_2 and K_m^{app} is the apparent Michaelis-Menten constant (Csöregi *et al.,* 1993). Where current (i/μA) is plotted versus the current divided by the concentration of the substrate {i/[H_2O_2]/(μA/μM)}, the slope of the line is the K_m^{app}. Kamin and Wilson (1980) have stated that a non-linear electrochemical Eadie-Hofstee plot is a qualitative indicator of mass transport limitation. A comparison of the free and immobilised enzymes shows the need for a higher substrate concentration to obtain half the saturation activity (K_m^{app}) for the immobilised enzyme preparation. Substrate access to the enzyme active site is not only affected by internal and external diffusional limitations but also by electrostatic interactions between the substrate and the porous material, by uniform or non-uniform enzymatic activity distribution in the porous structure and by the support geometry itself (Miyakawa *et al.,* 1999a; Miyakawa *et al.,* 1999b).

Other effects of immobilisation are partial loss of the enzyme's catalytic activity due to denaturation and a change in enzyme conformation due to the presence of the support matrix (Vishwanath, *et al.,* 1995).

1.6: Glucose oxidase biosensors, a case study:

Determining the concentration of glucose is very important. It is a popular research topic and these are the most well known biosensors. Glucose is especially important because of its major role in metabolic pathways. Control of glucose levels in the blood is controlled by the pancreas, which secretes the hormone insulin. When the body cannot control blood glucose levels, the patient becomes diabetic. There is a great need for diabetics to control their insulin levels. The ability of glucose biosensors to determine the concentration of glucose in their systems makes it easier for them to control their disease and lead as normal a life as possible (Magner, 1998; Uang and Chou, 2003). Since the original paper by Clark and Lyons (1962) describing the first glucose biosensor there has been immense research into glucose biosensors. The literature is full of papers relating to glucose biosensors, their applications and characterisation (Heller, 1996). However, most biosensors designed to measure the concentration of glucose do so in an indirect fashion. When GOx undergoes normal catalytic reaction a product, H_2O_2, is generated. This can then be measured at the surface of the electrode at a predetermined set potential. However endogenous materials (ascrobate and uric acid) within the blood matrix can lead to interference and the electrode can become fouled through protein adsorption (Magner; 1998, Marcinkeviciene and Kulys, 1993). This interference can be eliminated by decreasing the potential of the electrode. This is where the peroxidase enzymes are particularly useful. Peroxidases catalyse the reduction of H_2O_2 to water (see 1.7 below). They can use the H_2O_2 produced from the GOx reaction and produce electrons that are transported to the transducer where a signal is generated proportional to the concentration of analyte present. Sensors like these where two

enzymes are used to detect the presence of an analyte are termed bienzyme sensors (van de Velde *et al,* 2000). Many methods of measuring the concentration of glucose exist including the use of mediators and a second enzyme.

1.7: Peroxidase kinetics:

There is a great need to determine the concentration of H_2O_2 in chemistry, biology, in clinical situations, in the food and many other industries. Methods of detection have included UV-visible analysis, titrimetric analysis and electrochemistry (Wang *et al.,* 1999). The peroxidase reaction is a two-electron oxidation-reduction, with the reaction normally occurring in three distinct phases (Poulos and Kraut, 1980). The general catalytic reaction for soybean peroxidase has been detailed by Henriksen *et al.* (1999) as follows:

$$\text{SBP } (Fe^{3+}) \text{ porphyrin} + H_2O_2 \rightarrow \text{SBP } (Fe^{4+}{=}O) \text{ porphyrin}^{\bullet+} + H_2O$$

Resting enzyme *Compound I*

$$\text{SBP } (Fe^{4+}{=}O) \text{ porphyrin}^{\bullet+} + AH \rightarrow \text{SBP } (Fe^{4+}) \text{ porphyrin} + A^{\bullet}$$

Compound I *Compound II*

$$\text{SBP } (Fe^{4+}) \text{ porphyrin} + AH \rightarrow \text{SBP } (Fe^{3+}) \text{ porphyrin} + A^{\bullet} + H_2O$$

Compound II *Native enzyme*

Overall: $H_2O_2 + 2AH \rightarrow 2H_2O + 2A^{\bullet}$

Figure 1.7.1: The catalytic cycle of soybean peroxidase showing the two intermediate states compounds I and II (Henriksen, *et al.,* 1999), where AH is a reducing substrate.

Hydrogen peroxide oxidises ferric peroxidase in a two-electron step, forming the intermediate compound I (green in colour , this is referred to as a oxyferryl porphyrin π cation radical). This porphyrin radical accepts one electron from an organic substrate, yielding a substrate free radical and a oxyferryl heme intermediate (red in colour) known as compound II. Another one-electron reduction step from a second organic substrate molecule reduces compound II to the resting ferric peroxidase (Goodwin *et al.*, 1995; Dunford, 1999).

As can be seen from the above scheme, the peroxidase catalysis is a two substrate, and two-product reaction (Dunford, 1999). Cleland (1970) defines the catalytic reaction of peroxidases as an *Irreversible Bi-Bi Ping-Pong* reaction whereby the enzyme oscillates between two stable intermediate forms. Conventional *Ping-Pong* reactions are reversible with an upper finite limit with respect to rate. In an irreversible reaction, the rate of formation of the enzyme-substrate complex is fast compared to the rate of its dissociation and, therefore, initial rate conditions persist. As a result of this there appears to be no upper limit, and the larger the concentration of substrates, the faster the rate of reaction. A plot of the pseudo-first-order rate of compound I formation against H_2O_2 is linear and does not show saturation. This observed irreversibility should not be taken to mean that the back reaction to initial reactions has a zero rate, but that it is too small to measure. As the substrate concentration increases, saturation will occur or enzyme inactivation will eventually occur (Dunford, 1999). Dunford (1999) states, "it is a grievous error to try to analyse peroxidase kinetics in terms of k_{cat} or K_m". This is because there are 2 unknowns, the second-order rate constants for the formation of Cpds I and II. Due to the irreversibility of peroxidase reactions, equilibria between reactants and products

cannot be established and there is no Haldane reaction (Fersht, 2002). When reporting kinetic results, several groups have tried to standardise values, these include V_m/E, and $V_m/2K_m$ (Gilfoyle *et al.*, 1996, Smith *et al.*, 1990, Smith *et al.*, 1992). Smith *et al.*, (1990 and 1992) however do report a K_m value of [redacted] for ABTS. These various organic reducing substrates include colorimetric [3,5,3',5'-tetramethylbenzidine (TMB), 2,2'-azino-di-(3-ethyl-benzthiazoline-6-sulphonic acid (ABTS), *o*-phenyl diamine (OPD), and 3,3'-diaminobenzidine (DAB)}, fluorescent [homovanillic acid, (4-hydroxy-3-methpoxy-phenylacetic acid)], and chemiluminescent (luminol) compounds, (Ryan, *et al.*, 1994a). Several of the colorimetric reagents (e.g. OPD and DAB) are reportedly carcinogenic and, as a result, TMB and ABTS are the two reagents used in most activity and kinetic assays now (Ryan *et al.*, 1994a, Childs and Bardsley, 1975).

1.8: Peroxidase biosensors and signal generation a brief overview:

1.8.1: HRP biosensors:

As a result of HRP being a widely studied enzyme, it is also widely used in biosensor. The field of HRP biosensors is vast, and like GOx biosensors, a detailed review of the literature would be unduly long. HRP biosensors use many detection methods. Published methods using HRP include an amperometric immunosensor (Lu *et al.* 1997), mass balance (Martin *et al.* 2002), potentiometric methods (Ghindilis *et al.* 1996), photovoltaic spectroscopy (Wang *et al.* 2001), and optical and chemiluminescent methods (Choi, *et al.* 2001, Rubtsova, *et al.* 1998). For a greater understanding of the characteristics and mechanisms of HRP the following references are noteworthy; Dunford (1999); Veitch and Smith (2001).

1.8.2: SBP biosensors:

SBP has many advantages over HRP in its catalytic activity under many different conditions (as will be discussed later in Section 1.11). The first SBP biosensor was reported in 1995 by Vreeke *et al.* as a thermostable-wired enzyme electrode. They used a $Os(bpy)_2(PVP)$ mediator modified by an epoxide. Kenausis *et al.* (1997) also used a poly(4-vinylpyridine) polymer complexing the pyridine nitrogens to $Os(bpy)_2Cl^{+/2+}$ quaternised with 2-bromoethylamine. There have been few papers to date reporting the use of SBP in biosensors (see Table 1.9.1, page 22). The majority of papers discussing the incorporation of SBP into a biosensor system report the use of a mediator to aid in electron transfer from the active site to the surface of the electrode. It would be advantageous to construct a SBP biosensor that communicated directly with the electrode surface.

1.9: SBP and its applications to biosensors:

A major shortcoming of all heme-dependent peroxidases is their low operational stability, resulting from facile oxidative degeneration of the heme group (van de Velde *et al.,* 2000). HRP has a pH-activity profile ranging from neutral into the alkaline region. There is a need to measure H_2O_2 concentrations in the acid range of the pH scale, pH 2-6, where HRP cannot function properly. SBP, however, is an excellent candidate for use in this pH range (see Figure 1.9.1 for the action of SBP in a biosensor). Oxidation and reduction reactions are influenced by the buffer pH and SBP's wider working range affords it greater applicability in biosensors (Wang *et al.,* 1999). The first SBP biosensor was described by Vreeke *et al.* (1995) using an osmium based mediator ($Os(bpy)(PVP)Cl^{+/2+}$) partially quaternised with 2-bromoethylamine and using a vitreous carbon rotating electrode.

Until the use of SBP by Heller and Vreeke (1997), no sensors could be used in a realistic environment at physiological temperatures (37°C) for any reasonable time (~100 hours). In the clinical field, monitoring of glucose "*in vivo*" for diabetes mellitus, and of lactate for confirmation of hypoxia and ischemia, are vital in patient management (Heller and Vreeke, 1997). It would be highly desirable to provide a sensitive biosensor for the detection of H_2O_2, which would be stable at 37°C and higher for sustained periods of time. The use of thermostable SBP immobilised into a mediator now facilitates this (Heller and Vreeke 1997).

Operational stability of SBP can be greatly increased by generating H_2O_2 *in situ* from glucose and molecular oxygen. This avoids excessive initial H_2O_2 concentrations and hence, formation of compound III (an intermediary compound formed from compound II, it is created in the presence of an excess concentration of H_2O_2, and is a reversible dead-end compound, which slowly reverts back to native SBP, Dunford, 1999) and or irreversible inhibited SBP. Normally, SBP functions as a classical peroxidase, but it can be transformed into an oxygen transfer catalyst when coimmobilized with glucose oxidase (van de Velde *et al.*, 2000). H_2O_2 is electrochemically detected by its electrooxidation on a platinum electrode (or on other related inert Pt group metal electrodes) (Heller and Vreeke, 1997). Pt electrodes act as the basis of the systems described in this thesis.

Osmium-containing redox centres allow for electronic communication between the electrode surface and the SBP heme centre. The pyridin-*N*-ethylene groups of the Os containing mediator functions in increasing the hydration and providing primary

amines for cross-linking (Kenausis *et al.,* 1997). The current of "wired" peroxidase sensors is mass transport controlled over a broad concentration range and, thus, varies linearly with the concentration of H_2O_2 (van de Velde *et al.,* 2000). The long-term operational stability of the bi-enzyme (GOx-SBP) biosensor was investigated. The higher the glucose oxidase loading, the better the operational status at 37°C (Kenausis *et al.,* 1997). The oxidase is added into the mediator mix in great excess. Therefore, if 90% of the initial GOx activity is lost, enough activity remains to catalyse conversion of at least 90% of the substrate reaching the SBP-containing layer, reducing H_2O_2 to H_2O, which is sensed by the electrode (Heller and Vreeke 1997). van de Velde *et al* (2000) noted that a loading of 1.3μg GOx gave the biosensor a $t_{1/2}$ of 40 hours, a GOx loading of 52μg maintained 100% activity for more than 100 hours, while after 200 hours it had lost 10% activity.

The reaction sequence of the mediated peroxidase electrode is shown in Figure 1.9.1. Upon the addition of H_2O_2, SBP catalyses the reaction forming water, in the process, SBP goes through its catalytic cycle (Figure 1.7.1). This causes the mediator to go from its resting state of Os^{2+} to Os^{3+}. The osmium species is a one-electron donor used as the mediator to assist in electron transfer from the active site of SBP to the surface of the electrode.

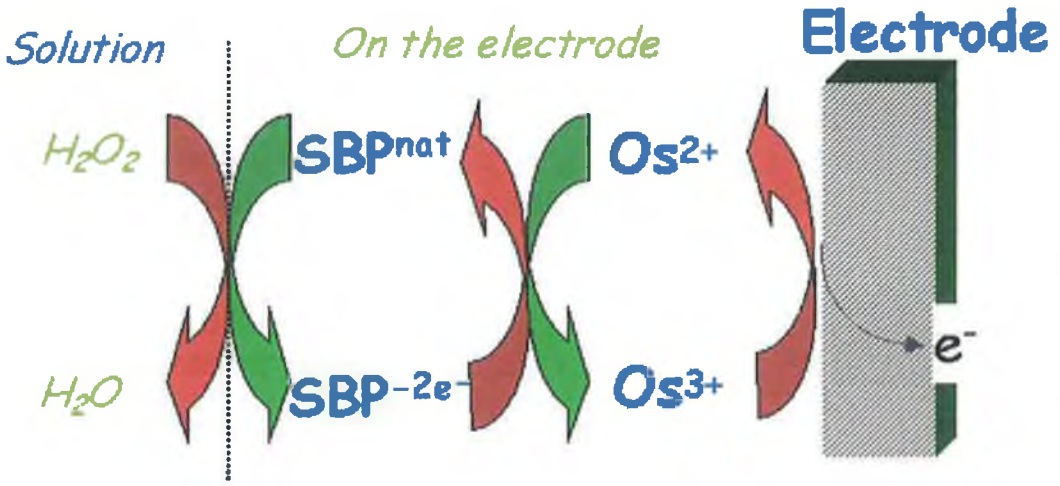

Figure 1.9.1: Mechanism of mediated bioelectrocatalytic reduction of hydrogen peroxide at a peroxidase-mediated modified electrode.

Table 1.9.1: Some SBP biosensors and their properties from the literature.

Electrode type ‡	Size of Electrode	Enzyme	Method of immobilisation	Mediator	Analyte measured	Method of measurement	Reference
Glassy carbon	4mm	SBP	Adsorption	PVA/PVP	H_2O_2	Amperometry	Wang et al. (2001)
Glassy carbon	4mm	SBP	Entrapment	Sol-gel	H_2O_2	Amperometry	Wang et al. (1999)
Glassy carbon	3mm	GOx/SBP	Entrapment	Pos-EA [1]	Glucose	Amperometry	Kenausis et al. (1997)
Glassy carbon	3mm	SBP	Entrapment	Pos-EA [1], PEGDGE[2]	H_2O_2	Amperometry	Heller and Vreeke, (1997)
Pyrolitic graphite (Rotating disk)	$0.2cm^{-2}$	SBP	Entrapment	DMPC [3]	H_2O_2	Amperometry /CV	Zhang *et al.* (2002)

‡ Disk electrode unless otherwise stated, [1] POs-EA: $Os(bpy)_2Cl^{+/2+}$ poly(4-vinylpyridine) quaternerised with 2-bromoethylamine, [2]PEGDGE: Poly(ethylene glycol) (400) diglycidylether, [3] DMPC: Dimyristoylphosphatidylcholine epoxidised olefins.

1.10: The biochemistry of soybean peroxidase:

Welinder (1992) classified the superfamily of peroxidases based on biological origin and thorough analysis of sequence alignment. The superfamily comprised 3 classes: Class I contains mainly bacterial peroxidases including cytochrome c peroxidase (CcP) and ascorbate peroxidase (APX); Class II includes the secretory fungal peroxidases lignin peroxidase (LiP), manganese peroxidase (MnP), and *Coprinus cinereus* peroxidase (CiP). Class III contains the plant secretory peroxidases including horseradish peroxidase C (HRP-C), its acidic isoenzyme A2 (HRP-A2), peanut peroxidase (PNP) and soybean peroxidase (SBP)(E.C. 1.11.1.7, www.chem.qmw.ac.uk/iubmb/enzym,e/rules.html).

All the peroxidases have a common catalytic mechanism for the deactivation of hydrogen peroxide but they can also take part in a wide range of physiological events (Nissum *et al.*, 1998). Nissum *et al.*, (1998) state that there is less than 20% similarity in amino acid composition between class III peroxidases, but they have highly conserved residues in the heme pocket playing a key role in the catalytic cycle.

The anionic SBP is isolated from the seed coat hull of the soybean plant (*Glycine max*). It is found as one isoenzyme in the hull, with a p*I* value of 4.1. SBP comprises approximately 5% dry weight of the total soluble protein of the hull (Schmitz *et al.*, 1997). To date the hull is the best single source of the enzyme (Munir and Dordick, 2000). SBP is cheap; the hulls of the seeds are the unwanted end products from the agricultural and food industries (Munir and Dordick, 2000). It has been shown that the enzyme is easily extracted and purified with good yields (Gray *et al.*, 1996). The enzyme is expressed in the hourglass cells (cells that control the opening and closing

of the stomata in the leaves) of the subepidermis of the seed coat of soybean 20-21 days after anthesis (the period during which a flower is fully open and functional) through maturation of the seed (Schmitz *et al.,* 1997; Henriksen *et al.,* 2001). SBP has an extinction coefficient of $90mM^{-1}.cm^{-1}$ at 403nm and pH 7.0 (Nissum *et al.,* 2001).

SBP has unusual stability with regard to temperature, pH and organic solvents (Henriksen *et al.,* 2001) see also 1.11 below. It is an anionic glycoprotein. Henriksen *et al.* (2001) determined that there are 13 α-helices and 2 β-pleated sheets within the protein. The apoenzyme has a molecular weight of approximately 40,662 Da. After deglycosylation this decreases to approximately 33,250 Da, as determined by MALDI-TOF analysis. This indicates that the sugar residues account for 18.2% of the apoenzyme (Gray *et al.,* 1996). There are six carbohydrate groups on five peptide fragments obtained after trypsin digestion. Five of the glycans [sugar residues *N*-linked to Asp in the sequence of Asn-X-Ser/Thr/Cys, where X can be any residue except Pro and Pro can't follow the tripeptide sequence (Creighton, 1993)] are attached at Asn16, Asn90, Asn104, Asn167 and Asn174 (Gray *et al.,* 1997). Resonance Raman analysis was carried out to determine the carbohydrate content. The average composition of the carbohydrate was 2 mol GlcNAc, 3.3 mol Man, 0.9 mol Fuc, and 0.7 mol Xyl (Gray *et al.,* 1996). Schmitz *et al.* (1997) showed that there was a decrease in peroxidase activity following chemical deglycosylation. Chen and Vierling (2000) determined the sixth glycan site residue as being Asn 185 and stated that it is common to most peroxidases. The molecular structure of SBP has been deposited in the RCSB Protein Data Bank with accession number 1FHF (see Figure 1.8), (Henriksen *et al.,* 2001). However, recently Welinder and Larsen (2004) have

updated the amino acid sequence of SBP and changed one amino acid residue (Figure 1.9), Ile-260-Thr. The first amino acid residue differs also from the Henriksen, 1FHF, structure by Gln-1-Pyr, this Pyr is pyrrolidone carboxylic acid. Welinder and Larsen (2004) also added two extra amino acids to the end of the sequence, these are Asp-305 and Ser-306, thus bringing the sequence length to 306 amino acid residues and differing from 1FHF, which has 304 amino acids in its sequence.

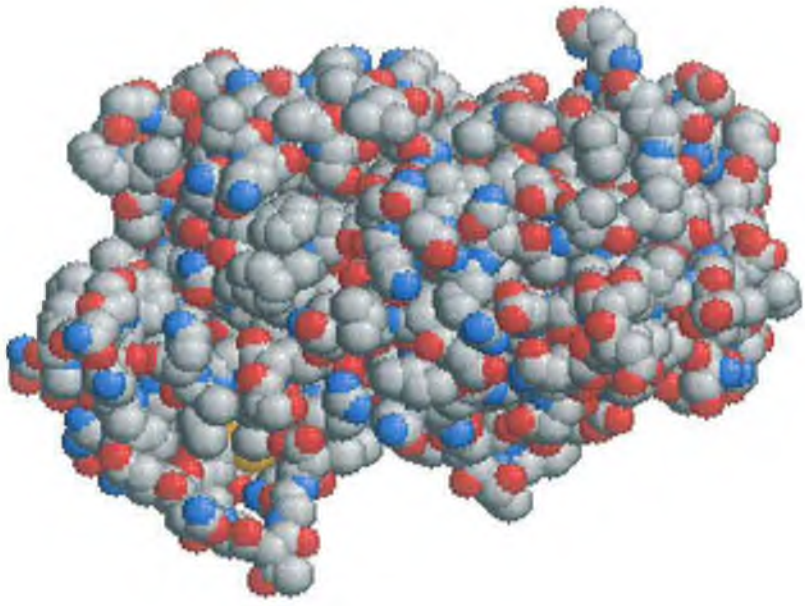

Figure 1.10.1: Structure of SBP as deposited in the PDB (Berman, *et al.* 2000; Bairoch 1993, www.rcsb.org/pdb.index.html, 2002) with accession number 1FHF, as determined by Henriksen *et al.* (2001). Structure is shown in the computer-modelling package RasMol (www.umass.edu/microbio/rasmol, 2001).

Determining the functions of peroxidases is very complex due to the numbers of isoenzymes in the peroxidase family. For SBP, there are at least 20 genes responsible

for the production of the enzyme. Cloning of these genes could help determine the function of the various enzymes *in vivo* (Chen and Vierling, 2000). Botanically, the seed coat acts as a barrier protecting the seed and prevents the seed from germinating at the wrong time. With breakdown of the seed coat, germination can occur. It has long been thought that plant peroxidases use lignin and other plant compounds as reducing substrates. Binding to, and polymerisation of, coniferyl alcohol indicates that SBP can efficiently catalyse reactions involving lignin precursors. Therefore, it is possible that SBP is involved in the lignification or suberisation processes of plants (Henriksen *et al.*, 2001). It is thought also that SBP could act as an antimicrobial agent, although it is itself not antimicrobial (Schmitz *et al.*, 1997).

In the last few years recombinant forms of SBP (rSBP) have been generated in bacterial vectors (Chen, and Vierling, 2000; Henriksen *et al.* 2001). Chen, and Vierling, (2000) generated a cDNA library and screened 2 x 10^5 clones for SBP activity. They isolated 4 clones exhibiting SBP activity (U51191 (GmEpa1), U51192 (GmEpa1), U50093 (GmEpb1) and U51194 (GmEpb2)) and characterised their production in *Escherichia coli.* Henriksen *et al.* (2001) generated a recombinant form of SBP (accession number 1FHF in the RCSB protein data bank) for crystallographic studies; an advantage of using rSBP is that it is unglycosylated in *E. coli* . This can be essential in crystallographic studies. To date no search on electronic databases could find applied studies (applications in biosensors or in other biotechnology fields) of recombinant SBP. It is only a matter of time, however before applications are found and utilised for rSBP.

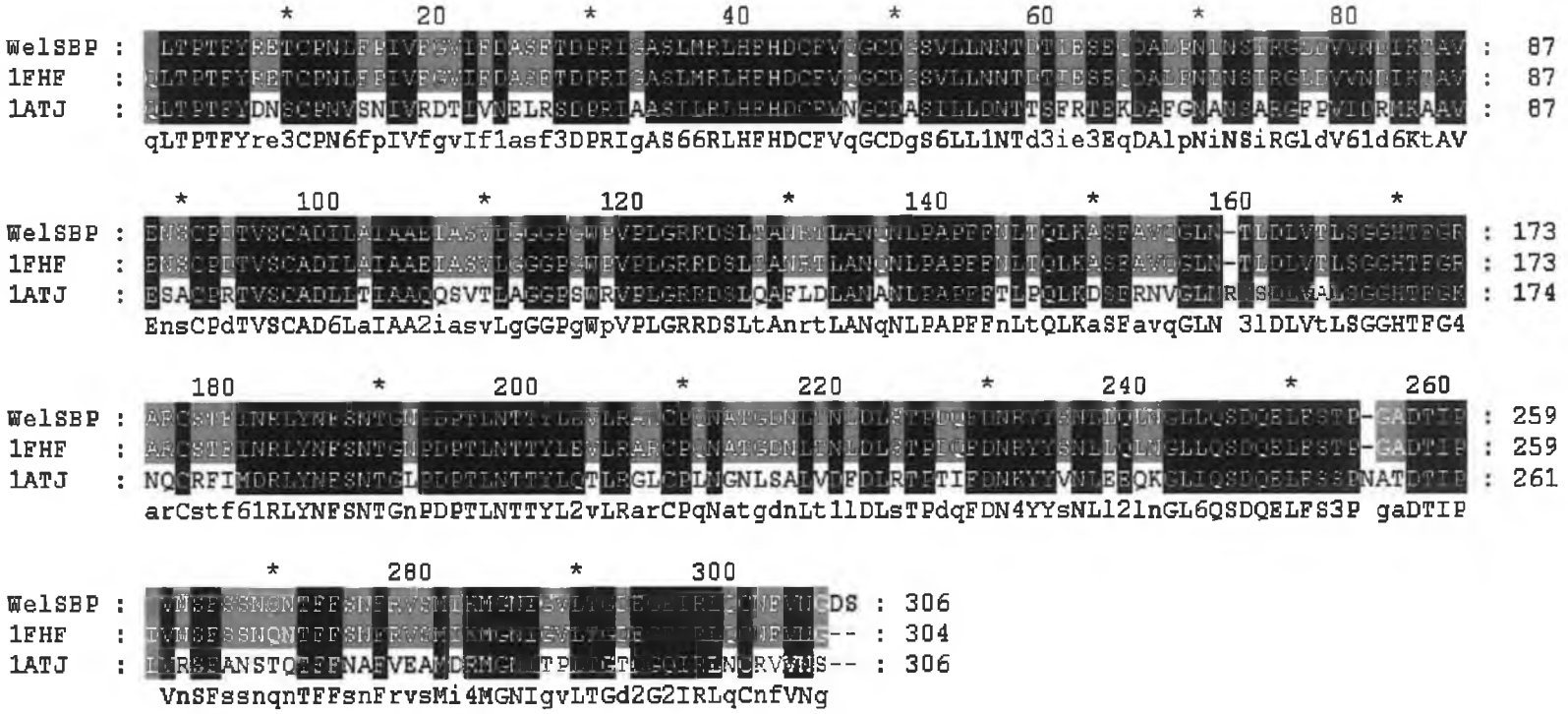

Figure 1.10.2: Sequence alignment of SBP (WelSBP, Welinder and Larsen, 2004), SBP, (1FHF, Henriksen, *et al.*, 2001) and HRP-C, (1ATJ Gajhede *et al.* 1997). The black background indicates sequence similarity between all enzymes, grey indicates similarity between two of the enzyme sequences. Positions 1 and 260 of WelSBP are coloured green with a red background to indicate a difference between this sequence and 1FHF. WelSBP and 1ATJ have 306 amino acid residues and 1FHF has 304 residues.

1.11: SBP stability and molecular properties:

Loss of heme from peroxidases leads to formation of an apoenzyme; this is well known to occur at elevated temperatures. The apoenzyme is expected to be less stable than the holo enzyme as the holo enzyme would retain the benefit of a structural entity (namely the heme group) bound in the active site centre. SBP unfolds due to the thermal melting of the protein. This is followed by a quasi-reversible loss of heme to give the apo-denatured SBP. Cooling of the enzyme solution to room temperature and addition of heme will regenerate the native enzyme. Upon formation of the apo-denatured SBP, the enzyme is irreversibly inactivated (McEldoon *et al.*, 1995). Soybean peroxidase is unusually highly thermostable and, as a result, has a number of unique catalytic properties (Nissum *et al.*, 2001). It has a high inactivation point of 90.5°C at pH 8.0 in a 1mM $CaCl_2$ buffer (McEldoon and Dordick, 1996). This is notably higher than HRP-C (81.5°C) and CiP (65°C) (Henriksen *et al.*, 2001). The optimal temperature for SBP catalytic activity has been reported to be 39°C (Schmitz *et al.*, 1997). It has been shown that SBP retains its heme prosthetic group more strongly than HRP, as a result maintaining catalytic activity for longer at higher temperatures. The heme group is tightly held in the active site centre by hydrogen and ionic bonds and by hydrophobic interactions. These interactions aid in maintaining a catalytically active conformation of the protein. Addition of heme induces changes in the secondary structure of the apoprotein to an active state (McEldoon and Dordick, 1996). SBP undergoes irreversible inactivation upon heating by the loss of the heme centre (Henriksen *et al.*, 2001). A first order deactivation is observed between 80 and 95°C. The half-life ($t_{1/2}$) of the enzyme at 70°C was not determined: after 12 hours no inactivation had been observed; however, the $t_{1/2}$ for 80.5°C was 2.5 hours. Upon cooling to 25°C

after exposure to elevated temperatures, SBP has been observed to undergo a loss in native secondary structure. Once the heme falls out of the active site centre, the apoenzyme is more susceptible to thermal deactivation (McEldoon and Dordick, 1996). Schmitz *et al.* (1997) experimentally showed that SBP maintained 80% of its specific activity at 55°C, 76% at 75°C, and 50% at 90°C, as determined by the guaiacol method.

SBP does not follow the usual two-state model of native and unfolded states present at equilibrium (N ⇆ U), (Amisha Kamal and Behere, 2002a; Amisha Kamal and Behere, 2002b). However, Amisha Kamal *et al.* (2002) published a method for SBP to determine the thermodynamic values by using high concentrations of the denaturant guanidine hydrochloride (GdnHCl). They measured the $\Delta G°(H_2O)$ from GdnHCl denaturation at 25°C at pH 7.0 as 47.0 $kJ.mol^{-1}$ while for apoSBP under the same conditions the value was 9.4 $kJ.mol^{-1}$. HRP-C has values of 16.7 $kJ.mol^{-1}$ and 9.2 $kJ.mol^{-1}$ for native and apoHRP (Amisha Kamal and Behere, 2002a).

SBP shows a very uncommon acid stability for class III peroxidases (Wang *et al.*, 2001a). It is very stable over a wide range of pH values (da Silva and Franco, 2000). In the literature the ranges are broad. Most reports agree that it is active in the range of pH 2-10 (Wang *et al.*, 2001a, b, McEldoon *et al.*, 1995, Wang *et al.*, 1999, Schmitz *et al.*, 1997). Schmitz *et al.* (1997) determined the optimum pH to be 6.3; however, Wang *et al.* (2001 a, b) found the optimum pH for their electrochemical work to be approximately 5.0. SBP is also highly stable at pH 2.4 at elevated temperatures (McEldoon *et al.*, 1995). When using SBP as a brominating biocatalyst, Munir Dordick (2000) determined the optimum pH range to be below pH 4.0.

The unusual acid stability of SBP compared with HRP can be understood with reference to the two enzymes' spectral properties. The Soret bands for both SBP and HRP at pH 3.0 had red shifts under acidic conditions. The absorbance peak of SBP changed from 402 to 407nm, whereas the HRP absorbance peak changed from 403 to 407nm. This fact is not unusual in itself, as it has been shown that the Soret band changes according to pH. After 15 minutes the spectra of the SBP and HRP were reread. The SBP spectral band remained unchanged; however, the peak band of HRP had decreased significantly, showing a new shoulder peak at 376nm. This peak at 376nm was determined to be that of free heme. This new peak at 376nm shows that the heme group of HRP falls out of the active centre at pH 3.0 leading to the loss of enzyme activity. In contrast SBP still retains its biocatalytic activity at pH 3.0 (Wang *et al.,* 2001a). From this, Wang *et al.* (2001a) were able to determine that SBP is a more stable enzyme than HRP with respect to the effects of pH. The food and fermentation industries need catalysts tolerant of acidic pHs. When analysing these low pH products for H_2O_2, the classic peroxidase HRP-C used in sensors and assay techniques is of little use due to its neutral to alkaline operating pH range. In these situations a peroxidase capable of operating in the acidic range is needed. It is here where SBP offers many advantages (Wang *et al.,* 2001a).

Resonance Raman spectroscopy has been a valuable means of characterising the active site structure of heme proteins. Spectral frequencies in the 900-1700cm^{-1} range yield information on the iron oxidation state, spin state and heme core size. Sixteen characteristic features were observed in this spectral range (Bedard and Mabrouk, 1997). The active sites of SBP and HRP are very similar. The active site iron is

mostly a high-spin 5 co-ordinate in heme and binding His as a fifth axial ligand (Bedard and Mabrouk, 1997 and Nissum *et al.* 1998). Nissum *et al.* (1998) carried out their analysis of SBP with a sample from Enzymol International (Ohio, USA), and one from Sigma-Aldrich (St. Louis, Missouri). The latter had an RZ value of 2.7, but a large proportion of the sample was low-spin heme, characterised by electronic absorbances at 403, 538, and 573 nm. No further explanation of this finding was given.

On addition of sodium fluoride, the Raman spectrum became typical of a fluorine-bound 6-co-ordinate high-spin heme with a Soret band at 402 nm. Both SBP and HRP spectra were blue shifted with respect to the corresponding spectrum of the fluorine complex of CcP (Nissum *et al.*, 1998). This feature of SBP is typical of Class III (plant) peroxidases.

All the heme peroxidases exhibit the same helix-rich fold in the heme cavity. The δ-meso heme edge of SBP is the most accessible in the peroxidase family. This is the site of electron transfer from the reduced substrate to the enzyme intermediates, compounds I and II. Isoleucine 74 influences the solvent access of the site. The distal cavity of SBP has the active site residues Phe41 and His42 in a different orientation from that of HRP, allowing more compounds to bind to the secondary solvent binding site and, as a result, increasing the activity of the enzyme. Isoleucine 74 is an important factor influencing solvent access. The C8 heme vinyl group interacts with the sulphur group of Met37 and affects the stability of the heme group by stabilisation/delocalisation of the porphyrin π cation of compound I at high pH levels (Henriksen *et al.,* 2001). Some applications of SBP are set out in Table 1.11.1:

Table 1.11.1: Some applications of SBP:

Enzyme	Substrates used	Application	Characteristics	Other info	Reference
SBP	Veratryl alcohol	Can be used in the removal of Cl from wastewater	pH range 2.4 - 12.0	Exhibits class II peroxidase characteristics	Nissum *et al.* (2001)
SBP	Lignin	Lignin degradation	SBP has strong oxidising properties	"	McEldoon, *et al* (1995)
SBP	Aqueous phenol	Can be used in the removal of phenol from wastewater	90% active; pH 5.7 – 9.0	Optimum pH 6.4	Wright and Nicel (1999)
SBP	"	"	PEG[1] added to prevent inactivation	35,000MW[2] PEG optimal for study	Kinsley and Nice (2000)
SBP	Bromine	Halogenation of compounds	Is carried out under mild conditions	Environmental alternative for halogenation	Munir and Dordic (2000)

[1] PEG: Polyethylene glycol. [2] MW: molecular weight.

Table 1. 11.1 Continued.

Enzyme	Substrates used	Application	Characteristics	Other info	Reference
SBP	AOX†	Cleaning of paper mill effluent	Removal of up to 95% of AOX† possible	Seed hulls used without purification	Pokora and Johnson (1993)
SBP	Cardonal	Anti-biofilm coating material	62% polymerisation of cardonal over 6 hours	Cardonal used in marine paints	Kim *et al.* (2003)
SBP	Aromatic substrates	Phenol removal from wastewaters	pH range 4 - 10	Addition of PEG to aid reaction	Caza *et al.* (1999)

†: AOX adsorbable organic halogens (pentachlorophenol, polychlorinated biphenyls)

1.12: Ferrocene-modified enzymes for incorporation into a biosensor system:

Ferrocene (Figure 1.12.1) is a well-studied, characterised and understood electrochemical mediator (Foulds and Lowe 1988, Frew and Hill, 1987; Price and Baldwin, 1980). Ferrocenes are highly versatile electron-transfer mediators and have a number of advantages. Ferrocenes show a wide range of redox potentials, brought about by substitution in the cyclopentadienyl rings (minus 50 to + 450mV versus SCE) (Cass, *et al.* 1984). They show electrochemically reversible one-electron redox properties, have pH-independent redox potentials and are not prone to autoxidation of the reduced form (Cass *et al.* 1985). Ferrocene is the reduced form and the oxidised form (known as a ferrocinium ion) is electrogenerated. Together, they mediate electron transfer from an enzyme active site to the electrode surface (Lange and Chambers, 1985). It has been shown that the oxidised ferrocinium ion is an efficient electron acceptor for glucose oxidase (Langue and Chambers, 1985; Frew and Hill, 1987). Substituted ferrocenes are available, affording different overall charges and a wide range of solubilities in different solvents. Ferrocenes are heat stable, and can be polymerised and used to modify other molecules. Substituents can be introduced on either or both of the cyclopentadienyl rings while maintaining the properties of a simple one-electron redox complex (Frew and Hill, 1987). Ferrocene and its derivatives have been used successfully as mediators in various enzyme electrode systems (García Armada *et al,* 2003 and Razumiene *et al.* 2003). Foulds and Lowe (1988) entrapped glucose oxidase in ferrocene-containing polypyrrole films, where the ferrocene acted to oxidise reduced glucose oxidase.

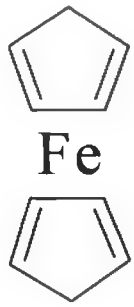

Figure 1.12.1: Structure of the electron transfer mediator ferrocene (bis(η^5-cyclopentadienyl)iron).

Ferrocenes have been used on many different electrode surfaces, including platinum (Gülce *et al,* 2003; Schuhmann, 1993), a platinum-ink layer printed onto a ceramic base electrode (Foulds and Lowe, 1988), an indium tin oxide (ITO) coated glass electrode (Ghosh (Hazra) *et al,* 1998), carbon paste (Patel and Karan, 2003; Sánchez *et al,* 1991), screen-printed carbon electrodes (Razumiene *et al.* 2003), graphite rods (Tkac *et al,* 2002), graphite powder (Oungpipat *et al,* 1995) epoxy graphite (Alegret *et al.* 1996) and graphite electrodes (Smolander *et al,* 1992).

Ferrocenes can be used in one of two ways in biosensors. The first method can be done by directly modifying the electrode surface (Smolander *et al,* 1992), by mixing carbon paste with ferrocene and either packing the mixture into a macroelectrode's cavity (Sánchez *et al,* 1991 and Oungpipat *et al,* 1995), Tkac *et al.* (2002) successfully adsorbed it directly onto the surface of a graphite electrode. The second strategy involves the incorporation of ferrocenes within a polymer chain. There are many examples of the latter in the literature. These include the incorporation of ferrocene into a B-polyethylenimine polymer (Chuang *et al,* 1997), a ferrocene

carboxylic acid polypyrrole polymer (Ghosh (Hazra) *et al,* 1998), ferrocene-poly(allylamine) cross-linked to glucose oxidase using epichlorohydrin (Calvo and Danilowicz, 1997), a poly(vinylferricinium) redox polymer (García Armada *et al,* 2003; Patel *et al,* 2003), and [(Ferrocenyl)amidopropyl] pyrrole, with [(Ferrocenyl)amidopentyl]amidopropyl)pyrrole, Foulds and Lowe (1988). Other ferrocene-containing mediators include poly(ethylene glycol)-bound ferrocene (Schuhmann, 1993), and the polymer polyvinylferrocenium perchlorate (Gülce, *et al,* 2003). Yet another method of using ferrocene was illustrated by Kataky *et al.* (2003) who used ferrocenes linked to a cyclodextrin. Bartlett *et al,* (1987) compared ferrocene-carboxylic acid to ferrocene-acetic acid and ferrocene-butanoic acid in a GOx biosensor. Ferrocene-acetic acid gave an improved overpotential for oxidation and improved reactivity towards glucose, than the other two ferrocene derivatives studied.

Riklin *et al* (1995) devised a novel method for site-specific positioning of ferrocene into redox proteins. The cofactor FAD is removed from the protein and modified with ferrocene groups. Then the apoprotein is reconstituted with the modified cofactor. There appeared to be no change in activity of the enzymes from the literature. This treatment facilitates electron transfer from the protein's redox-site to the electrode surface by reducing the distance the electron has to travel. In a further development, Katz *et al,* (1997) developed a multilayer GOx network on a gold electrode, using a cystamine monolayer, which was attached to a isothiocyanate-functionalised monolayer. This bilayer was then reacted with the ferrocene-modified GOx. Recently, Razumiene *et al.* (2003), have based their "bioorganometallic" strategy of mediator design on similar work of Katz *et al,* (1997) and Riklin *et al.*

(1995) who combined a redox-active organometallic compound and an organic moiety, similar to a substrate for a peroxidase (in their case, HRP). They used three ferrocene derivatives: 4-ferrocenylphenol, 2-ferrocenyl-4-nitrophenol and *N*-(4-hydroxybenxylidene)-4-ferrocenylaniline. These three compounds were synthesised and studied as electron transfer mediators between the coenzyme pyrroloquinoline quinone (PQQ) of GOx and alcohol dehydrogenase (ADH) and a carbon electrode surface in a screen-printed carbon electrode set-up.

Degani and Heller (1987) covalently attached ferrocene to lysine residues of GOx (Figure 1.26). Heller and Degani (1988) went on to develop a glucose biosensor but using ferrocylacetic acid. Investigating a bienzyme biosensor Kulys and Schmid (1990) found that the fungal peroxidase from *Arthromyces ramosus* (ARP) exhibited greater electrochemical reduction of H_2O_2 than did HRP. They ascribed this to the different enzyme structures. ARP carbohydrate content is only 5% whereas HRP's is approximately 18%. The electrons likely have to travel a greater distance to reach the electrode surface in the case of HRP. Attachment of electron transfer moieties to the carbohydrate can increase the electron transfer rate. Schuhmann (1995) developed a biosensor similar to that of Degani and Heller (1987) using ferrocenecarboxaldehyde and GOx. His method involves a complex multi step preparation of the ferrocene and its subsequent incorporation to the oxidised carbohydrate moieties of GOx.

1.13: Increasing enzyme stability by chemical modification:

Franks (1993) defines enzyme stability as possessing catalytic activity in a particular environment and remaining active whilst being exposed to certain deleterious conditions that can promote chemical deterioration or conformational changes. An important factor in the use of proteins/enzymes in industrial, biotechnological and medical fields is stability. This stability relates to enzyme production, distribution, and actual use at the last stage and limits the applications of proteins/enzymes (Česi *et al,* 1993 and Brugger *et al,* 2001). An enzyme derives its stability from noncovalent forces, van der Waal's forces, disulphide bonds between cysteine residues, hydrogen bonding, solvation, electrostatic forces, hydrophobic bonding, and packing contributions (Creighton, 1990, Sowdhamini, and Balaram, 1992, Tyagi, and Gupta, 1998a). In the use of proteins and enzymes in biotechnology, it is important to ensure that proteins remain stable *in vitro* (Ó'Fágáin, 2003, Sowdhamini, and Balaram, 1992).

Stability is lost as a result of denaturation, i.e. loss of the enzyme's tertiary structure or the transformation of a protein to a non-native, inactive conformation (Sowdhamini and Balaram, 1992, Ó Fágáin, 1995). The reversible and the irreversible deactivation of the enzyme can be explained by modification of the conventional two-state deactivation model;

$$N \leftrightarrows D \rightarrow I$$

where N and D represent the native and the reversibly denatured forms of the enzyme and I represents the irreversibly inactivated enzyme (Lumry and Eyring, 1954).

To maintain an active enzyme in a diverse milieu the structural integrity of the protein must be maintained. There are two general methods to maintain freely soluble enzyme activity in adverse environments: (i) recombinant technologies, and (ii) chemical modification. Mozhaev (1992) argues that chemical modifications can challenge the recombinant methods in improving enzyme stability.

1.14: Chemical modifications of proteins:

Chemical modifications of proteins and enzymes can increase their stability against high temperatures, solvents, pH, and can increase the shelf life of a protein or enzyme (Tyagi, and Gupta, 1992). Lysine residues are often targeted, as they have a reactive amine side chain. The ε-amine of Lys has a pK_a of 9.4 and modification of this ε-amine group alters the positive charge of the residue, when using most homobifunctional reagents (Khajeh, *et al,* 2001).

The main methods to chemically modify proteins and enzymes are as follows:

1. Cross-linking using homo/hetero bifunctional reagents.
2. Immobilisation.
3. Hydrophilisation,
4. Chemical aggregation,
5. Production of cross-linked enzyme crystals (CLECs)

Reaction conditions and the nature of the reagent being used to modify the protein/enzyme are important in controlling the extent of modification. Factors that can influence the outcome of modification include (Tyagi and Gupta, 1992):

1. The chemical nature of the bifunctional reagent being used.
2. Chemical specificity of the homo/hetero bifunctional reagent,
3. Hydrophobicity/hydrophilicity of the bifunctional reagent,
4. The cross-linking distance or span of the homo/hetero bifunctional reagent,

It is also possible to modify the oligosaccharide glycans of the target enzyme. Cross-linking is the most widely known and used method of chemically modifying an enzyme. There are three main types of cross-linkers: (i) zero-length, (ii) homobifunctional and (iii) heterobifunctional cross-linkers.

1.14.1: Zero-length Cross-linking reagents:

This is the smallest available type of crosslinker. It forms a chemical bond between two groups without itself being incorporated into the product and with no additional atoms being added (Hermanson, 1996). The water-soluble carbodiimide [1-(3-dimethylaminoproypl)-3-ethylcarbodiimide hydrochloride] (EDC) that is used to couple carboxylic acids to amines is a well-known example (Hoare and Koshland, 1966). EDC forms an amide bond between carboxylic acids or phosphates and amines, by activating the carboxyl group to form an active O-acylisourea intermediate. This intermediate reacts readily with nucleophiles and an amide bond is formed between the carboxyl group and the added amine. EDC is ideal for use in bioconjugation, as both it and the isourea by-product are water-soluble and can be removed by dialysis or by passing the reaction solution through a gel column

(Hermanson, 1996; Rich and Singh, 1979). Figure 1.14.1.1 depicts the reaction mechanism of EDC with a carboxylic acid and an amine group.

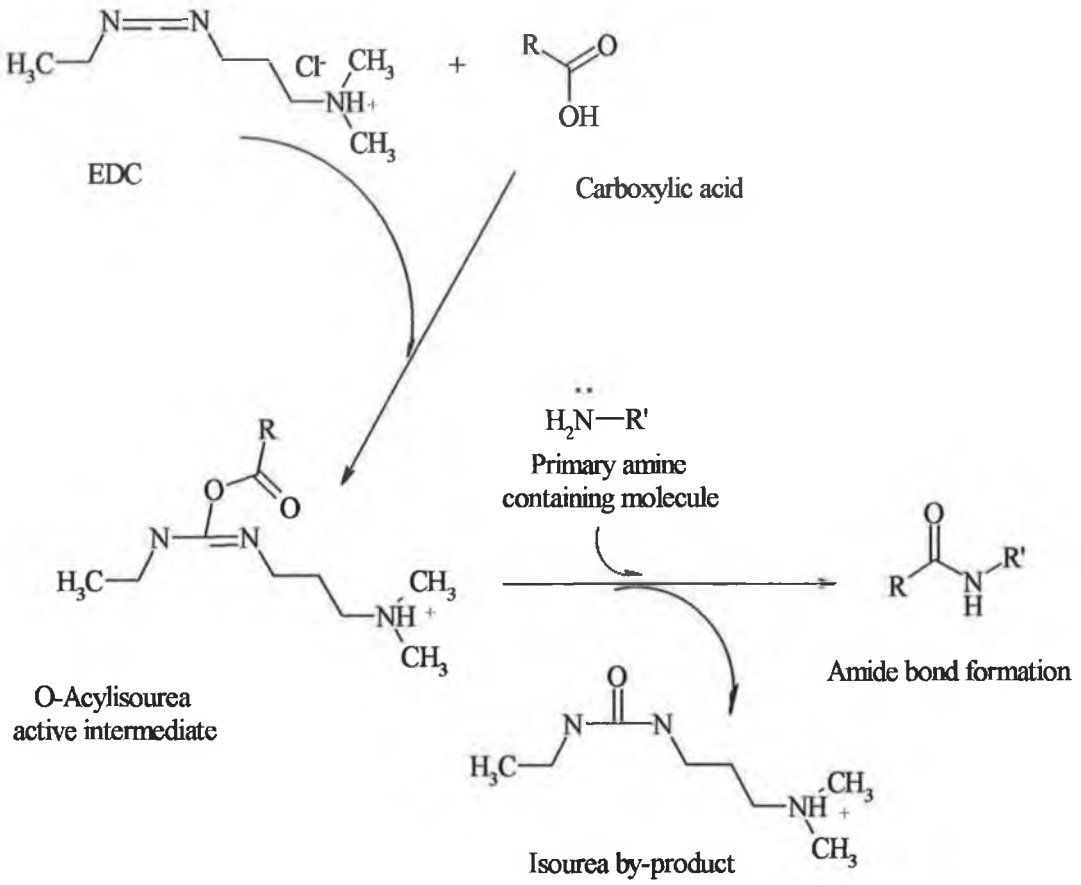

Figure 1.14.1.1: Activation of a carboxylic group by EDC and reaction with a primary amine to form an amide bond and the isourea by-product (www.probes.com, 2001).

The highly reactive O-acylisourea intermediate reacts with a nucleophile, such as a primary amine, to form an amide bond (Carraway and Koshland, 1972). *N*-hydroxysuccinimide (NHS) can be added to aid in the carbodiimide induced coupling of the acid to the amine (Rich and Singh, 1979, http://chem.ch.huji.ac.il/~eugeniik/edc.htm, 2002).

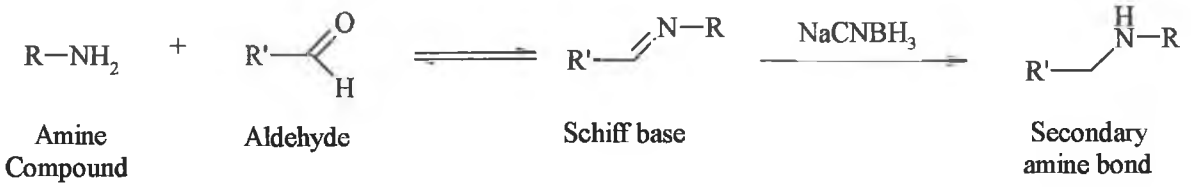

Figure 1.14.1.2: The reaction of an amine and an aldehyde group. This results in the formation of the reversible "Schiff base" intermediate which is then reduced to a secondary amine using sodium cyanoborohydride.

Aldehydes are reactive and can be modified into other groups (including Schiff bases) using different reagents. Addition of sodium cyanoborohydride ($NaCNBH_3$) to the reaction medium will reduce the Schiff base intermediate to a single bond creating a secondary amine link between the starting carbonyl and amine groups (Hermanson, 1996). Sodium cyanoborohydride is preferred over borohydride as it is less aggressive in reducing aldehyde functional groups to hydroxyls.

In this study, the EDC/NHS reaction was used to create secondary amines on SBP (Section 2.24). This modified SBP aided the development of the soybean peroxidase biosensor (Chapter 5) and a similar reaction was also used in an attempt to increase its stability (Chapter 7).

1.14.2: Homobifunctional crosslinking reagents:

Here there are two identical reactive groups. These reagents couple like functional groups typically two thiols, amines, acids or alcohols. The reactive ends are usually separated by a carbon spacer chain and are predominantly used to form intramolecular crosslinks.

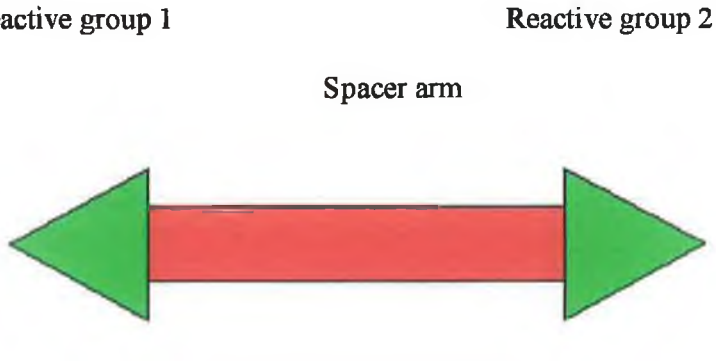

Figure 1.14.2.1: General design of a homobifunctional cross-linking agent. The two reactive groups are identical and are usually located at the two ends of the spacer group. The length of the spacer arm can be designed to fit between the functional groups to be conjugated.

Knowledge of the primary sequence and tertiary structure of the target protein/enzyme does help to determine the choice of homobifunctional cross-linking reagent. Even though a particular enzyme has many residues that can be modified does not mean that the modification will succeed if the residues do not present themselves in a manner conducive towards modification.

1.14.3: Ethylene diamine:

Diamine modification of proteins can have a dramatic effect on the overall net charge through the elimination of negative charges on carboxyl groups. Ethylene diamine is popular for protein modification, due to its small length and few hydrophobic interactions (Hermanson, 1996). While Ethylene diamine is not a cross-linker by itself in the presence of EDC and NHS it can act like a cross-linker.

Diamines can also be used to modify carbohydrate groups. One can create amine reactive sites on a sugar by oxidising with sodium *m*-periodate. Periodate cleaves vicinal hydroxyls to form highly reactive aldehyde groups. When the amine reacts with the aldehyde it is reduced to a secondary amine, as discussed previously with reference to EDC (Section 1.14.1).

1.14.4: Adipic acid dihydrazide (AADH):

Glycoproteins as discussed above, can participate in cross-linking modifications through their carbohydrate moieties (Česi *et al.* 1993 and Kozulić, *et al.* 1987). Aldehyde groups on periodate oxidised sugars will react spontaneously with hydrazides to form a hydrazone group. This hydrazone is a form of Schiff base and is reduced to a secondary amine as previously described (Hermanson, 1996). The reaction scheme is detailed in Figure 1.14.4. The first step is to oxidise the carbohydrate moiety to generate aldehyde groups. The second step is the covalent attachment of AADH (a homobifunctional cross-linker) to the aldehyde groups (Section 2. 29). When the protein is exposed to a molar excess of AADH one of the hydrazine groups binds to one aldehyde group of an oxidised sugar moiety. The second hydrazine group can then bind to another aldehyde group or remain free to be conjugated to another protein moiety at a later stage (Bystrický, *et al.* 1999).

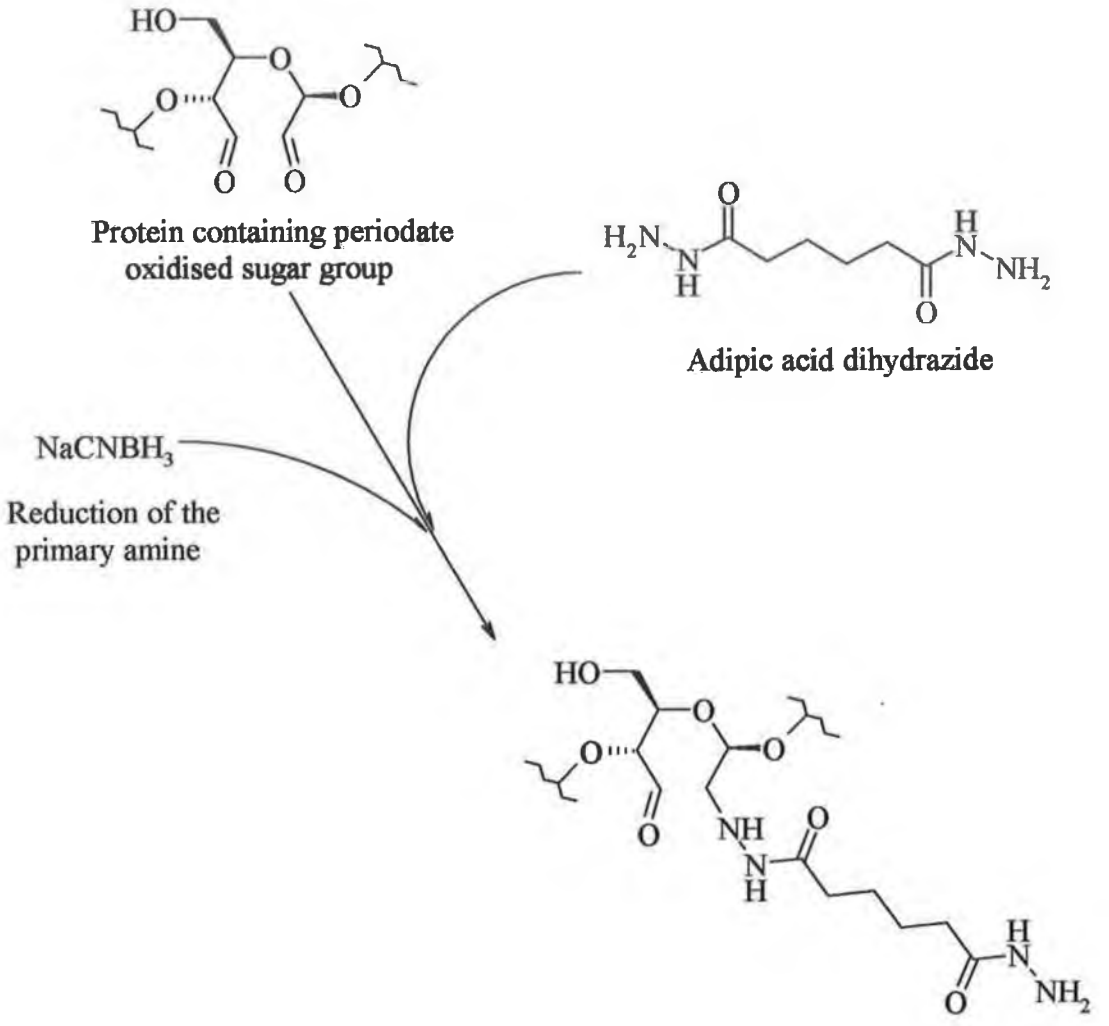

Figure 1.14.4: Glycoproteins may be treated with sodium *m*-periodate and then reacted with AADH to form a hydrazone link. This results in a hydrazide linkage.

1.14.5: Heterobifunctional cross-linking reagents:

Heterobifunctional crosslinking reagents possess reactive groups with dissimilar chemistry, allowing the formation of crosslinks between unlike functional groups. As with homobifunctional reagents, heterobifunctional crosslinking reagents can form multiple intermolecular crosslinks to yield high molecular weight aggregates, but conditions can be more easily controlled so as to optimise the stoichiometry of the target molecules. Thus, heterobifunctional crosslinking reagents are very useful for preparing conjugates between two different biomolecules (Haughland, 2001).

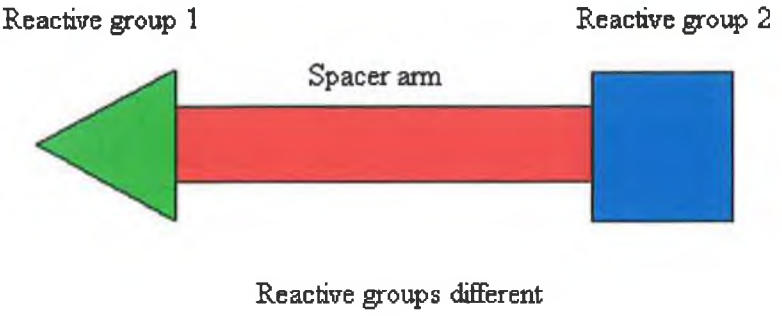

Figure 1.14.5.1: General structure of a heterobifunctional cross-linking reagent. The molecule has two different end groups, which can react with different residues. The length of the spacer arm can be varied to fit between the functional groups to be conjugated.

A commonly used heterobifunctional crosslinking reagent is *N*-Succinimidyl 3-(2-pyridyldithio)propionate, (SPDP) (Figure1.14.5.2) which crosslinks an amine and a sulfhydryl groups.

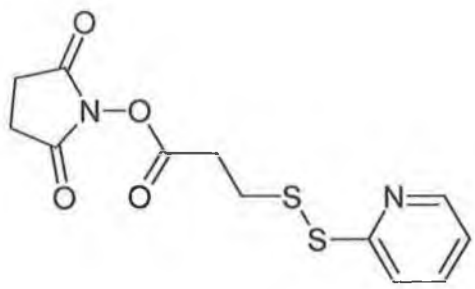

Figure 1.14.5.2: The structure of the heterobifunctional crosslinking reagent *N*-Succinimidyl 3-(2-pyridyldithio)propionate.

1.15: Immobilisation:

An immobilised enzyme, by definition, is a protein physically localised in a certain region of space, or converted from a water-soluble region of space to a water-insoluble immobile one (Gianfreda and Scarfi, 1991). Immobilisation often results in the increased stability of the enzyme; however, this may not be the primary reason for immobilising the protein in the first place (Ó Fágáin, 1997, Clark, 1994). Enzymes are often immobilised because of the economic costs involved in their isolation and purification, to allow their reuse, or use in bioreactors, and to prevent contamination of the product formed (Smith, *et al.* 2002; Isgrove *et al.* 2001). It is often the case that immobilised enzymes on solid platforms perform better than free enzymes in various applications. Immobilised enzymes are used in the medical diagnostic,

therapeutics, chromatographic packing of columns, in electronics, organic synthesis and biosensors (Nakanishi, *et al.* 2001 and Jiang *et al.* 2000).

There are five different types of immobilisation, namely:

1. Encapsulation in microcapsules (Figure 1.19),
2. Entrapment in gels, beads or fibres (Figure 1.20),
3. Covalent binding to a surface or material (Figure 1.21)
4. Adsorption to a surface or material (Figure 1.22) and
5. Intermolecular cross-linking bifunctional reagents (Section 1.18.2).

1.15.1: Encapsulation:

Encapsulation (Figure 1.15.1.1) of enzymes within small spherical capsules (liposomes), which have a semi-permeable membrane (Nafion membrane), prevents leaching of the enzyme into the bulk solution. This is because the enzymes are bigger than the pore diameter of the microcapsule, while smaller substrate and product molecules are able to diffuse through the pores. The semi-permeable membrane is often an inert polymer such as polystyrene, nylon (Isgrove *et al.* 2001) or Nafion (Wang and Dong, 2000).

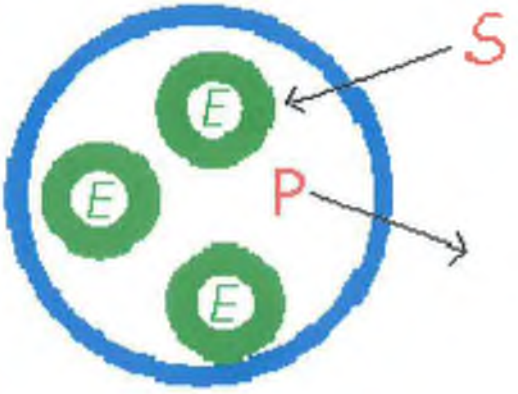

Figure 1.15.1.1: Encapsulation of enzymes in a semi-permeable membrane. The green circles marked E are the enzymes, and the surrounding blue circle is the membrane.

1.15.2: Physical entrapment:

Physically entrapping (Figure 1.15.2.1) an enzyme in a gel matrix is a mild method of immobilisation on or at an electrode surface. The degree of cross-linking can often be controlled, especially with synthetic polyacrylamide gels and sol-gels (Wang and Dong, 2000; Smith *et al,* 2002; Rosatto, *et al.* 2002); this then determines the pore size of the gel (M^{c}Cormack *et al.* 1998). Another method of entrapment is the addition of the enzyme to a mediator complex in a biosensor system, such as the $Os(bpy)_2(PVP)_{10}$ used in the work reported in Chapters 4 and 5. Natural materials for the entrapment of enzymes include calcium alginate (Bucke, 1987 and Hertzberg, *et al.* 1992), chitin (Krajewska, 1991) and its derivative chitosan (Zhou *et al.* 2002) and the use of the hydrocolloid κ-carrageenan (Chibata *et al.* 1987; Crumbliss *et al.* 1993). Liposomes (Alfonta *et al.* 2001,) and lipid membranes (Tang *et al* 2003) are also used.

Figure 1.15.2.1: The entrapment of enzymes in an inert gel membrane matrix. The green circles marked E are the enzymes the red lines are the water insoluble fibres; the enzymes are able to move within the matrix but cannot leach out.

1.15.3: Covalent attachment:

Covalent attachment of enzymes to surfaces of solid matrices (Figure 1.15.3.1) can confer increased resistance to adverse pH, temperature, and solvents. If however, the sites for covalent attachment are near or at the active site, access to the active site can be blocked, causing a decrease in activity. The surfaces of biosensors can be activated and linked to a spacer molecule, which can then be covalently attached to an enzyme, resulting in an immobilised modified enzyme. Calvo and Danilowicz (1997) discuss the advantages of using mediators in biosensors and of immobilising enzymes to these mediators. In one example, they immobilised glucose oxidase (GOx) to the mediator ferrocene-poly(allylamine) using epichlorohydrin (Figure 1.15.3.2), giving a redox hydrogel. Heller (1992) constructed a three-dimensional electrically wired enzyme, cross-linked to the Os-based polymer (Figure 1.15.3.3).

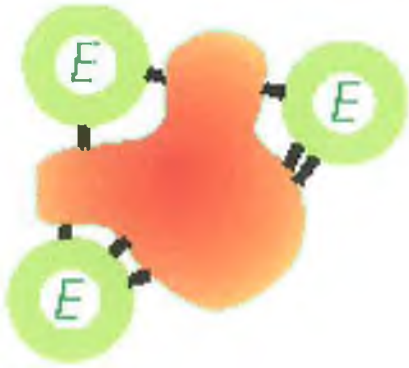

Figure 1.15.3.1: Covalent attachment of enzymes to an insoluble material. The green circles marked E are the enzymes, the red shape is the insoluble material and the black lines are the covalent bonds attaching the enzyme to the insoluble material.

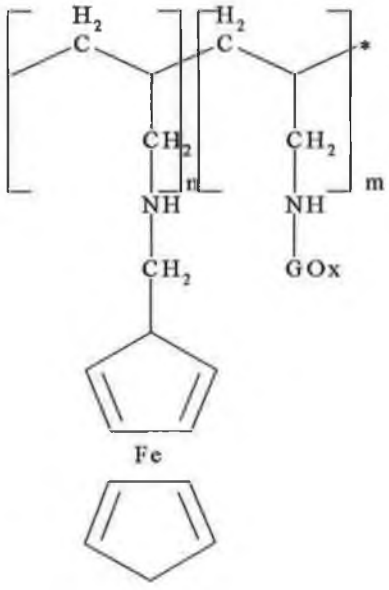

Figure 1.15.3.2: The enzyme-mediator modification. The GOx enzyme has been covalently attached to the mediator ferrocene-poly(allylamine) using epichlorohydrin. The resulting product is a redox hydrogel (Calvo and Danilowicz, 1997).

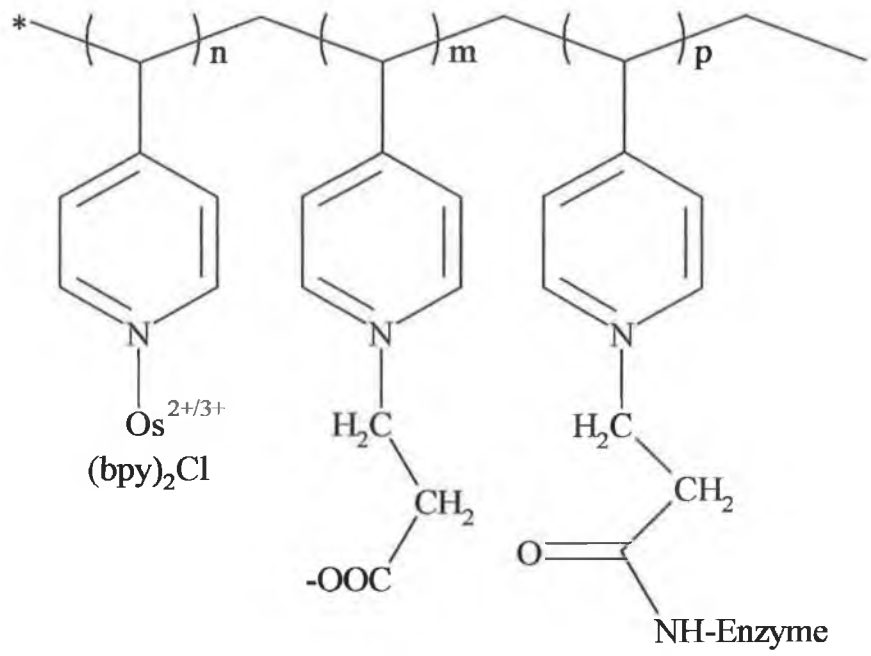

Figure 1.15.3.3: An electrically wired enzyme (GOX) Os based polymer mediator (Heller, 1992).

1.15.4: Adsorption:

The simplest method of immobilisation is adsorption (Figure 1.15.4.1) of enzymes to an insoluble surface or carrier. Anionic or cationic exchange resins, activated charcoal, silica gel, clay, and porous glass are all materials for adsorbing enzymes (Scheller and Schubert, 1992). As well as being simple in application, the process can also be reversible: by changing the pH, ionic strength or temperature, the enzyme can be released from its immobilising matrix if desired, as leaching is a drawback to immobilisation. Sun *et al.,* (2004) adsorbed HRP onto the surface of active carbon on a glassy carbon electrode to investigate the characteristics of direct electrochemistry of HRP adsorbed onto a surface.

Figure 1.15.4.1: Adsorption of enzymes to an insoluble material. The green circles marked E are the enzymes the red shape is the water insoluble material

Immobilisation of proteins/enzymes is crucial for the performance of biosensors (Löfås *et al.* 1995). Often the surface of an electrode is modified so as to immobilise an enzyme. Cysteamine monolayers formed on the surface of gold colloids permitted immobilisation of HRP (Yi *et al.* 2000). Thiol groups are immobilised directly onto gold electrodes and the enzyme can then be immobilised to the thiol group though the N3 modified portion of the thiol group (Mizutani, 1999). The microenvironment produced by immobilisation can present a unique situation (Findl, *et al.* 1985). There can be a change in the enzyme's activity and the K_m can be altered due to restricted diffusion of the substrate. V_{max} can also be altered by a partial change in the enzyme conformation inactivating following immobilisation. Ensuring a uniform dispersion of enzyme in the matrix is also important (Schmidt, *et al.*, 1992; Scheller and Schubert; 1992).

1.16: Outline of research undertaken:

Peroxidases are said to be ubiquitous in nature (Dunford. 1994) performing numerous tasks. It has been found that the peroxidase from the soybean plant has unusual thermal and solvent properties (M^{c}Eldoon and Dordick. 1996). SBP is found in the hulls of the seed and is readily extracted and purified. The fabrication of a redox biosensor from cheap sources would find numerous applications in many fields using biosensor technology. Hydrogen peroxide has been normally detected using a HRP based biosensor, considering the ease of obtaining large amounts of a cheap, easy to purify enzyme that has increased thermostability, solvent and pH tolerances; SBP may have the potential to challenge HRP as the main peroxidase used in the biosensor detection of the important analyte H_2O_2. The feasibility of using SBP an Pt microelectrodes as the basis of a biosensor is explored in this thesis. Initially the biosensor (25μm diameter platinum electrode) the mediator $[Os(bpy)_2(PVP)_{10}Cl]^+$ to shuttle electrons from the SBP active site to the electrode. Next ferrocene carboxylic acid was covalently attached to SBP in an attempt to improve electron transfer. Later experiments used a cavity-etched microelectrode to determine if direct electron transfer from SBP to Pt could take place. Finally, SBP was chemically modified in attempts to increase its stability still further. The results of these experiments are set out and discussed in the following chapters.

CHAPTER 2

MATERIALS AND METHODS

Materials:

The following materials were sourced from **Sigma-Aldrich (Dublin):** ABTS, acryl stock, adipic acid dihydrazide, ammonium persulphate [$(NH_4)_2S_2O_8$], borax, bovine serum albumin, citric acid, coomassie blue, dextran, dialysis tubing MWCO 12400 Da, 1-(3-dimethylaminoproypl)-3-ethylcarbodiimide hydrochloride (EDC), ethylene diamine, ethylene glycol-*N*-hydroxysuccinimide, ferrocene carboxylic acid, HRPA2, HRPC, *N*-hydroxy succinimide (NHS), glycine, lysine, MOPS, potassium bromide, potassium dihydrogen phosphate, Sephadex G-25, soybean peroxidase, sulphosalicylic acid, sodium acetate, sodium-*m*-periodate, sodium cyanoborohydride, sodium dodecyl sulphate, *N,N,N',N'*-tetramethylethylenediamine (TEMED), 3,3',5,5'-tetramethyl benzidine (TMB), 2,4,6-trinitrobenzenesulfonic acid (TNBS).

Amersham (UK): Sephadex G-25.

Pierce (MSC, Dublin): Bicinchoninic acid (BCA) and micro-BCA kits, [1-(3-dimethylaminoproypl)-3-ethylcarbodiimide hydrochloride] (EDC).

BDH (Lennox, Dublin): Sodium sulphite, hydrogen peroxide (30% v/v), $FeCl_3.6H_2O$.

Fischer Chemicals (Dublin): Sodium hydroxide, Tris-(hydroxymethyl) aminomethane (TRIS), Ethanol, Glycerol.

Merck: Sodium dihydrogen phosphate, disodium hydrogen phosphate, Tween 20, mercaptoethanol, trichloroacetic acid.

S. and J. Juniper Co. Essex, England: Iron (Fe) hollow cathode lamp for Perkin Elmer atomic absorption spectrometer.

Quest International (Cork): Soybean peroxidase (Food grade).

Instruments:

ALC multispeed centrifuge.

Atomic absorption spectrometer 3100, Perkin Elmer.

BioRad power Pac 1000, MSC.

Corning 240 pH meter,

HITACHI, S3000N Scanning Electron Microscope,

MT and C6CP Lauda water baths.

Multiplate reader; Labsystems Multiskan MS.

Unicam UV/VIS spectrophotometer.

660 CHi potentiostsat CHI, Texas USA,

2.1: Protein determination using the Bicinchoninic acid assay (BCA):

This assay utilised the micro-plate protocol described in the Pierce kit insert and as outlined by Smith *et al.* (1985). Fresh bovine serum albumin (BSA) was diluted from the stock solution (2 mg/mL). The diluent was the buffer in which the protein was to be assayed. Dilutions used were in the range of 2000-20 μg/mL.

Preparation of the working reagent (WR): A 1:50 dilution was made of the BCA working solutions B to A. Control (buffer, used for blank) or sample 25 μL was pipetted into the appropriate microwell. To this, 200 μL of WR was added. The solution was then shaken for 30 seconds. The plate was covered and incubated at 37°C for 30 minutes. After incubation the microwell plate was dried and allowed to cool to room temperature. The colour generated from the reaction was measured at 560 nm. Absorbance readings obtained for unknown concentrations of protein were determined from the standard curve.

2.2: Protein determination using the Micro-bicinchoninic acid assay (μBCA):

The micro-bicinchoninic acid assay utilises a higher BCA concentration and an increased incubation time and temperature (Pierce kit insert). It is used to detect protein concentrations in the range of 0.5 to 20 μg/mL. Fresh bovine serum albumin (BSA) was diluted from a stock solution (2 mg/mL). The diluent was the buffer in which the protein was to be assayed. Dilutions used were in the range of 0 – 20 μg/mL of BSA.

Preparation of the Working Reagent (WR): A 50:48:2 dilution was made of the BCA working solutions A to B to C respectively (Reagent A: sodium carbonate, sodium bicarbonate and sodium tartarate in 0.2M sodium hydroxide, Reagent B: aqueous solution of BCA™ detection reagent and Reagent C: 4% cupric sulfate pentahydrate). One hundred µL of control (buffer, used for blank) or sample was pipetted into the appropriate microwell. To this, 100µL of WR was added. The solution was then shaken for 30 seconds. The plate was covered and incubated at 60°C for 60 minutes. After incubation the microwell plate was dried and allowed to cool to room temperature. The colour generated from the reaction with protein was measured at 560 nm. Absorbance readings obtained for protein samples were determined from the standard curve. All standards and unknown samples were assayed in triplicate.

2.3: Preparation of buffers:

2.3.1: 3-(*N*-Morpholino) propanesulfonic acid, (MOPS): 25 mM pH 7.0

2.3.2: Citric acid/Na citrate: 100 mM pH 5.5

2.3.3: Phosphate buffer: 100 mM NaH_2PO_4:100 mM Na_2HPO_4, pH 7.0

2.3.4: Borax (Sodium tetraborate)/NaOH: 50 mM, pH10.0

2.3.4: Borax (Sodium tetraborate)/HCl: 50 mM, pH 8.5,

2.3.5: ABTS buffer: 200 mM NaH_2PO_4:100 mM Citric acid, pH 5.5

2.3.6: Tris-(hydroxymethyl) aminomethane, (Tris): 100 mM

2.3.7: Acetic acid/Sodium Acetate: 200 mM, pH 5.0.

2.3.8: Bis-Tris: 10 mM, pH 6.0.

All buffers were adjusted to their respective pH values using 5M NaOH or 5M HCl, with the exception of phosphate buffer, which was adjusted using the conjugate acid or base. All buffers were prepared and used at room temperature (~ 20°C) useless

otherwise stated. All buffers for use in assays using 96 well microtitre plates had Tween 20® added to a final concentration of 0.002%. This was to prevent possible enzyme denaturation through contact with polystyrene (Berkowitz and Webert, 1981)

2.4: Buffer exchange and removal of unused materials:

2.4.1: Gel filtration:

Gel filtration was carried out as described by Helmerhorst and Stokes (1980). Sephadex G-25 (10 g) was suspended in 100 mL buffer. The slurry was slowly stirred continuously overnight to hydrate the beads fully. Slurry (25 mL) was poured into an empty column and left to settle, making sure not to let the column dry out. The column was then sealed and stored at 4°C until needed. Immediately before use, the column was centrifuged using an ALC multispeed centrifuge at 1800 revolutions per minute (rotor diameter, 7.5cm) for 3 minutes at room temperature. The eluted liquid was discarded. The sample was applied to the dried column and centrifuged as before.

2.4.2: Dialysis tubing:

Dialysis tubing was also used to remove unreacted reagents and to exchange buffer as described previously by O'Brien (Transfer report, 1999).

2.5: UV-visible spectrum of soybean peroxidase and Reinheitzahl determination:

Broad scan spectra of native and chemically modified SBP were run on a UV-VIS spectrophotometer using dedicated PC software (Unicam UV2, with Vision 1.3 software). The scan was run from 800 – 250nm. Smoothing was set at medium.

Quartz cuvettes were used and the appropriate buffer used as blank. Where required the RZ value (A_{403}/A_{280}) was calculated and recorded.

2.6: Extinction coefficient:

The concentration of SBP solutions was calculated by measuring absorbance at 403 nm where the millimolar extinction coefficient has a value of 90 mM^{-1}. cm^{-1} (Henriksen *et al.*, 2001).

2.7: SBP assay utilising 3,3',5,5'-Tetramethylbenzidine dihydrochloride (TMB):

3,3',5,5'-Tetramethylbenzidine dihydrochloride (TMB, Josephy, *et al.* 1982) was used as the reducing substrate in the catalytic activity assay. This colourless reagent produces a blue colour that can be spectrophotometrically measured at 620nm (Liem *et al.*, 1971). One milligramme of TMB was dissolved in 200 µL dimethylsulphoxide [DMSO] (final concentration 2%) and added to 9.8mL of 100 mM citric acid buffer pH 5.5. . To this solution, immediately prior to the assay, 4 µL H_2O_2 (30% v/v) was added and mixed to give a final concentration of 0.04% H_2O_2. To 50 µL sample or blank (buffer solution), 150 µL reaction solution was added, mixed and allowed to react for 150 seconds (the optimum time and volume of H_2O_2 needed was determined at room temperature). Absorbances of all samples were read in triplicate simultaneously at 620 nm (Ryan *et al.*, 1994b).

2.8: Optimisation of the TMB assay:

The optimum SBP concentration, H_2O_2 concentration, and time for the standard TMB assay, were determined using a "checkerboard" experimental design in a 96 well micro-plate.

2.8.1: Optimisation of enzyme, substrate concentration and time for analysis:

Varying concentrations of SBP were pipetted in triplicate horizontally across the plate. Then, varying concentrations of the oxidising substrate were pipetted into the wells in columns. All substrate concentrations were determined in triplicate. The developing colour reaction was measured over time. The samples absorbances were read every 15 seconds and plotted against time to determine the optimum time of analysis.

2.9: Determination of free amino groups using the TNBS assay:

Determination of amino groups with 2, 4, 6-trinitrobenzenesulphonic acid (TNBS) was performed according to Fields (1971). The reaction is carried out in borax buffer at pH 9.5. A standard curve using α-*N*-acetyl-$_L$-Lysine was constructed. A 10mM solution of α-*N*-acetyl-$_L$-Lysine was prepared in distilled water; from this, standards in the range of 10 mM –50 mM were prepared. To 100 µl of enzyme (≅50 – 100 µM) or standard, 500 µl of borate buffer (0.1 M Borate buffer in 0.1 M NaOH pH 9.5) and 400 µl of ultra pure water were added. TNBS (20 µl, 5% v/v) was added and the solution was mixed. The test tubes were covered with tinfoil and left in the dark for 5 min. The reaction was terminated by the addition of 2 mL of 1.5 mM sodium sulphite in 0.1 M NaH_2PO_4. Absorbances were read at 420 nm, a standard curve was constructed and the samples were determined from the curve.

2.10: Determination of residual catalytic activity:

Enzyme preparations were prepared in 25 mM MOPS pH7.0. A standard TMB assay (Section 2.7) performed on each sample was regarded as 100% catalytic activity. Samples were dialysed (Section 2.3) overnight into 25 mM MOPS pH 7.0, removed from the dialysis tubing and assayed by the TMB method. Activity was expressed as a percentage of the initial activity (100%) and recorded. Samples were again dialysed into 25 mM MOPS pH 7.0 buffer overnight at 4°C, with stirring and were again assayed for residual catalytic activity by the TMB assay. This was done to determine the loss of SBP activity as a result of dialysis.

2.11: Thermal profile of catalytic activity:

This method is used to determine the temperature at which the enzyme begins to lose catalytic activity. A SBP solution is exposed to a range of temperatures for a set time, after which an aliquot of solution is removed, stored on ice to prevent refolding and assayed for remaining activity.

A 100 μg/L solution of SBP was prepared in 25 mM MOPS buffer pH 7.0. Two water baths are used in the experiment (MT Lauda and C6 CP Lauda). Initial temperature was taken as 20°C.

The SBP solution was left at 20°C for 10 minutes and then a 25 μL aliquot is removed and stored on ice. The water baths are preheated to their set temperatures; as one is being used the other is ramping up to the next temperature. The samples

were left in the heated bath ranging from 20 - 60°C in 10°C increments and to temperatures from 65-100°C in 5°C increments for 10 minutes and a 25 µL aliquot of enzyme is removed and stored on ice. When these incubations have been completed, samples were assayed for residual catalytic activities using the TMB method (Section 2.8).

2.12: Thermal inactivation assay:

A water bath was equilibrated to an elevated temperature close to the determined T_{50} (the temperature of half inactivation). SBP solutions were added at 15-second intervals to allow removal of sample aliquots at set times. At 15-second intervals, 50µL samples were removed into a micro-plate well and stored on ice. Samples were taken at 0, 1, 2, 4, 6, 8, 10, 15, 30, 60, and 120 minutes. The microplate containing all the samples was then warmed to room temperature (20°C) and assayed for activity by the TMB assay (Section 2.8). The values obtained were expressed as percent residual activity (where activity at time 0 = 100%) and plotted. From this graph, the half-life ($t_{1/2}$) can be calculated via computer fitting of data to single exponential decay (Enzfitter®: Biosoft, Cambridge, U.K.).

2.13: Kinetic analysis using 2,2'-Azino-di-(3-ethyl-benzthiazoline-6-sulphonic acid), (ABTS):

This method of Childs and Bardsley (1975) had been adapted to a micro-plate protocol by D. O'Brien (1999, unpublished). A 10 mM stock solution of ABTS was prepared in buffer (200 mM Na_2HPO_4/100 mM Citric acid pH 5.5). A 100mM stock solution of H_2O_2 was prepared in distilled water. For Michaelis-Menten kinetic

analysis, concentrations of the ABTS from 100mM to 0mM were prepared by serial dilution in buffer. SBP was prepared in 25 mM MOPS buffer pH 7.0 at a concentration that would give absorbance readings within the desired range (0.1-0.9). Into a microplate well 20 μL of the appropriate concentration of ABTS, 5 μL of H_2O_2, and 180 μL of ABTS buffer were pipetted followed by 20 μL SBP to initiate the reaction. The blank was the zero concentration ABTS. The microtitre plate was shaken as the initiating enzyme solution was added and the absorbance at 405 nm read every 30 seconds for 10 minutes. The change in absorbance per minute ($\Delta A.min^{-1}$) was measured for each substrate concentration.

2.14: Characterisation of Quest International SBP:

Two samples, each 2.5 mg/mL (20 mL), were prepared in 25 mM MOPS pH 7.0. Sample #1 was used as prepared. Sample # 2 was mixed for 20 minutes at room temperature and then centrifuged for 3 minutes at 1800 rpm (rotor diameter 7.5cm). The supernatant was removed and stored and the pellet discarded. Initial catalytic activity was determined using the TMB assay (Section 2.7). A temperature profile (Section 2.11) was performed and the residual catalytic activity determined. A thermal inactivation assay (Section 2.14) was carried out; and the residual catalytic activity was determined. Results for the two-enzyme preparations were compared.

2.15: Investigation into possible proteolysis:

The crude Quest SBP was screened for the presence of contaminating proteases by the method of Bickerstaff and Zhou (1993). Native protein will bind to the dye (Coomassie blue) but proteolyzed fragments cannot bind, so there will be a progressive decrease in absorbance at 595nm. This decrease is related to the amount

of protease activity in the enzyme preparation (Bickerstaff and Zhou, 1993). Using the Coomassie blue dye-binding assay (Bradford, 1976) the possible presence of proteolytic activity in the SBP preparation from Quest International was investigated.

Preparation of protein reagent:

Coomassie Brilliant Blue G-250 (100 mg) was dissolved in 50 mL 95% (v/v) ethanol. 100 mL 85% (v/v) phosphoric acid was added to the stain. This solution was then diluted to 1.0 L with distilled water (Bradford, 1976).

Proteolysis studies of SBP (Quest):

Trypsin (Bovine) and Soybean peroxidase both from Sigma-Aldrich and Quest International respectively (each 1 mg/mL) were prepared in 100mM phosphate buffer pH 7.0. Sigma SBP was assayed as a negative control and bovine trypsin (trypsin is prone to autolysis) as a positive control. Samples were incubated in a water bath at 20°C. Samples were taken at 0, 1, 2.5, 5, 10, 15, 30, 60, 120, 240, and 300 minutes, mixed with the protein reagent, left for 5 minutes and read at 595 nm to determine the residual protein content.

2.16: The determination of molecular weight using gel electrophoresis (SDS PAGE):

This method was adapted from Laemmli, (1970). The resolving (buffer A) and stacking buffer (buffer B) were prepared as follows: Buffer A: 750 mL 2 M TRIS/HCl, pH 8.8, 40 mL 10% (w/v) SDS, and 210 mL distilled water. Buffer B: 500 mL 1 M TRIS/HCl, pH 6.8, 40 mL a 10% (w/v) SDS, and 460 mL distilled water. A 10X running buffer was prepared as follows: 30.25g TRIS/HCl, 144g

Glycine and 100 mL 10% (w/v) solution of SDS were made up to 1000 mL with distilled water. A 4X loading buffer was prepared as follows: 20 mL distilled water, 5 mL 0.5 M TRIS/HCl pH 6.8, 4 mL Glycerol (neat), 8 mL 10% (w/v) SDS, 2 mL β-mercaptoethanol (neat), 1 mL of bromophenol blue 1% (w/v)

Table 2.1: Preparation of separating gel (10% Acrylamide):

Solution	Volume (mL)
Acrylamide (30% v/v)	3.30
Buffer A	2.50
Water	6.00
10% (w/v) $(NH_4)_2S_2O_8$	0.05
TEMED	0.01

Table 2.2: Preparation of stacking gel (10% Acrylamide):

Solution	Volume (μL)
Acrylamide (30% v/v)	670
Buffer B	1000
Water	3000
10% (w/v) $(NH_4)_2S_2O_8$	50
TEMED	10

To prepare the samples, 15 μL of sample and 5 μL of the 4X loading buffer were boiled for 4 minutes. Molecular weight markers (5 μL) and samples (20 μL) were loaded into separate wells. The gels were run at 200 volts, constant voltage for approximately 45 minutes.

Gels were removed from the gel plates and washed in distilled water. They were then stained using a Coomassie-based protein stain for 3 hours and were washed in distilled water for 1 hour to remove unbound dye. Gels were imaged or scanned onto a PC for analysis.

2. 17: Nondenaturing/Native polyacrylamide gels:

Nondenaturing or native polyacrylamide gels allow the electrophoresed protein or enzymes to remain active. Samples are resolved by their charge and size. These gels were run in TRIS based buffer at pH 8.8.

The 4x separation buffer comprised 1.5 M Tris-HCl pH 8.8 (100 mL). The 4x-stacking buffer was 500 mM Tris-HCl, pH 6.8 (100 mL). The 30.8% v/v acrylamide stock solution was sourced commercially. Ammonium persulfate (10% w/v, $(NH_4)_2S_2O_8$) was freshly prepared. The running buffer pH 8.8, contained TRIS (25 mM), Glycine (192 mM), and the volume was brought to 1.0 L with distilled water. The 5x sample buffer contained 1 M TRIS-HCL (final concentration 312.5 mM), glycerol (50%, v/v), and 1% bromophenol blue (final concentration 0.05%). All samples were prepared in buffer containing less than 0.1M salt.

Table 2.3: All separating gels were made up as 8% acrylamide gels as follows:

Solution:	Volume (mL)
Acrylamide 30% v/v	5.34
Separating buffer	5.00
H_2O	9.66
10% AP	0.10
TEMED	0.01

Once the separating gels were poured, a solution of water:ethanol (1:1 v/v) was layered over the gels until they had set. The water:ethanol layer was poured off and the stacking gel was then poured.

Table 2.4: All stacking gels were made up as 5% acrylamide gels as follows:

Solution:	Volume (mL)
Acrylamide 30% v/v	1.34
Stacking buffer	2.00
H_2O	4.60
10% AP	0.06
TEMED	0.01

Once the stacking gel was poured the combs were inserted and the gels were allowed to set.

Nondenatured molecular weight standards were made as detailed in the product information. Carbonic anhydrase, chicken egg albumin and bovine serum albumin were used with all gels. These standards (15 μL) were used in individual wells of the gel and run with the samples. Samples (20 μL) were mixed with the sample buffer and applied to the gel. Samples and molecular weight standards were applied to the gels under running buffer. The gel box was placed in a container of ice to maintain enzyme activity. A constant voltage of 100V was applied for 105 minutes. The gels after this time were removed from the gel plates and washed exhaustively in distilled water. One gel was stained using a protein stain for 3 hours then washed in distilled water for 1 hour to remove unbound dye and the gels were imaged or scanned onto a PC.

2. 18: Isoelectric focusing:

2.18.1: Preparation of the IEF solutions:

The 50X anode (lower) buffer comprised 4.7 g phosphoric acid (85%), brought to 100 mL with distilled water. The 10X cathode (upper) buffer contained 3.5g arginine (free base), 2.9 g lysine (free base), brought to 100 mL with distilled water. The upper buffer was deoxygenated by bubbling nitrogen gas through it for 45 minutes. The 2X sample buffer contained: 2.0 mL 10X cathode buffer and 3.0 mL glycerol brought to 10 mL with distilled water. The fixing solution was prepared using 3.46 g sulphosalicylic acid and 11.46 g trichloroacetic acid (TCA) brought to 100 mL using distilled water. The staining solution contained 58 mL distilled water, 20 mL MeOH, 20 mL Stain A and 2 mL Stain B this solution was prepared fresh before use.

2.18.2: Sample preparation:

Before loading the samples onto the precast gel the wells should be washed out using distilled water. Ten microlitres of sample buffer and sample were each added to an eppendorf tube, the solution was mixed and 15 μL of the mixture was loaded onto the gel. Standard *p*I markers (5 μL of each) were loaded into a separate well. The plastic strip covering the anode was removed and the anode buffer covered the anode gel strip. Salt concentrations in the samples were less than 100 mM to avoid interference.

Table 2.5: The gel was run under the following conditions:

Voltage:	Time (minutes)	Current (mA/gel)
100V constant	60	5
200V constant	60	5
500V constant	30	6

Following electrophoresis, the gels were removed from the cassette and placed into fixing solution for 30 minutes, then into staining solution for 3 hours. Following this the gel was destained in distilled water for 3 hours, making sure a clean background was obtained. Gels were then imaged and analysed on a PC.

2.19: Optimisation for the purification of SBP:

2.19.1: SBP sample preparation:

Twenty-one mL of 2 mg/mL, SBP (Quest International) was prepared in 50 mM NaCl, 10 mM Bis-Tris pH 6.0. The sample was stirred at room temperature for 20 minutes, and then centrifuged at 1800 rpm (rotor diameter 7.5cm) for 3 minutes. The supernatant was removed and stored and the pellet was discarded. One mL of the enzyme preparation was removed and stored at 4°C as control for all further analysis.

2.19.2.Sepharose ™high performance column preparation:

A Q-Sepharose anion exchange column (2.5cm x 7cm) was equilibrated in 100 mL of 50 mM NaCl, in 10 mM sodium acetate, pH 4.7. Crude enzyme (above, 20 mL) was applied and the column was washed with 100 mL 50 mM NaCl, 10 mM Bis-Tris buffer, pH 6.7, at 1mL per minute. SBP was eluted from the column using a NaCl gradient of 50-500 mM NaCl in 10 mM Bis-Tris, pH 6.7 and fractions (5 mL) were collected.

Peroxidase activity was determined by the TMB assay (Section 2.7) and fractions were also assayed for protein concentration using the BCA protein assay (Section 2. 1). Results were graphed and the aliquots showing the highest peroxidase activities were collected, 100 μL removed from each for analysis and the relevant fractions were pooled.

Next the column was equilibrated with 10mM sodium acetate buffer, pH 4.0 (100 mL) at 4°C at 1 mL per minute. Pooled fractions from the Bis-TRIS elution were applied to the column followed by a 100 mL wash of 10 mM sodium acetate buffer pH 4.0 at 1 mL per minute. SBP was eluted using a gradient of 0-500 mM NaCl in 10 mM sodium acetate; pH 4.0 and fractions (5 mL) were collected.

Peroxidase activity was determined by the TMB assay (Section 2.7) and fractions were also assayed for protein concentration using the BCA protein assay (Section 2. 1). Results were graphed and the aliquots showing the highest peroxidase activities were collected, 100 μL removed from each for analysis and the relevant fractions were pooled.

2.20: Organic solvent tolerance assay:

SBP was prepared at 1mg/mL concentration in 25 mM MOPS pH 7.0. The organic solvent to be tested was diluted with 25 mM MOPS pH 7.0 in 10% increments from 0% to 90% v/v. SBP samples were exposed to solvent for 90 minutes at 20°C in a temperature controlled water bath, removed and diluted down to assay concentration. Remaining catalytic activity was assayed using the TMB method (Section 2.7), and

results were expressed as percent residual activity with respect to aqueous solution (Native, control enzyme preparation = 100%). All solvent tolerance assays were carried out in triplicate and results are of three separate determinations. Solvents used were acetonitrile, methanol, dimethyl sulfoxide, and tetrahydro furan.

2.21: Oxidation of SBP carbohydrate moieties:

Using sodium *meta*-periodate, it is possible to specifically oxidise glycoproteins at their sugar residues and introduce aldehyde or ketone functionalities (Hermanson, 1996).

$NaIO_4$ (50 mM) solution was prepared in distilled water. A 53.5 µL aliquot of this was added to 20 mL SBP in 25 mM MOPS pH 7.0 and reacted at room temperature for 120 minutes, in the dark, on a magnetic stirrer. The reaction was stopped by passing the solution through a Sephadex G-25 column (Section 2.3.1) or dialysing the sample overnight into 25 mM MOPS pH 7.0 (Section 2.3.2).

2.22: Modification of SBP by the introduction of additional amine groups:

(This method was used for the dextran dialdehyde and ferrocene carboxylic acid modifications). To the oxidised enzyme preparations (Section 2.21) 100-215 µL 1M ethylene diamine was added and allowed to react at room temperature with stirring for 90 minutes. Different volumes were used for the different chemical modifications [dextran dialdehyde (Section 2.26) and ferrocene carboxylic acid (Section 2.29)].

2.23: Introduction of ferrocene carboxylic acid (FCA) moieties onto the peroxidase surface:

Two millilitres of SBP solution (3.5 mg/mL) was prepared in 25 mM MOPS pH7.0 and mixed with 400 μL 50 mM $NaIO_4$; this mixture was reacted for 2 hours in the dark (Section 2.21). An aliquot (500 μL) was removed after the reaction was completed and stored at 4°C for analysis as detailed below. Six hundred microlitres of 95% (v/v) ethylene glycol was added to quench the reaction; the solution was mixed and left for 10 minutes. Next two hundred and fifteen microlitres 1.0 M ethylene diamine was added and reacted for 90 minutes, with stirring, at room temperature. The native and modified samples were dialysed (Section 2.3.1) overnight into 25 mM MOPS pH 7.0 at 4°C. After dialysis, 500 μL was removed and stored for analysis. To the modified enzyme preparation was added 200 μL sodium cyanoborohydride (100 mM) in 0.1 M NaOH. Reaction was allowed to proceed at room temperature in the dark for 90 minutes with stirring. The solution was then dialysed into 25 mM MOPS pH 7.0 with overnight stirring at 4°C. Five hundred microlitres of the modified enzyme were removed for analysis. *N*-hydroxysuccinimide (NHS) at 2 mM was added to the modified SBP preparation and allowed to react for 5 minutes. To this modified (aminated) enzyme was added 150 μL 10 mM FeCOOH/EDC solution, in 25 mM MOPS pH 7.0. The reaction was carried out with overnight stirring at 4°C. Next both samples (Native and modified) were dialysed overnight, stirring at 4°C. Another 500 μL was removed for analysis. Analyses at each step were: protein concentration (BCA assay), Activity assay (Percent recovery), TNBS assay for free amino groups, and atomic absorption analysis (elemental Fe determination).

After a successful modification, electrochemical analysis (Section 2.31-33) can be performed. This includes cyclic voltammetry, to determine enzyme-mediator response to varying the potential, and chronoamperometry analysis to investigate the response to changes in current in response to additions of enzyme substrate.

2.24: Atomic absorption analysis:

2.24.1: Instrument set-up (Perkin Elmer 3100):

The lamp (Fe, hollow cathode lamp) was placed into the lamp chamber. (Average lamp current was ~ 20 mA). Slit width was set to 0.2 nm and the wavelength dial adjusted as indicated on the lamp (248.3 nm). The system went through the initial set-up. The current value of the lamp (20 mAmp) was entered and the interval time was set at 1 second. The energy icon was pressed; energy value is to be as high as possible. Adjustment of the wavelength dial increases the light energy to a maximum, one then adjusts the fine-tuning knobs above the lamp until the light energy is again maximal. Once this has occurred the Gain icon was pressed. Absorbance should be at ~ 0.2, and at this stage autozero is pressed. The oxidising agent and compressed air are turned on and the mixture ignited. For iron analysis, it is recommended to let the instrument to warm up for 10 minutes (Perkin Elmer manual, 1990).

2.24.2: Iron analysis:

The oxidant flow rates should be 5 mL/min for, and the fuel 3 mL/min. When sampling, the tube was put into the air and the instrument autozeroed. Next, deionised water was introduced, and the instrument autozeroed again. Then the standard or sample was introduced. Standards were checked to calibrate the

instrument. The analyser was shut down by turning off the oxidant and fuel on the instrument, followed by the fumehood and finally the gas taps on the wall. The analyser was turned off and the lamp removed.

2.24.3: Sample analysis:

A standard curve was constructed from $FeCl_3.6H_2O$ in the range of 2.0 – 0.0625 mg/L. Ultra pure water was used to prepare the buffer and standards (25 mM MOPS pH 7.0). The instrument was blanked with 25 mM MOPS pH7.0. Before analysis of native and chemically modified SBP, standard iron solutions were analysed to ensure the instrument gave a linear response over the range being investigated.

2.25: The use of the zero-length cross-linker EDC and the importance of using *N*-hydroxysuccinimide (NHS):

Initial chemical modifications were carried out in the presence of the zero-length cross-linker (EDC) only. Subsequent modifications using EDC incorporated the use of *N*-hydroxysuccinimide (NHS). NHS stabilises the formation of an active ester functional group, which is necessary for the successful chemical modification of the enzyme. The conjugation chemistry is discussed in the introduction.

2.26: Modification of SBP by the attachment of dextran dialdehyde:

2.26.1: EDC/Ethylenediamine modification of SBP

To 1mL SBP (1 mg/mL in 100 mM Na_2HPO_4 pH 4.5), 4 mg EDC were added. The reaction was allowed to proceed for 1 hour at room temperature, with stirring. Samples were dialysed overnight against 50 mM $NaBr_4O_7$/HCl pH 8.5. One hundred microlitres of 1.0 M ethylenediamine (1% v/v) were added and the reaction allowed

to proceed for 90 minutes. Samples were then dialysed (Section 2.3.1) overnight against 50 mM $NaBrO_4$/NaOH buffer pH 10.0.

2.26.2: Dextran Oxidation

One gramme sodium *meta*-periodate ($NaIO_4$) was added to 12.5 mL dextran (average molecular weight: 66,900) in distilled water (20 mg/mL) and the mixture was incubated at room temperature for 2 hours. The oxidised dextran was then dialysed overnight at 4°C with 3 changes of distilled water.

2.26.3: Dextran modification of the aminated peroxidase:

One hundred and ten microlitres dextran dialdehyde 20 mg/mL (~10% v/v) were added to peroxidase samples, and the reaction allowed to proceed for 72 hours, before termination by the addition of 100 µL ($NaCNBH_3$, 100 mM) in 0.1 M NaOH. This solution was mixed at room temperature for 90 minutes, then dialysed overnight against 25 mM MOPS pH 7.0 to remove unreacted products and to change the buffer.

2.27: Modification of SBP by the cross linking reagent adipic acid dihydrazide:

The method of Brugger *et al,* (2001) and Kozulić, *et al,* (1987) was adapted to modify SBP. Twenty millilitres of 5 mg/mL SBP was prepared in 200mM sodium acetate pH 5.0. A 500 µL aliquot was removed for analysis. Carbohydrate moieties of the SBP were oxidised in the presence of 12.5 mM $NaIO_4$, for 120 minutes at room temperature with stirring and the reaction was then stopped by dialysis (Section 2.3.1) of the oxidised SBP against 200 mM Sodium acetate pH 5.0 overnight. A 500 µL aliquot was removed for analysis. To 900 µL of oxidised SBP was added 0.5 mM

adipic acid dihydrazide (AADH, 100 μL). Reaction was allowed to continue for 30 minutes at room temperature with stirring and was then stopped by dialysis (Section 2.3.1) against 200 mM Sodium acetate pH 5.0 overnight. A 500 μL aliquot was removed for analysis.

Reaction of AADH with SBP is facilitated through a Schiff base; in order to stabilise this bond, the sample was reduced with $NaCNBH_3$. One hundred microlitres of 100 mM $NaCNBH_3$ in 100 mM NaOH was added to 1000 μL of modified SBP at room temperature for 90 minutes with stirring. The reaction was stopped by dialysis (Section 2.3.2) into 200 mM Sodium acetate pH 5.0 overnight. A 500 μL aliquot was removed for analysis. The stored SBP samples were assayed for free amine groups by the TNBS assay (Section 2.9) as described by Bystrický, *et al.* (1999).

2.28: Characterisation of chemical modification:

To determine if a chemical modification had been successful, several assays were carried out to characterise modified fractions. These were:

1. Temperature profile (Section 2.11),
2. Thermal inactivation (Section 2. 12),
3. Michaelis-Menten kinetics (section 2.13),
4. Gel electrophoresis (Section 2.16-18),
5. Electrochemistry (Section 2. 31-33).

2.29: Synthesis and characterisation of an Osmium containing metallopolymer complex:

The mono substituted metallopolymer was prepared by refluxing $Os(bpy)_2Cl_2$ with a ten fold excess of PVP (i.e. one osmium moiety per ten pyridine units) to give the structure shown in Figure 2.1. (bpy, 2,2'-bipyridyl; PVP, polyvinyl pyridine), (Hogan, 1999). The reflux was performed in the dark in 100% ethanol for 72 hours. The product was precipitated into diethyl ether, and the solid was collected after the diethyl ether had evaporated. The reaction scheme for the synthesis of the mediator is shown below:

$$Os(bpy)_2Cl_2 + (PVP)_{10} \xrightarrow{\text{Ethanol}} [Os(bpy)_2(PVP)_{10}Cl]^+ + Cl^-$$

The cyclic voltammogram for an electroactive species in solution has the following characteristics: the curves (anodic and cathodic) are non-symmetrical, the difference in cathodic and anodic peak potentials (ΔE_p) $\approx$ 59/n mV, and $i_p \propto \sqrt{v}$ (Schreurs, and Barendrecht. 1984). Experimentally, a ΔE_p of 59mV is rarely observed due to small distortions caused by the resistance of the electrolyte. The ratio of the i_{pc}/i_{pa} (peak anodic/cathodic currents) for a diffusion-controlled process is 1. However, deviations have been measured for osmium complexes. The major criterion for distinguishing if a system is controlled by semi-infinite linear diffusion is a linear plot of the peak current versus the square root of the scan rate.

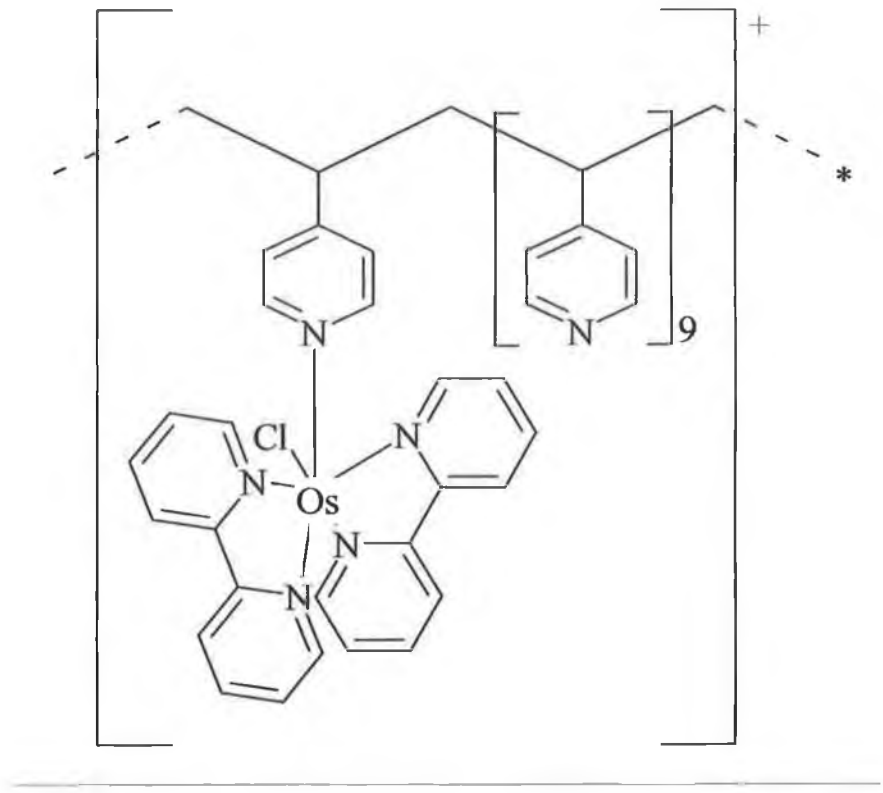

Figure 2.29.1: Structure of the electron-transferring mediator $[Os(bpy)_2(PVP)_{10}Cl]^{+}$.

The slope of the peak heights of the line with respect to the square root of the respective scan rate ($v^{1/2}$ versus i_{pa}), can be entered into the Randles-Sevçik relationship to determine the diffusion coefficient of the system.

$$i_p = 2.69x10^5 D.v^{1/2}.C.A..n^{3/2} \qquad \textit{equation 2.1}$$

Where i_p is peak current, D is the diffusion coefficient, v is the scan rate, A is the geometric area of the microelectrode, C is the concentration of the redox active species, and n is the number of electrons transferred (Southampton Research Group, 2001).

For an ideally reversible system under semi-infinite linear diffusion control, a plot of ip versus $V^{1/2}$ will result in a straight line, and if the values for A, n, and C are known the diffusion coefficient describing homogeneous charge transport through the polymer can be determined. The diffusion coefficient was determined for the mediator immobilised onto the surface of the electrode only. As will be discussed later, the SBP-mediator displayed diffusion limitations and the diffusion coefficient could not be calculated.

2.30 Fabrication of microelectrode:

Soft glass was used as the external support for the electrode. The conducting material chosen was platinum (Pt). Platinum has been widely studied as an electrochemical electrode: it is electrochemically inert and is robust enough to be put into biological buffers without compromising either its own chemistry or the biological activity of the entity being investigated. The top of the glass tube was partially closed by placing the tip into a Bunsen flame and rotating it to aid in the symmetrical closing of the glass. A tin-annealed copper wire was used as the starting wire; to this a hook up wire was attached by spot soldering it to the tin annealed copper wire. The hook-up wire was kinked to prevent it from breaking during polishing. The platinum wire (25μm diameter) was wrapped around the hook-up wire and spot-soldered to it to ensure the electrical signal would be transferred. The platinum wire was passed though the partially closed end. This end was then completely closed by placing it into a flame; the glass tube was rotated to ensure a proper seal resulted. A cyclic voltammogram (CV) was performed and recorded. The microelectrode was then placed into a solution of distilled water and left overnight. It was then removed and

dried in the air. Another CV was carried out and compared to the previous one. If there is no leakage, the two voltammograms should be superimposable. The tip of the microelectrode was polished on very fine sand paper to remove any remaining protruding platinum wire. The electrode was then mechanically polished on decreasing sizes of silica (0.5 and 0.03 μM) on moistened emery polishing paper for ten minutes at each size, being held at 90° to achieve equal polishing to all areas of the electrode. To aid this process, it was rotated in a figure of eight while being polished. The electrode was rinsed in distilled water after each polishing and finally sonicated for five minutes.

The polished electrode was placed into a solution of 1.0 M H_2SO_4. By measuring the area under the reduction peak of the oxide curve of the voltammogram from Figure 2.3 it is possible to calculate the actual surface area of the microelectrode, using the following equation (Hogan, 1999):

$$A = A_p/420 \times 10^{-6}\ C.\ cm^2 \qquad \textit{equation 2.2}$$

Where A = area of electrode, A_p= area under the peak and C = charge of reactive species. Assuming that a perfect disc was formed the geometric surface area was calculated from the equation (Hogan, 1999):

$$A = \pi r^2 \qquad \textit{equation 2.3}$$

The ratio of real to geometric surface areas gives the electrode's surface roughness. Roughness ratio of ~ 1.0-3.0 is desired. If the roughness lies outside these values, the polishing is repeated until the actual surface area falls within the desired range.

2.31: Preparation of the potentiostsat for analysis of the biosensor:

Figure 2.31.1, details the parameters necessary to be controlled for a CV to be carried out.

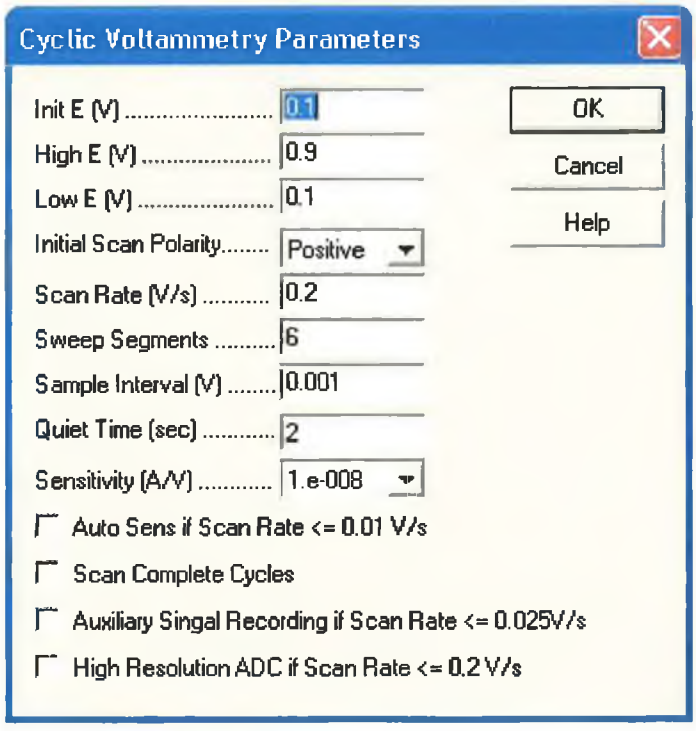

Figure 2.31.1: Set-up parameters for the running of a cyclic voltammogram, from the CHI potentiostat.

Figure 2.31.2 depict the parameters needed for amperometric i-t curves to be performed.

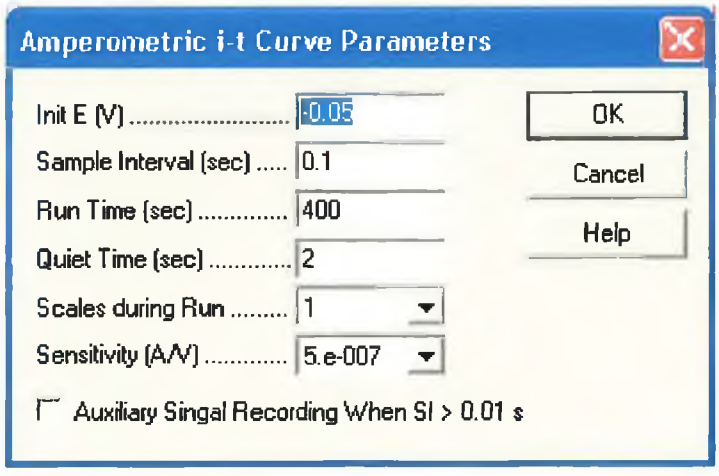

Figure 2.31.2: Set-up parameters for the running of an amperometric time-current (i-t) curve, from the CHI potentiostat software.

2.32: Preparation of the electrochemical cell:

Voltammetry is the measurement of the current flowing through the electrode as a function of the potential applied to the electrode. The resulting graph is recorded as a voltammogram. Figure 2.5 shows the working configuration of the three-electrode system, used in all experiments. This comprises a working electrode (WE), a reference electrode (RE), and an auxiliary electrode (AE). In the system used here a potentiostsat controls the potential.

Operation of the electrochemical cell was carried out at room temperature in a 10 mL buffer solution (25 mM MOPS/NaOH pH 7.0, 20°C) containing the three-electrode voltammetric cell, comprising the H_2O_2 sensor. All potentials (mV) were referred to

the KCl saturated Ag/AgCl reference electrode (Kulys and Schmid, 1990). A PTFE cap was placed over the glass cell. All cyclic voltammograms were obtained in an oxygen-free buffer (Iwuoha *et al.* 1994), achieved by purging the system with nitrogen (N_2), or argon (Ar) gas for at least 15 minutes. A nitrogen/argon atmosphere was maintained over the solution during experiments (Chattopadhyay and Mazumdar, 2000).

2.33: Description of the cyclic voltammogram in an acidic environment for the elucidation of electrode characteristic features:

In an acidic solution, the overall reaction is as follows:

$$2H^+ + 2e^- \longrightarrow H_2$$

In electrochemistry, two features can be observed when performing potential analysis: the evolution of hydrogen, and the evolution and the reduction of oxygen.

Hydrogen is adsorbed onto the surface of the electrode by the following reaction:

$$H^+ + e^- \longrightarrow H_{ads}$$

This plays a very important function in the mechanism of the hydrogen evolution reaction, by changing its thermodynamic and kinetic properties. This adsorption of hydrogen occurs at a potential where: $-\Delta G^{\theta}_{ads}/F$ (free energy of adsorption/Faraday). The adsorption of hydrogen on metals can be detected using cyclic voltammetry. The voltammogram shows there are two peaks for the adsorbed hydrogen; these have been

attributed to being strongly and weakly adsorbed hydrogen. The strongly adsorbed hydrogen is more positive because a higher free energy of adsorption is needed for the larger shift in potential. Hydrogen evolution occurs at intermediate values of ΔG^{θ}_{ads}, which result in a reasonable covering of adsorbed hydrogen atoms on the surface of the electrode metal. (Lambrechts and Sansen, 1999)

2.34: Immobilisation of SBP and mediator onto platinum microelectrode:

In order to observe an electrical signal from the SBP/mediator complex, it must be immobilised onto the electrode surface. To immobilise the SBP and mediator, a solution containing SBP (1000 μg/L) and the osmium-containing mediator $\{[Os(bpy)_2(PVP)_{10}Cl]^+$, (0.1 M)$\}$ was prepared. The tip of the electrode (5 mm) was immersed in the solution at 4°C for 3 hours. The electrode was then removed and allowed to air dry for 5 minutes. A CV was carried out to ascertain if the SBP and mediator had immobilised onto the electrode surface. Cyclic voltammograms were carried out at and repeated at various scan rates to determine the diffusion capabilities of the biosensor.

2.35: Scanning electron microscopy imaging:

The scanning electron microscope (Hitachi S3000N) was used to image the surface of the platinum microelectrodes. The microelectrode was placed in BlueTac™ and mounted on the SEM stage. It was placed into the vacuum chamber and the vacuum was applied. The filament was saturated and the electron gun aligned. Excitation voltage was set at 15-20 kV, the working distance at 27 mm and the spot size set to 3. The images obtained are from the secondary electron detector. To obtain images of

the platinum wire in the electrode, the stage was tilted to 45°. The sample was imaged, recorded onto a PC and analysed.

2.36: Etching of the platinum microelectrode:

Aqua regia was used to etch a cavity in the platinum microelectrodes. This was prepared by mixing neat hydrochloric acid (HCl) (specific gravity 1.18, purity 37%) and nitric acid (HNO_3), (specific gravity 1.42, purity 70%) in a ratio of 3:1. The tip of the 25 μm platinum electrode was immersed in the aqua regia (heated to approximately 75°C and stirred on a heated stirring plate) and allowed to react for a number of hours. The extent of etching of the platinum at different times was investigated by SEM image analysis (Section 2.35). Upon successful etching, the electrode was tested for an electrical signal and was characterised electrochemically (Section 2.31-33). To determine if direct electrochemistry was possible, native and ferrocene-modified SBP were each packed into the cavity on their own, signals determined (CV and i-t curves) and the results obtained from each biosensor set-up were compared.

2.37: Immobilisation of SBP onto etched platinum microelectrode:

To ensure the cavity formed was clean after etching (Section 2. 36) and image analysis (Section 2.35) the electrode was washed in a sonic bath (NEY ULTRAsonik. 230V~, 1 Amp, 50/60Hz, 240W) for 5 minutes. The bottom was removed from an eppendorf tube and the electrode inserted through the new bottom opening. SBP solution (250 μL) was pipetted into the eppendorf. The electrode and the solution were inverted 5 times to allow any air in the cavity to be replaced with solution. The electrode/eppendorf was kept at 4°C for 5 hours to allow deposition and

immobilisation of the SBP into the etched cavity. A CV was carried out to ascertain if the SBP had immobilised onto the electrode surface. Cyclic voltammograms were carried out and repeated at various scan rates to determine the diffusion capabilities of the resulting biosensor.

CHAPTER 3

Characterisation of crude and purified SBP

3.1: Protein determination:

3.1.1: The bicinchoninic acid assay:

The BCA assay was used to quantify the amount of protein in SBP preparations as described in Section 2.1. SBP concentrations were determined before and after purifications, modifications and all assays. Bovine serum albumin (BSA) was used to construct the standard curve (Figure 3.1).

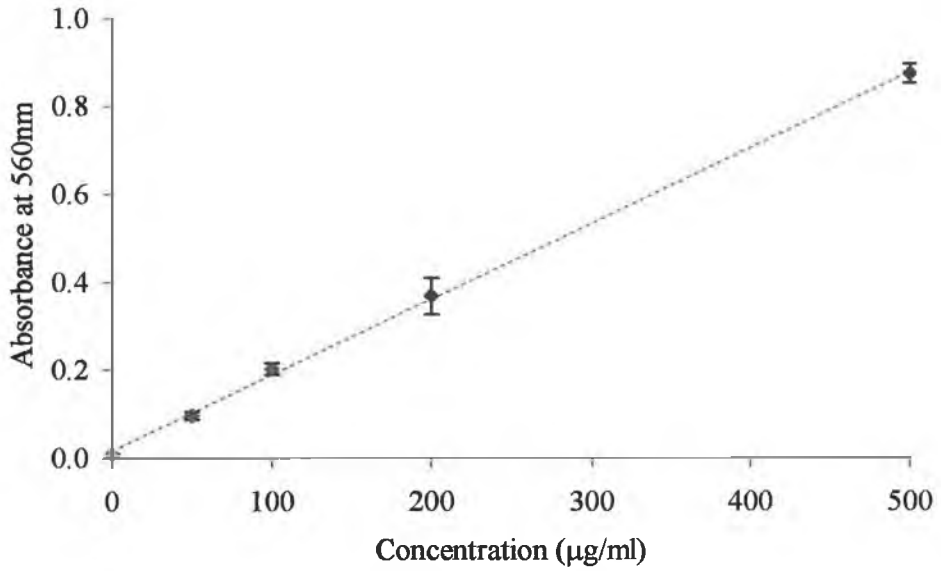

Figure 3.1: Standard curve of bovine serum albumin (BSA) for the determination of protein present in a sample, as determined by the BCA method.

3.1.2: The micro-Bicinchoninic assay:

The micro-BCA assay was used to quantify the amount of protein in the range of 0-20 μg/mL in SBP preparations as described in Section 2.1.2. SBP concentrations were determined before and after purifications, modifications and all assays. Bovine serum albumin (BSA) was used as the standard protein (Figure 3.2).

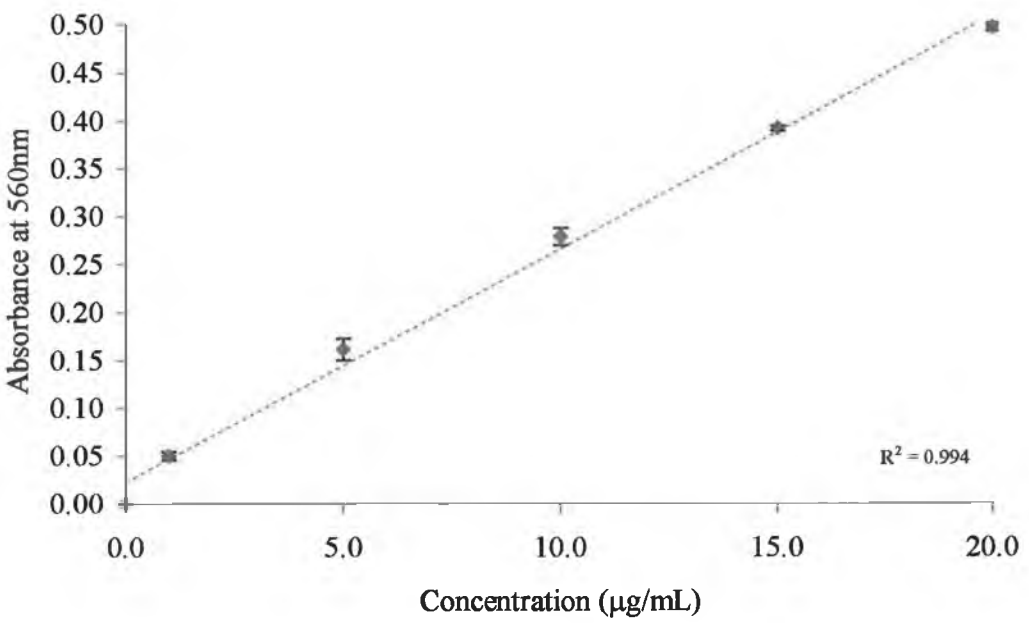

Figure 3.2: Standard curve of bovine serum albumin (BSA) by the micro-BCA assay for the determination of protein present in a sample.

3.2: Determination of amine groups and RZ number:

The TNBS assay was used to determine the number of free lysine and free amine groups in the SBP polypeptide before and after certain chemical modifications (Figure 3.3).

After successful amidation (Sections 2.23, 2.24 and 2.27), the number of amines should increase. This is illustrated in Chapter 7 (Table 7.1). *N*-α-acetyl-$_L$-lysine was used to construct the standard curve for this assay as it only has one amine group available. The standard curve is shown in Figure 3.3. Sequence analysis (Figure 1. 10.2) of SBP shows that there are three lysines.

The UV-visible spectrum of 1mg/mL SBP in 25 mM MOPS pH 7.0 was determined. A Soret peak was observed at approximately 403 nm and is attributed to the absorbance of the iron in the heme. The Reinheitzahl (RZ) purity ratio (A_{403}/A_{280}) is determined from these absorbances. This was calculated to determine the purity of the SBP preparations and was typically 2.9. The absorbance peak at approximately 280 nm is assigned to the aromatic amino acid residues, with a contribution from the heme (Dunford, 1999).

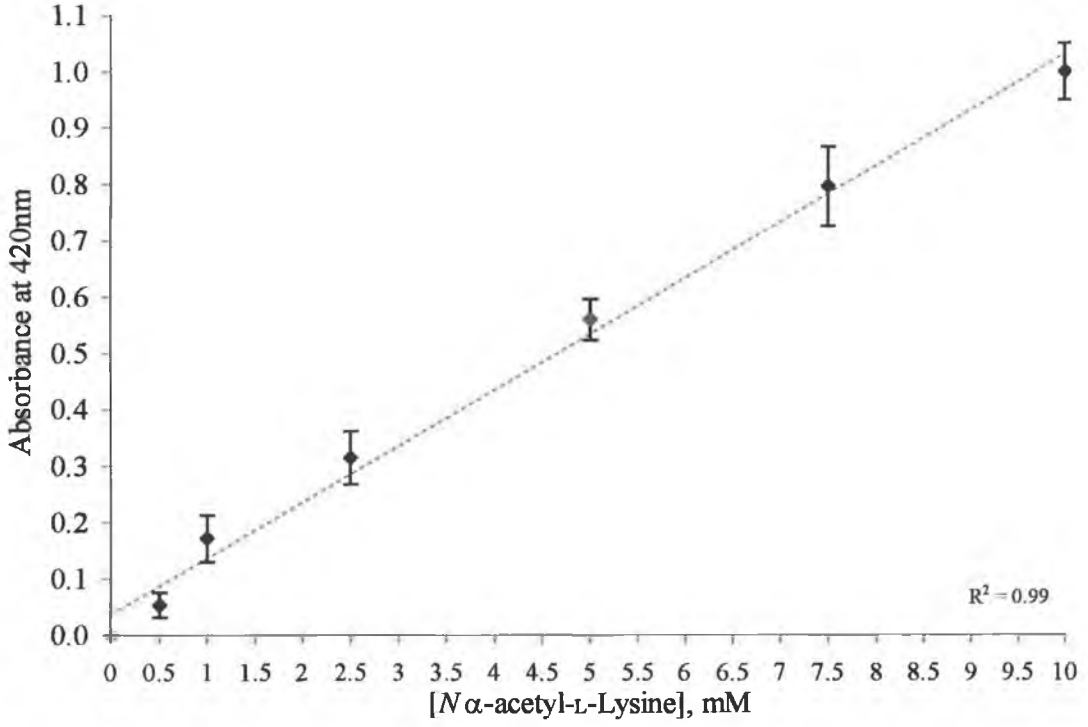

Figure 3.3: Standard curve of *N*-α-acetyl-$_L$-lysine for the determination of amines.

3.3: Optimisation of SBP (from Quest International):

The SBP used in this investigation was a food grade preparation and needed to be characterised. Optimisation of the TMB assay was performed according to Section 2.7. The TMB assay used here was modified from that of Ryan *et al.* (1994b). Three experiments were performed in order to determine the optimum time for assay, the

optimum concentration of SBP and the optimum concentration of hydrogen peroxide. Figure 3.4 illustrates the optimum time for reading the TMB assay. The absorbance is linear ($r^2 = 0.99$) up to 6 minutes and 30 seconds. The time for analyses was taken at 2 minutes 30 seconds.

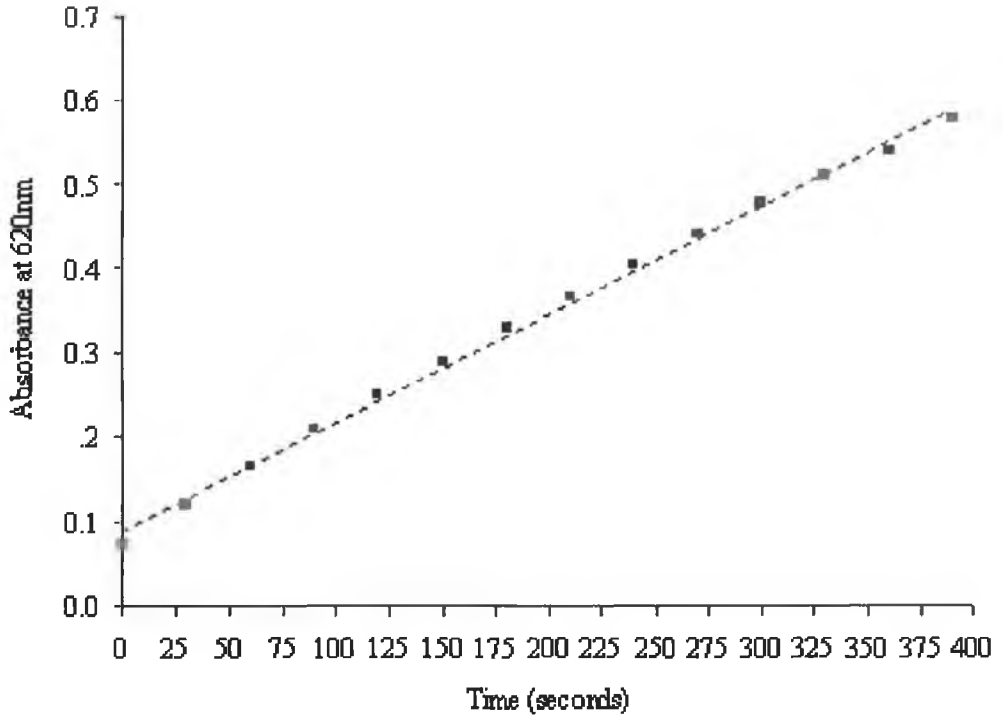

Figure 3.4: Assay to determine the optimum time of analysis for the catalytic activity assay (TMB assay). Optimum time was determined to be 2 minutes 30 seconds.

Figure 3.5 shows the concentration range for SBP from Quest International in the TMB assay. The concentration dependence is linear between 25-1000 µg/L and has an R^2 value of 0.99. The time taken for the assay was 2 minutes and 30 seconds (Figure 3.4).

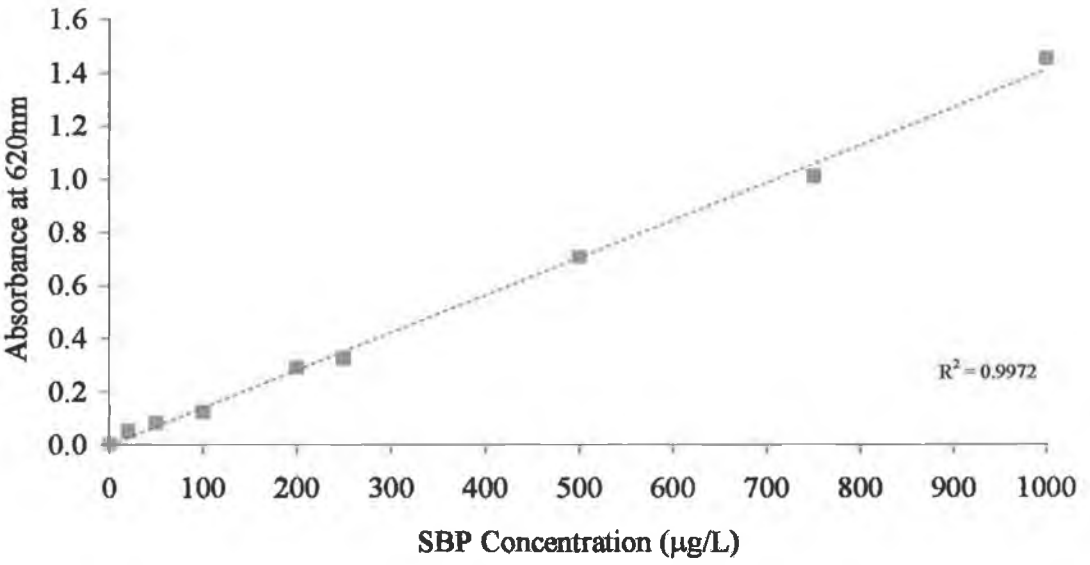

Figure 3.5: Optimisation of enzyme concentration as determined by the colorimetric TMB assay at 150 seconds. The sample was prepared as a 1 mg/mL solution in 25 mM MOPS pH 7.0 and diluted appropriately.

Figure 3.6 investigated the concentration of H_2O_2 needed for the TMB assay to yield a satisfactory absorbance at the time of analysis. A H_2O_2 concentration was desired that would prevent formation of compound III, a dead-end intermediate of the enzyme formed in the presence of a large excess of H_2O_2 (Dunford, 1999).

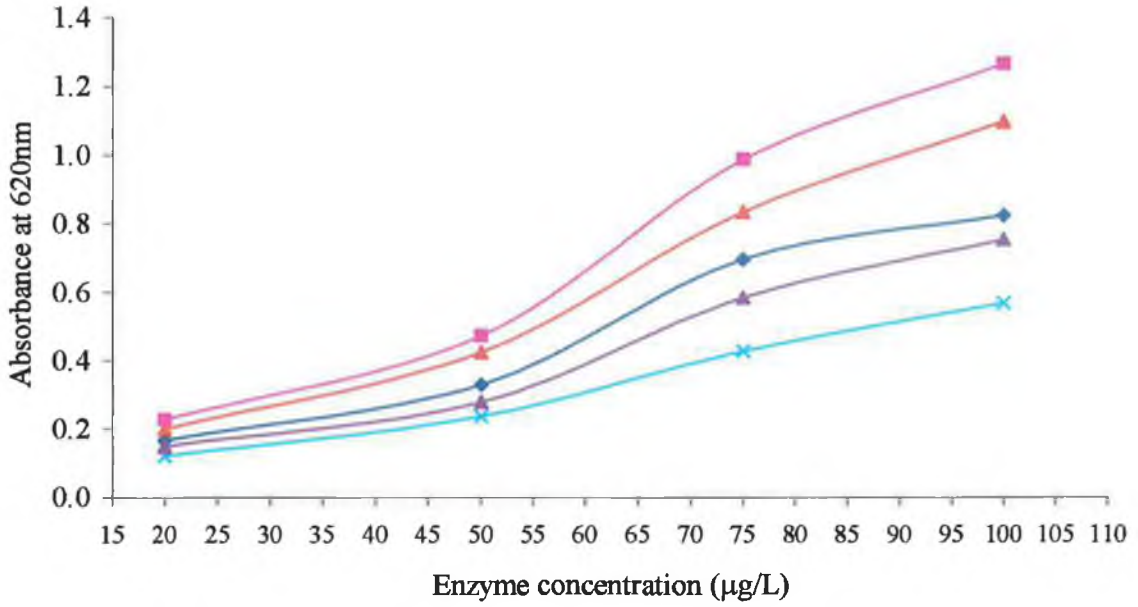

Figure 3.6: Graph showing the relationship of H_2O_2 and absorbance to SBP concentration in the TMB assay. From this, a final concentration of 0.04% v/v H_2O_2 in the TMB assay was desired, assay time was 2 minutes 30 seconds. All enzyme solutions were prepared and used at 1 mg/mL in 25 mM MOPS pH 7.0, samples were blanked against 25 mM MOPS pH 7.0. ♦ 0.03%, ■ 0.04%, ▲ 0.05%, x 0.06% and ▲ 0.07% final concentration of substrate.

3.4: Proteolytic activity in SBP samples:

The possible presence of proteolytic activity in the SBP crude commercial preparation was investigated using the Coomassie blue method described in Section 2.16. Bovine trypsin was included as a positive control, and SBP from Sigma as a negative control. As can be seen from Figure 3.7, there was no discernible proteolytic activity in the Quest SBP preparation.

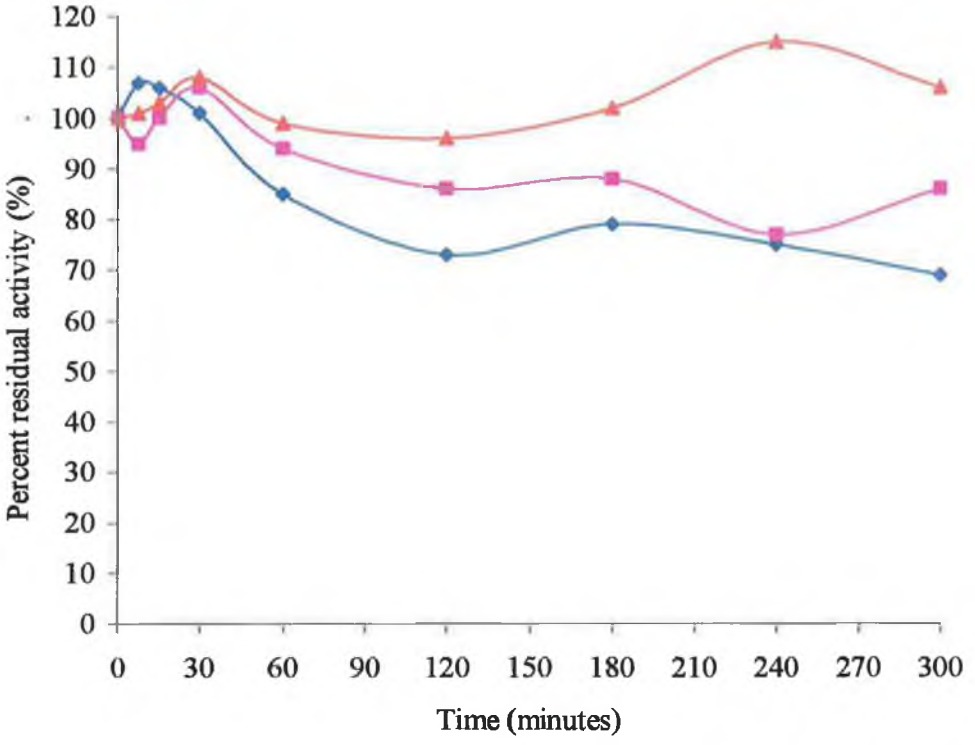

Figure 3.7: Investigation of possible proteolysis on three enzyme preparations. Bovine trypsin was used as a positive control in 25 mM MOPS, pH 7.0. Over the 300 minutes of the experiment no significant proteolysis was seen in the Quest International preparation of SBP. ♦Trypsin (Sigma), ■ SBP (Sigma) and ▲ SBP (Quest International).

3.5: Thermal activity of soybean peroxidase:

3.5: Thermal profile of SBP:

A thermal profile was performed as described in Section 2.11. The T_{50} was determined by inspection to be 73°C (Figure 3.8). It was decided to use this temperature for the thermal inactivation assay.

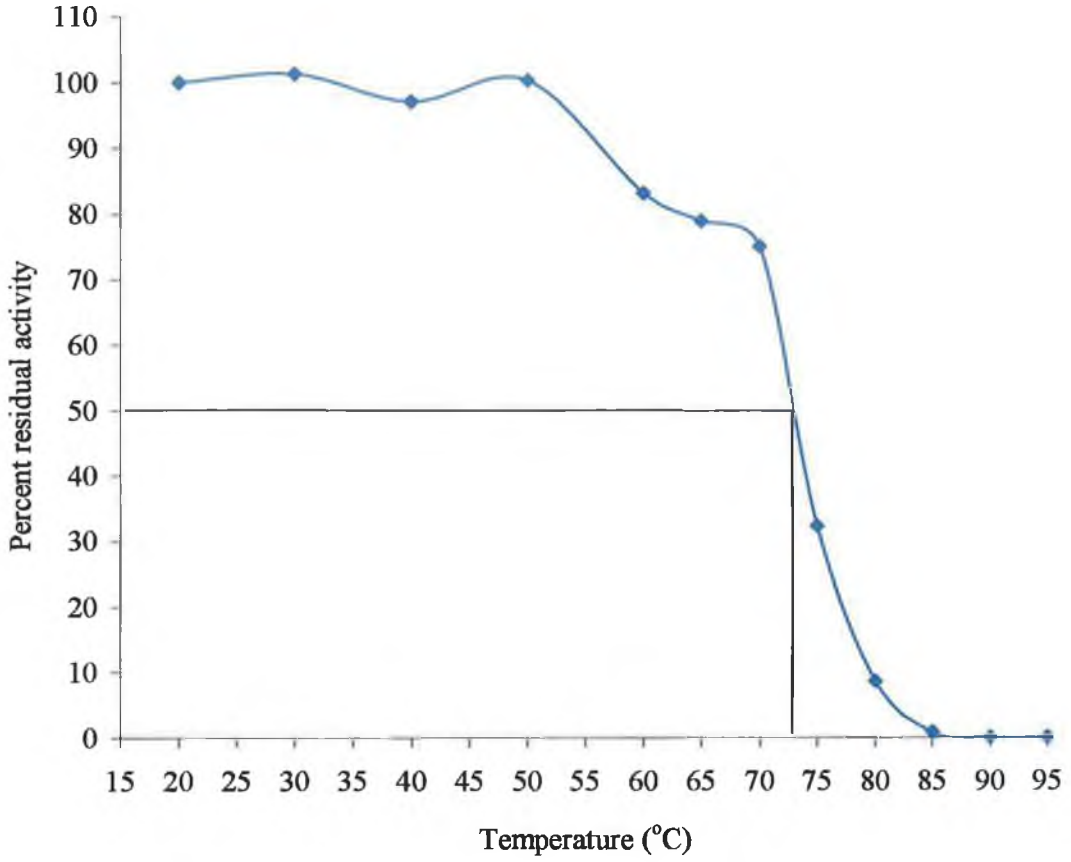

Figure 3.8: Temperature profile to determine the T_{50} of soybean peroxidase. The SBP was prepared in 25 mM MOPS pH 7.0. Incubation was for 10 minutes at each temperature point.

3.5.2: Thermal inactivation assay of SBP:

The thermal inactivation assay was performed at 73°C, the $t_{1/2}$ determined from Figure 3.9 according to section 2.12. The values obtained from the thermal inactivation assay were analysed using the Enzfitter program, and the data were fitted to first order exponential decay. The half-life was calculated from the data output of the Enzfitter programme using the formula, ln2/rate constant (0.693/k).

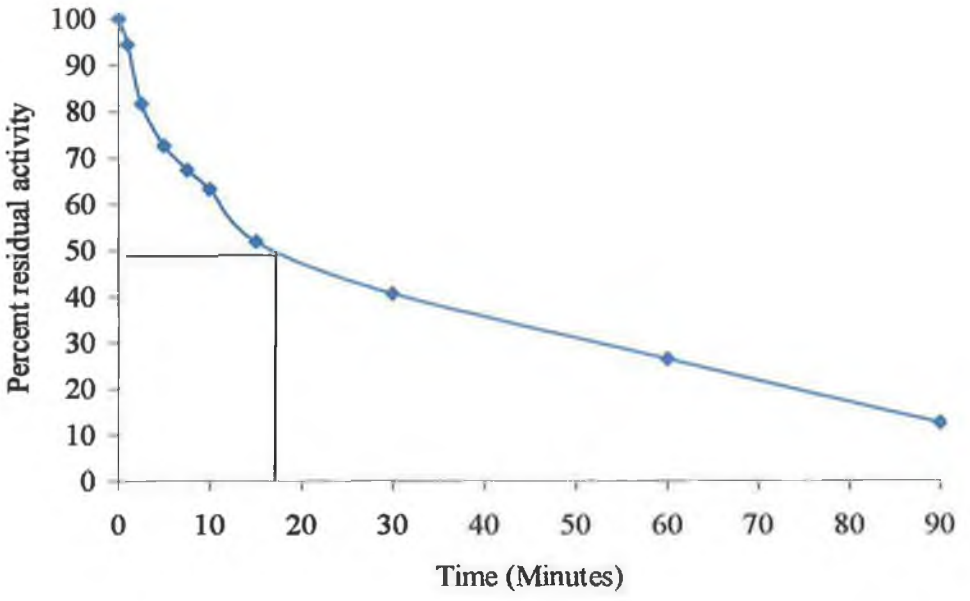

Figure 3.9: A thermal inactivation assay for Quest SBP at 73°C. Samples were stored on ice until time of assay by the TMB method.

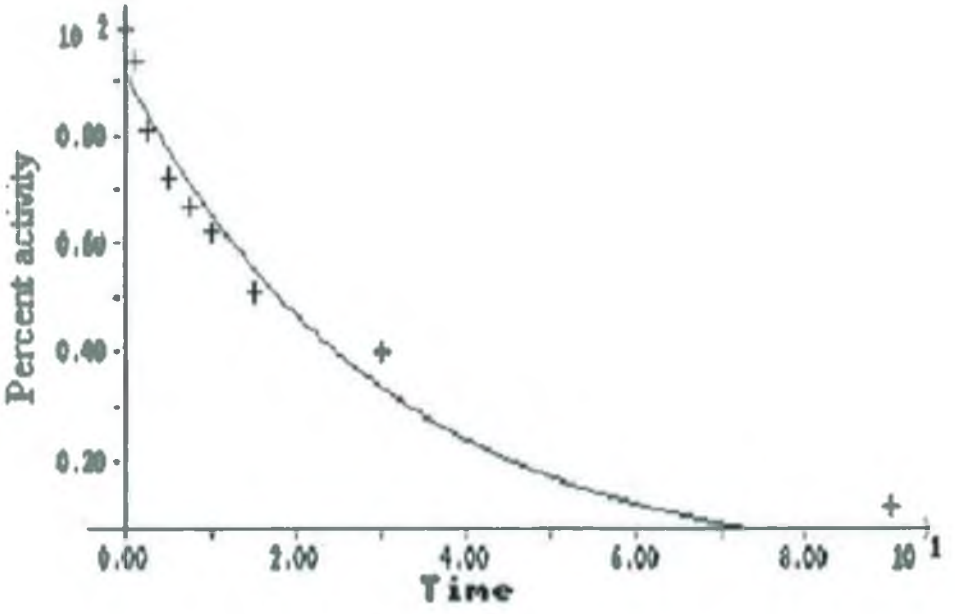

Figure 3.10: The $t_{1/2}$ for native SBP was determined to be 18 minutes, ($k = 0.0385 \pm 0.003$, Enzfitter). Data used for this calculation were obtained from Figure 3.9 and fitted to single (first order) exponential decay.

3.6: The Effects of solvents on SBP:

The effects of the solvents (acetonitrile (ACN), tetrahydrofuran (THF), methanol (MeOH) and dimethylsulphoxide (DMSO)) on the catalytic activity of SBP are investigated. Solvents have many different effects on the activity of enzymes: they can increase the activity or decrease, and the same solvent can affect the activity in different ways at different concentrations.

3.6.1: SBP in aqueous solution and solvent mixtures:

Figures 3.11 to 3.14 show the effects of increasing solvent concentrations on SBP (Section 2.13). Figure 3.11 shows that only after 50% v/v ACN is there any effect on the activity. Activity decreases to 70% of that in aqueous solution at 80% (v/v) ACN and increases again slightly at 90% (v/v) ACN.

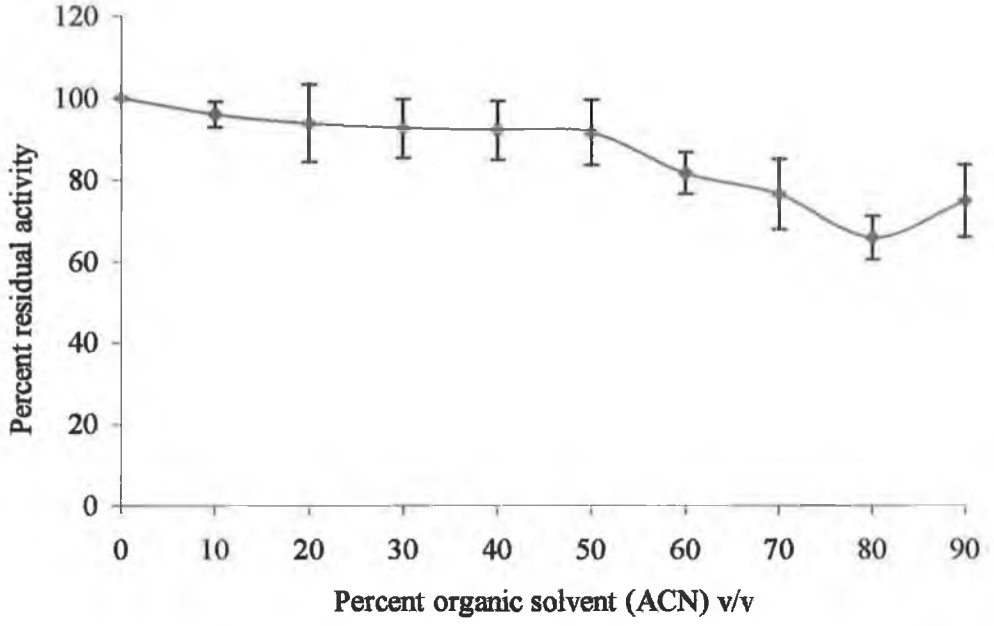

Figure 3 11: Activity of Quest International SBP, at 50 μg/L in 25 mM MOPS pH 7.0, in increasing concentrations of acetonitrile. Enzyme was exposed to the solvent for 60 minutes, at 25°C. Residual activities were then measured by the TMB assay.

Figure 3.12 shows the effect of THF on SBP. The activity is not greatly affected by increasing THF concentrations, but does decline to approximately 80% of aqueous activity at 90% THF (v/v).

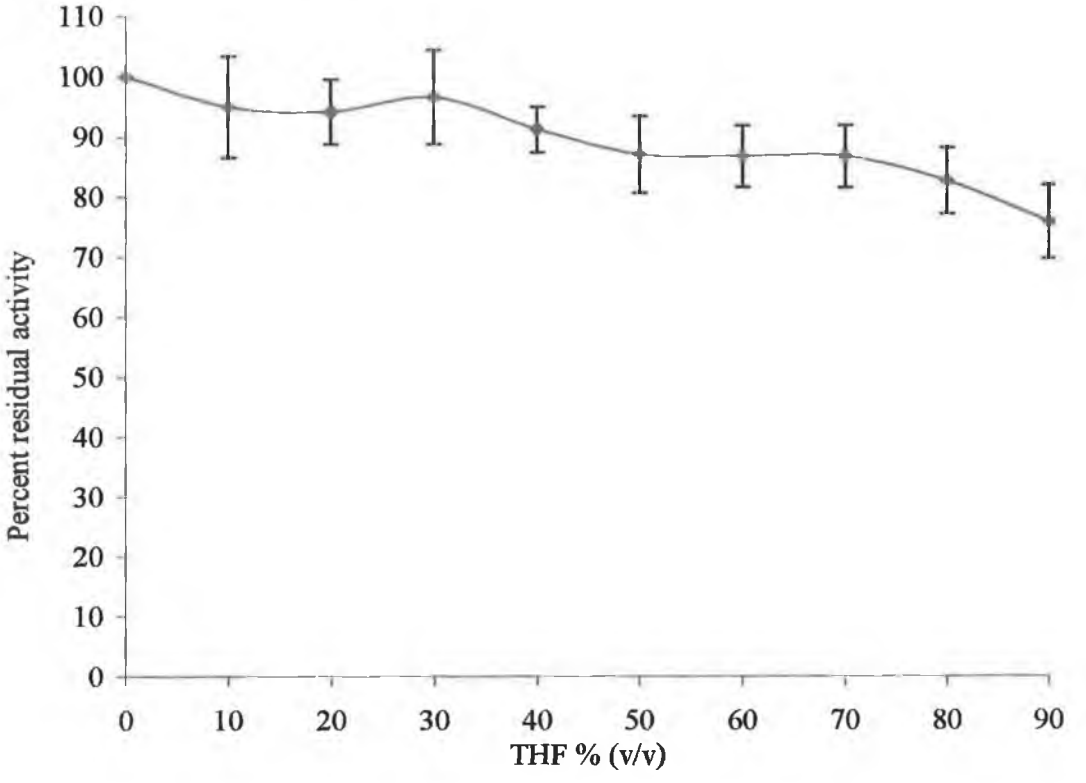

Figure 3.12: Activity of Quest International soybean peroxidase from, at 50 µg/L in 25 mM MOPS pH 7.0, in increasing concentrations of THF. The enzyme was exposed to the solvent for 60 minutes, at 25°C. Residual activities were then measured by the TMB assay.

It can be seen in Figure 3.13 that SBP activity is reduced to approximately 10% above 70% (v/v) DMSO. This can be partially explained by induced unfolding of the native enzyme. The enzyme assumes the most favourable thermodynamical conformation; this conformation however does not allow the normal catalytic cycle to occur (Klibanov, 1986).

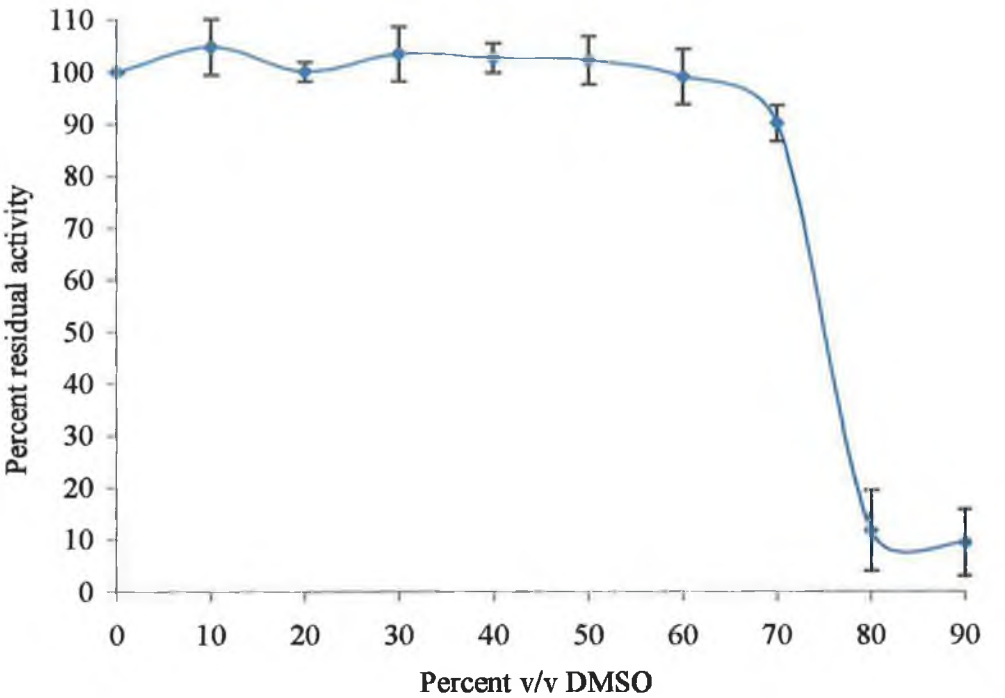

Figure 3.13: Activity of Quest International soybean peroxidase at 50 µg/L in 25 mM MOPS pH 7.0, in increasing concentrations of DMSO. The enzyme was exposed to the solvent for 60 minutes, at 25°C, before residual activities were measured by the TMB assay.

Methanol (Figure 3.14) shows an apparent increase in activity at 50% v/v, when observing the standard error bars. This may be explained by the enzyme becoming unfolded so that the substrate can enter the access channel easier and react with the active site of the SBP. Above 50% (v/v), SBP activity is seen to decrease to 60% of aqueous activity at 90% (v/v) MeOH.

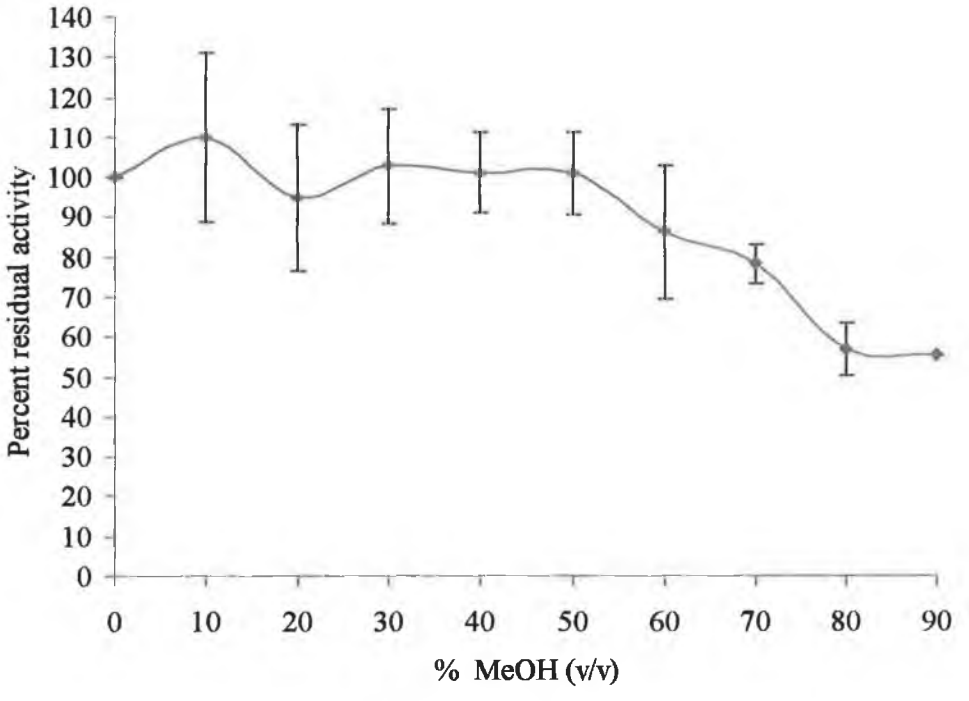

Figure 3.14: Activity of Quest International soybean peroxidase at 50 μg/L in 25 mM MOPS pH 7.0, in increasing concentrations of methanol. The enzyme was exposed to the solvent for 60 minutes, at 25°C. Residual activities were then measured by the TMB assay.

Following activity assay of SBP in these solvents, kinetic analysis (Section 2.21) was carried out using the ABTS assay (Section 2.13). Michaelis-Menten graphs were plotted, with insets of the Lineweaver-Burk transformation. SBP (1mg/L) was exposed to the solvents for 60 minutes, then diluted to assay concentration 50μg/L and assayed using the ABTS assay. The H_2O_2 concentration was from 0 – 10mM.

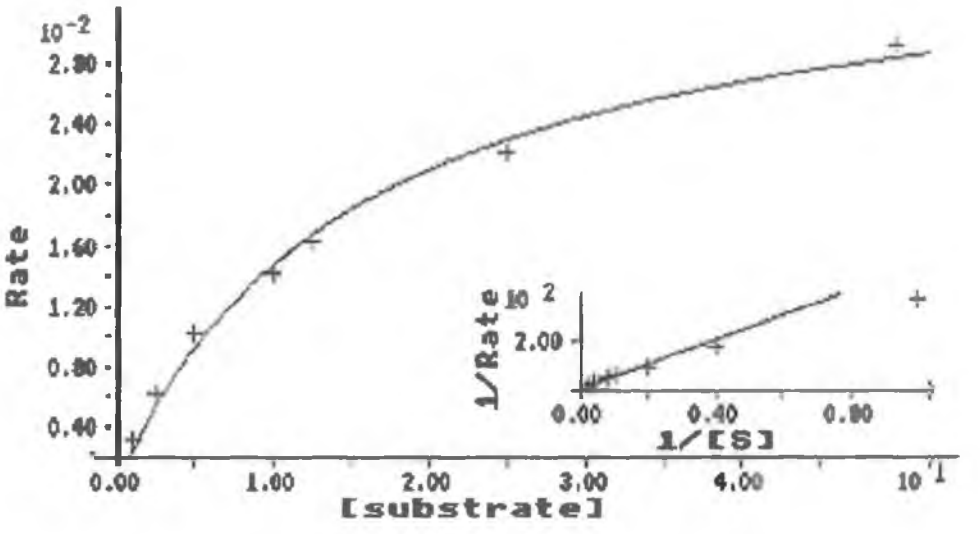

Figure 3.15: Steady-state kinetic analysis of SBP in 25 mM MOPS pH 7.0 with ABTS. Plots were drawn using the software package Enzfitter®. The rate (ΔA_{405}/min) is the change in absorbance at 405 nm over the time of the assay.

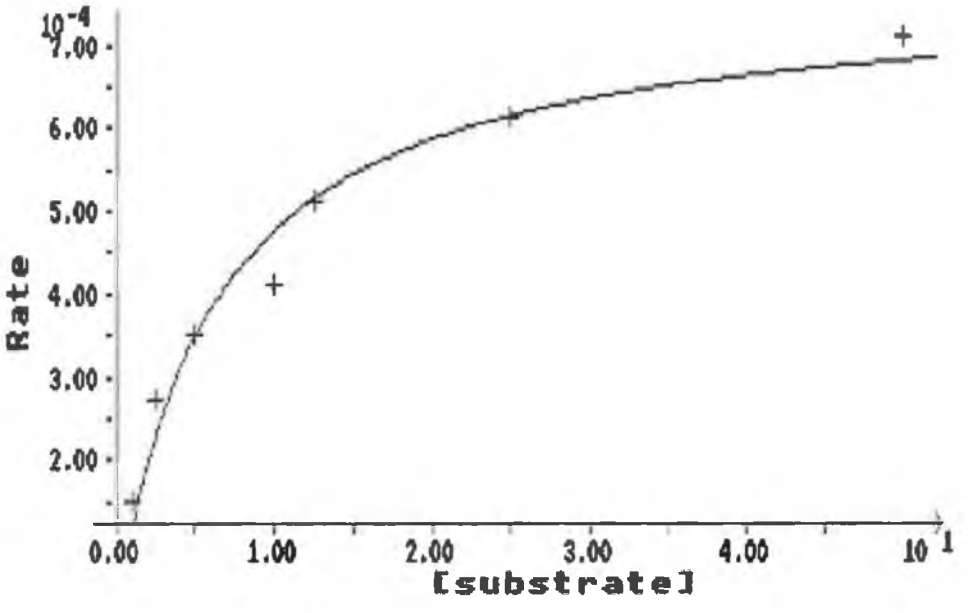

Figure 3.16: Steady-state kinetic analysis of SBP in the presence of 90% v/v DMSO with ABTS. Plots were drawn using the software package Enzfitter®. The rate (ΔA_{405}/min) is the change in absorbance at 405 nm over the time of the assay.

3.7: SBP purification:

The food grade SBP was further purified as outlined by Nissum *et al.* (2001). SBP was passed through two anion-exchange columns utilising two gradient buffer systems, as detailed in Section 2.20. Figure 3.17 shows SBP eluting from the first column utilising a linear gradient (50-500mM NaCl in 10mM bis-Tris-Cl buffer, pH 6.0). A protein peak with low SBP activity elutes first over fractions 2-15 (TMB assay, Section 2.7). Fractions 31-49 also had a notable protein concentration but only 4 fractions had peroxidase activity (Fractions 44-47). These four fractions eluted at approximately 475mM NaCl, were pooled and an aliquot removed for analysis (Section 2.13). The peroxidase active fractions were then applied to the second column (Figure 3.18). The RZ or purity number (Section 2.5) of the crude and purified preparations of SBP were assayed to determine if the value had increased. The RZ (A_{403}/A_{280}) for crude SBP was calculated to be 2.2, the RZ from the 1st Column (Q-Sepharose, pH 6.0) was found to be 2.5 and the RZ value for the final purification column (Q-Sepharose, pH 4.7) was calculated to be 2.8.

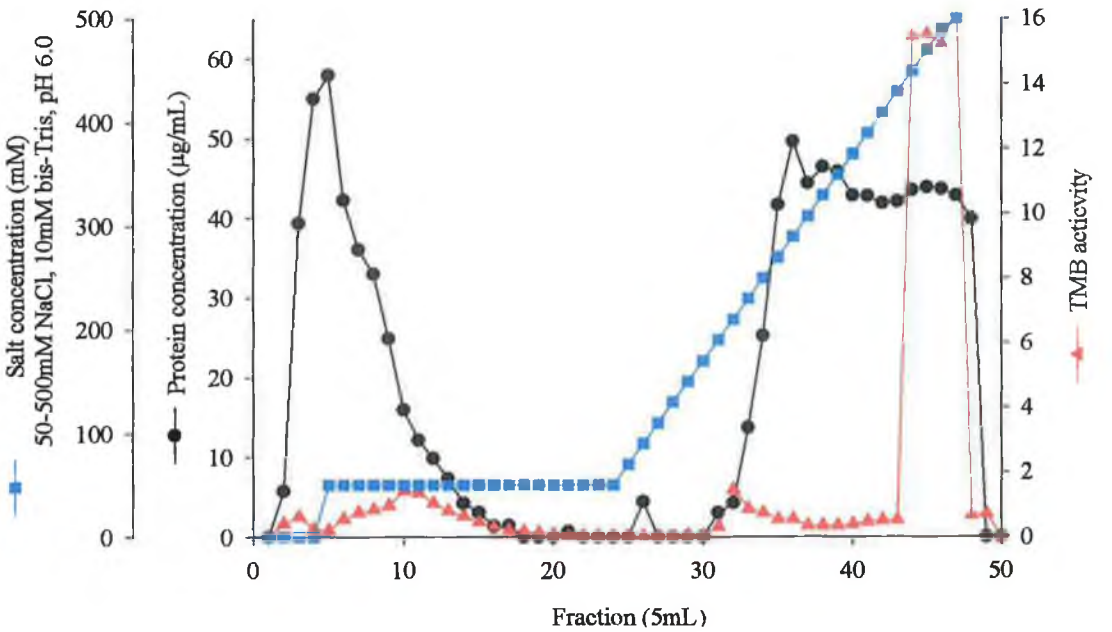

Figure 3.17: SBP eluted from Q-Sepharose column, (50-500 mM NaCl gradient in 10 mM bis-Tris-Cl buffer, pH 6.0). Fractions showing peroxidase activity were pooled and applied to the second column. —●— Protein concentration as determined by the BCA method, —■— salt gradient (50-500 mM NaCl in 10 mM Bis-Tris, pH 6.0), —▲— catalytic activity (TMB assay).

Figure 3.18 shows the SBP sample (from the bis-Tris column) eluting from the second, sodium acetate column in a linear salt gradient (0-500 mM NaCl in 100mM sodium acetate buffer, pH 4.7). Protein elutes first over fractions 2-13; these showed no peroxidase activity. Fractions 31-49 had increased protein concentration but, again only 4 fractions had peroxidase activity (Fractions 42-45). These latter fractions were pooled and an aliquot removed for kinetic analysis (Section 2.13). The peroxidase-active fractions eluted from the column at approximately 380 mM NaCl. The peroxidase active pooled fractions were assayed and, with the results from Figure 3.17, a purification table was constructed (Table 3.2).

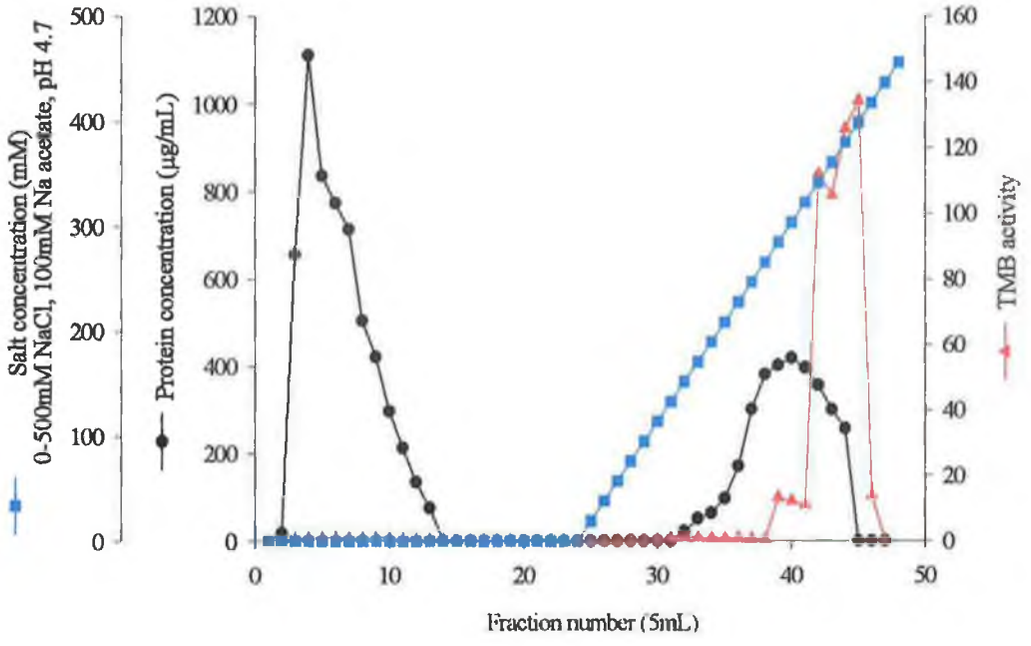

Figure 3.18: SBP eluted from Q-Sepharose column, (0-500 mM NaCl gradient in 10 mM sodium acetate buffer, pH 4.7). Fractions showing peroxidase activity were pooled and applied to the second column. —●— Protein concentration (BCA method), —■— Concentration of salt, —▲— catalytic activity (by TMB assay).

Table 3.2: Purification table for Soybean peroxidase (Quest International) as described in Section 2.20.

Purification step	Volume (mL)	Total activity, (μmol/min/mL) *	Total protein (μg/mL) ®	Specific activity nmol/min/μg *	Purification factor	Percent recovery (%)
Crude Enzyme	20	4.70	2342	0.002	1	100.0
Q-Sepharose, pH 6.0[1]	20	11.40	478	0.024	12	242.6
Q-Sepharose, pH 4.7[2]	20	7.35	63	8.57	428	156.4

* Here Activities were determined by the ABTS assay.
® Protein concentrations were determined by the BCA assay.
1. 50 mM NaCl, 10 mM Bis-Tris pH 6.0
2. 50 mM NaCl, in 10 mM sodium acetate, pH 4.7

3.9: Discussion:

HRP is the peroxidase traditionally studied in enzymology, in industry and in the biosensor fields. However, in recent years, another class III peroxidase, SBP has been found to have improved thermostability, sensitivity, tolerance to pH and solvents compared with HRP (M^{c}Eldoon and Dordick, 1996;Schmitz *et al.* 1997; Gaspar *et al.* 2001 and Amisha Kamal and Behere, 2003).

It was from consideration of these favourable properties that SBP was investigated with regard to developing a biosensor for the detection of hydrogen peroxide in solution. The enzyme preparation obtained for this work was of food grade quality from Quest International. Before any work for the biosensor could be done, a general investigation of the SBP had to be carried out.

The TMB assay has been reported as an ideal assay to determine the activity of peroxidase enzymes (Ryan *et al.* 1994b). As SBP was a new peroxidase to the host laboratories, the time of assay and suitable concentrations of the enzyme and substrate (H_2O_2) needed to be calculated. The optimum time for analysis was determined by allowing the assay to proceed over time and observing the linear extent of the product-time plot. The optimum time was estimated to be 2 minutes 30 seconds. The concentration of SBP was found to give a linear formation of product over a wide range from 25-1000μg/L SBP (time: 2 minutes 30 seconds). The optimum concentration for H_2O_2 (30% v/v) was determined to be 0.04% v/v final concentration. These compare well to Ryan *et al.* (1994b) values for HRP, where 2 minutes is the optimum time of assay, and 0.003% is the optimum concentration of H_2O_2.

M^{c}Eldoon and Dordick (1996) described the unusually high thermal stability of SBP. In this work, the thermal profile of SBP gave a T_{50} of 73-75°C as compared to 65°C for HRP under similar conditions. A thermal inactivation of native SBP at 75°C indicated from Enzfitter analysis (Figure 3.10) a half-life of 14 minutes 30 seconds

SBP is catalytically active after removal from the solvent and assay by the TMB assay (Section 2.7) with respect to all the solvents tested (ACN, THF, MeOH, and DMSO) up to 50%. ACN, THF, MeOH show a gradual decrease in activity at concentrations higher than 60%. DMSO is the only solvent investigated that gave drastic changes in activity at high solvent concentrations. Above 70% the activity falls significantly to 10 ± 6%. Santucci *et al.* (2002) saw a similar trend (Table 3.1) with respect to kinetic activity with HRP. It is thought that DMSO causes unfolding of the tertiary enzyme structure, leading to the loss of the haem group from the active site (Santucci *et al.* 2002). DMSO is used in the TMB reaction (Section 2.7), but its concentration there is well below the concentration of inactivation.

The food grade SBP was purified according to the method outlined by Nissum *et al.* (2001). The RZ values were determined and there was an increase from the crude to the purified enzyme of 2.2 to 2.8 (Table 3.2). After passing through the anion exchange column, pH 6.0 there is an increase in the activity of SBP, and this has been attributed to the removal of inhibitory substances. The total protein decreased in the two columns and the specific activity was seen to increase, which resulted in a purification factor of 428.5 being recorded and a recovery of 156%.

A denaturing SDS gel (12.5%) showed a protein band above the 41KDa molecular weight marker identifying the purified SBP protein as having a molecular weight slightly above 41KDa. This is within the weight that Henriksen *et al.* (2001) state for the native form of SBP (44KDa). The crude preparation of SBP had many bands illustrating the heterogeneous makeup of the preparation. Gels were of poor quality and are not shown. The ferrocene-modified preparation of SBP shows a faint band higher than the purified native SBP. This is in agreement with the addition of the modifying groups ferrocene carboxylic acid. An IEF gel showed many bands in the crude SBP sample, again showing the heterogeneous nature of the preparation. The purified SBP sample shows a band just above *pI* 4.2. This agrees with the recorded *pI* value for SBP of 4.3 (Henriksen *et al.* 2001).

With this understanding, the SBP preparation can be used in electrochemical sensor configuration for H_2O_2 detection. The development of such systems is described in Chapters 4, 5 and 6 of this thesis. In this Chapter the food grade SBP from Quest has been extensively characterised in terms of its physical stability and kinetic properties. A purified SBP sample was obtained by published chromatographic techniques (Nissum *et al.* 2001) as shown by electrophoretic analysis. Further work is planned on the purified enzyme. No chemical modifications have been carried out to date on the purified SBP for use in biosensors. For the development of a sensor, a crude SBP preparation was used to show that it was possible to construct a sensitive working biosensor from unprocessed commercial materials. Purification steps would add to the cost of any such prototype biosensor.

CHAPTER 4

Electrochemistry of native SBP with the mediator $[Os(bpy)_2(PVP)_{10}]^+$

4.1: Plotting convention in this study:

Shown in Figure 4.1 is the convention for plotting current-potential curves that is used in this report. Cathodic currents related to reduction are plotted in an upward direction and anodic currents related to oxidation are plotted in a downward direction.

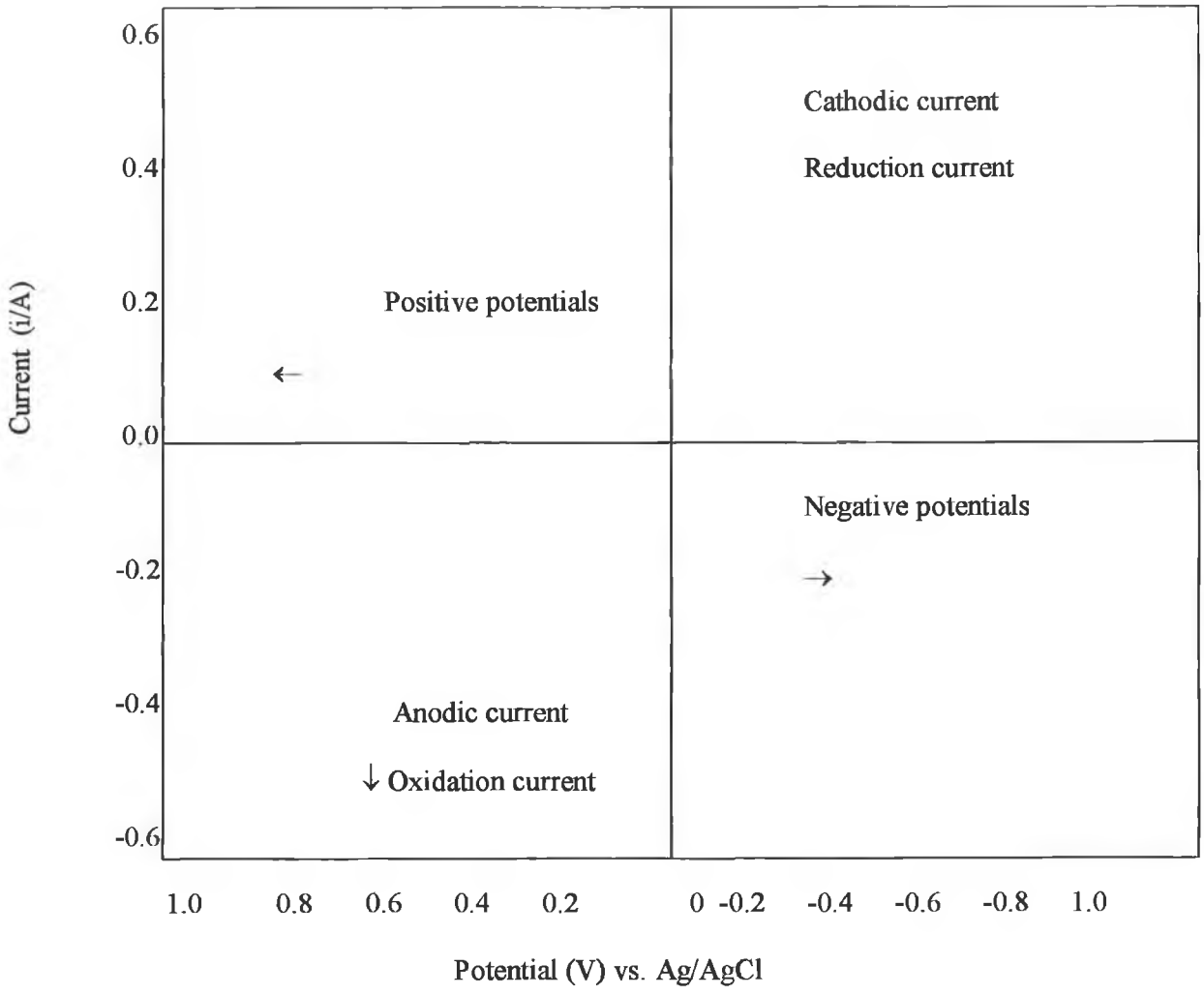

Figure 4.1: The convention used in this report for the plotting of current-potential curves (cyclic voltammograms) (Lambrechts and Sansen, 1996).

4.2: Schematic of an electrode:

Figure 4.2 depicts the structure of the microelectrode used to fabricate SBP-based biosensors.

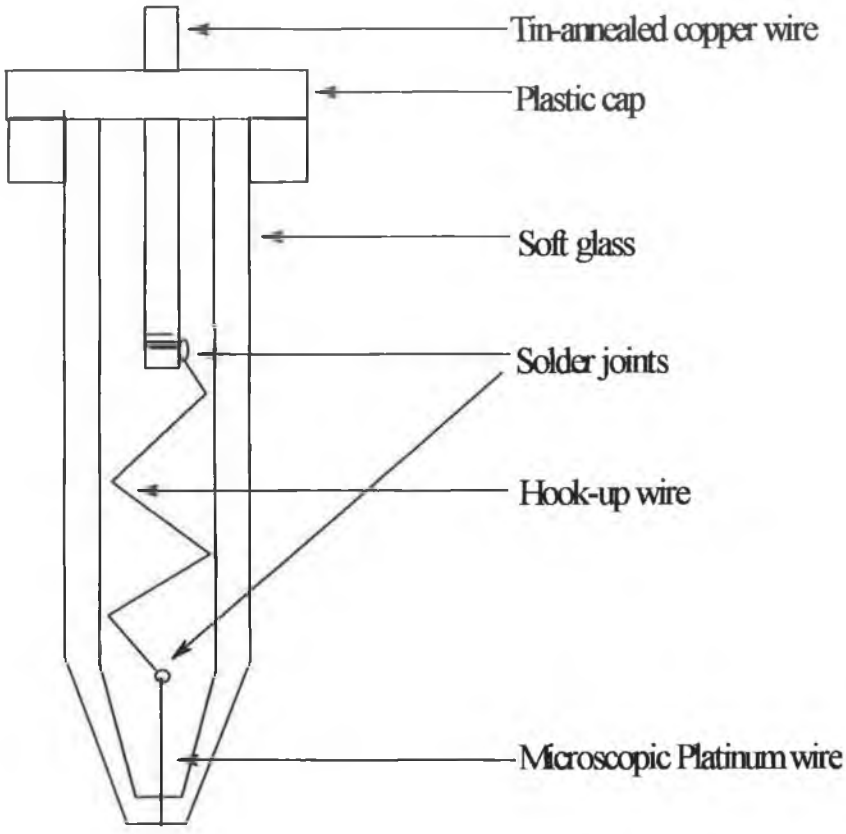

Figure 4.2: Schematic cross-section of a platinum microelectrode.

4.3: Characterisation of a platinum microelectrode in H_2SO_4:

When a triangular potential wave is applied to the Pt electrode in a 1.0M H_2SO_4 solution, several peaks are observed (Kissinger and Heineman, 1983). These peaks are associated with the generation of hydrogen and oxygen. The peak at approximately – 0.9 V corresponds to the reduction of adsorbed hydrogen, the peak at approximately – 0.6 V corresponds to the oxidation of the hydrogen layers, the peak

at approximately + 0.8 V corresponds to the formation of adsorbed oxygen and platinum oxide layers, and the peak at – 0.3 V approximately corresponds to the reduction of the oxide layer versus a Ag/AgCl reference electrode (Lambrechts and Sansen, 1996).

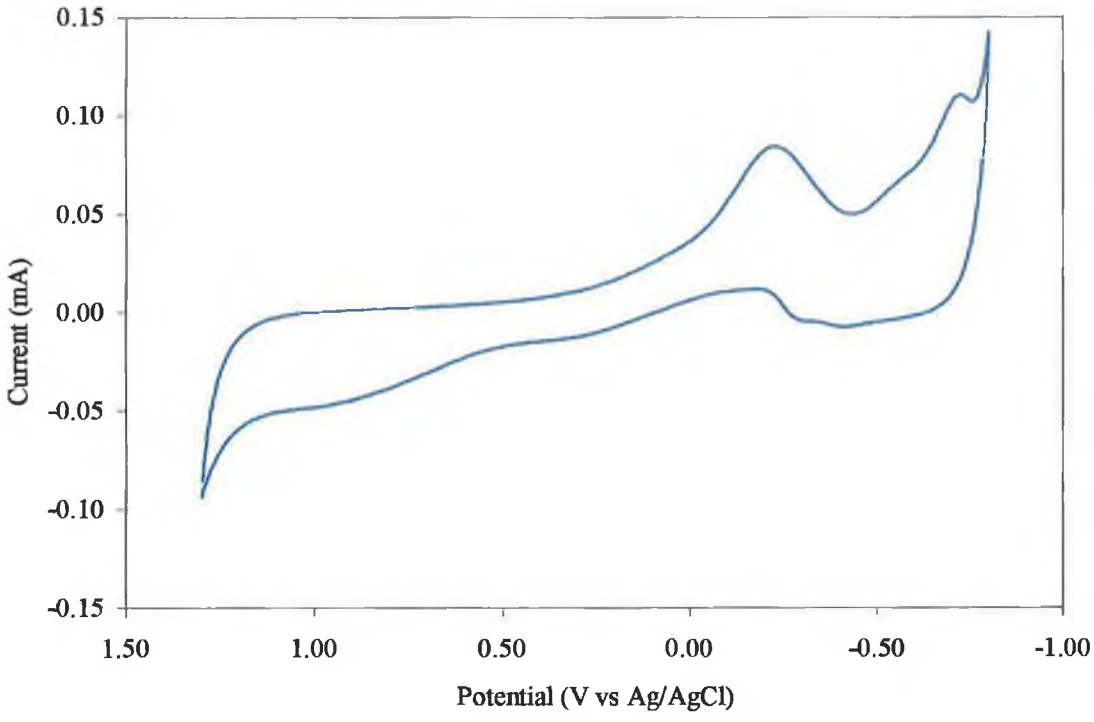

Figure 4.3 Cyclic voltammogram of a Platinum microelectrode (25 μm radius) in 1.0 M H_2SO_4. The scan rate was 0.2 V/s.

The size and roughness of the electrode are determined, this is performed to characterise the electrode. From Figure 4.3, the area under the reduction of the oxide layer peak is calculated using the CHI software. From these calculations, the roughness of the electrode is estimated.

Table 4.1: Surface roughness of the fabricated 25 μm radius platinum microelectrode. For a definition of the terms, and an explanation of the calculations, please refer to the materials and methods section (Section 2.34).

Microelectrode	Radius (μm diameter)	Geometric surface area (cm^2)	Actual surface area (cm^2)	Surface roughness
Platinum	25	4.9×10^{-6}	9.6×10^{-6}	1.9

4.4: Cyclic voltammetry of a bare platinum microelectrode:

The electrode was placed in a deoxygenated buffer solution and cycled over a potential range. The potential range scanned was + 0.1 to + 0.9 V, at a rate of 0.2 V/s. The resulting CV was recorded and is seen in Figure 4.4. No reduction or oxidation events occur over the potential range. This is representative of a clean electrode, and was used to determine if a given electrode had been polished sufficiently and to ensure there was no interference between the buffer (25 mM MOPS/NaOH, pH 7.0) and the electrode surface during the CV cycle.

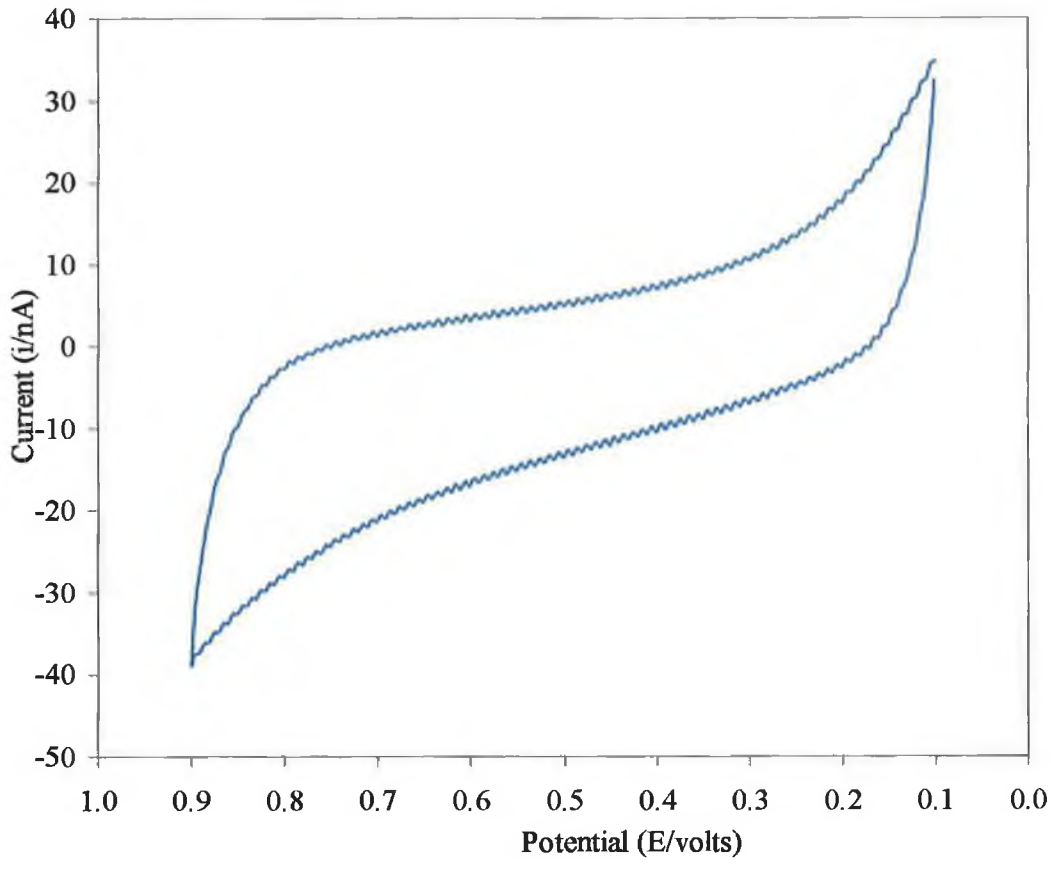

Figure 4.4: A cyclic voltammogram showing the electrochemical response of a 25 μm Pt microelectrode in 25 mM MOPS/NaOH buffer pH 7.0. The scan rate was 0.2 V/s.

4.5: Direct electrooxidation of hydrogen peroxide at a platinum microelectrode:

At high potentials greater than + 0.80V the direct electrooxidation of H_2O_2 can occur. Given that this work is focused on mediated electron transfer the potential range should be restricted to values less positive than that required for direct H_2O_2 oxidation. For some glucose biosensors using GOx, the generation of H_2O_2 is measured and the concentration of glucose is determined indirectly. However, there

are many biological matrices that can cause interference (ascorbic acid is electrochemically reactive; protein absorption; can physically foul the surface of the electrode). These substances are also electroactive at the potential of direct H_2O_2 electrooxidation (+ 0.9 V) at a platinum microelectrode. In numerous cases, a mediator is used, which facilitates electron transfer and the electron reaction can proceed at a value close to the thermodynamic potential.

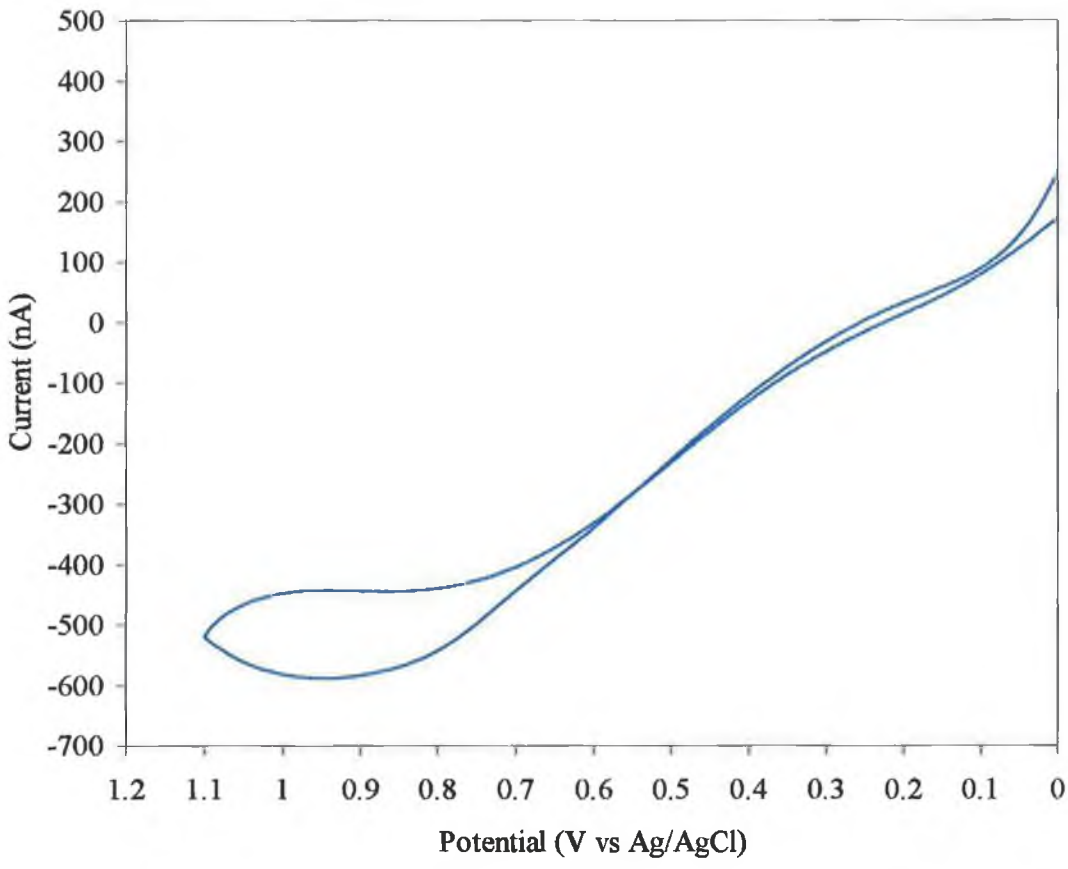

Figure 4.5: Cyclic voltammogram of H_2O_2 at the surface of a Pt microelectrode over the potential range of + 0.9 - 0.1 V. The scan rate was 0.2 V/s, hydrogen peroxide concentration 20 μM.

Initially, to ensure that SBP has been immobilised (Section 2.35) on the electrode surface the electrode was placed in a solution of TMB (Section 2.7). After 3 minutes, the solution had turned blue. This indicated the presence of SBP on the electrode surface.

4.6: Electrochemistry of the Osmium containing mediator:

A CV of the Os containing metallopolymer was run at different scan rates from 0.2 to 5.0 V/s; the resulting scans were recorded and are shown in Figure 4.6. As the scan rate is increased, the oxidation and reduction peak currents increased. The resulting i_{pc} or i_{pa} were plotted against the square root of the scan rate and a straight line was observed (Figure 4.7), indicating that the process operating under semi infinite linear diffusion control. If the system is diffusion controlled and not influenced by adsorption of the electroactive species, the peak current should scale linearly with the square root of the scan rate. This was in fact the case and is illustrated in Figure 4.7.

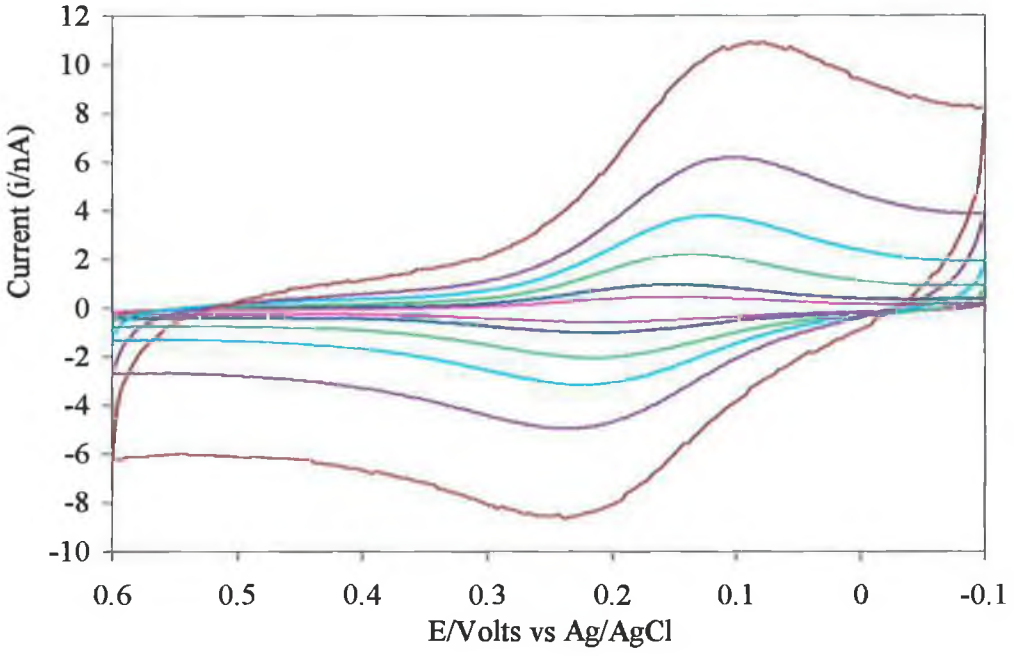

Figure 4.6: Cyclic voltammograms on a 25 μm radius Pt microdisk for the redox electron mediator $[Os(bpy)_2(PVP)_{10}Cl]^+$ in 25 mM MOPS/NaOH buffer pH 7.0. The inner most curve is 0.1 V/s, followed 0.2, 0.5, 1.0, 2.0, and 5.0 V/s respectively.

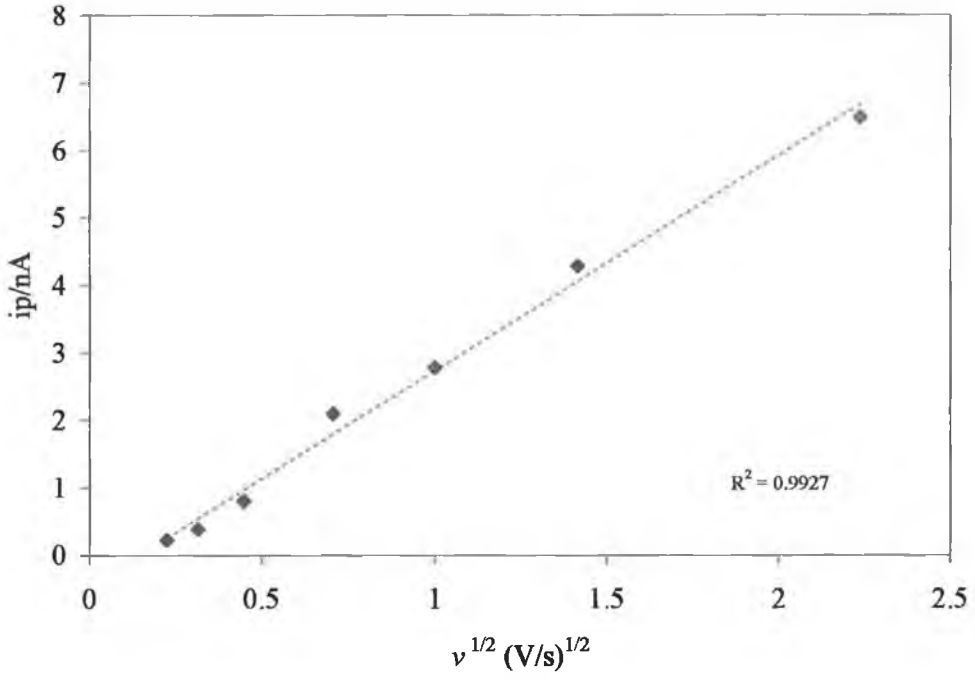

Figure 4.7: Plot of i_{pc} versus $v^{1/2}$ for cyclic voltammograms for the redox electron mediator $[Os(bpy)_2(PVP)_{10}Cl]^+$ in 25 mM MOPS/NaOH buffer pH 7.0. The peak currents were obtained from data in Figure 4.6.

4.7: SBP – Osmium mediator film:

A CV of SBP and the Os containing mediator was run at different scan rates from 0.2 to 5.0V/s. The resulting scans were recorded and are shown in Figure 4.8. As the scan rate was increased, the oxidation and reduction peaks increased in response and, correspondingly, the current also increased. The resulting i_{pc} or i_{pa} were plotted against the square root of the scan rate, giving a straight line, once again indicating that the process is operating under semi infinite linear diffusion.

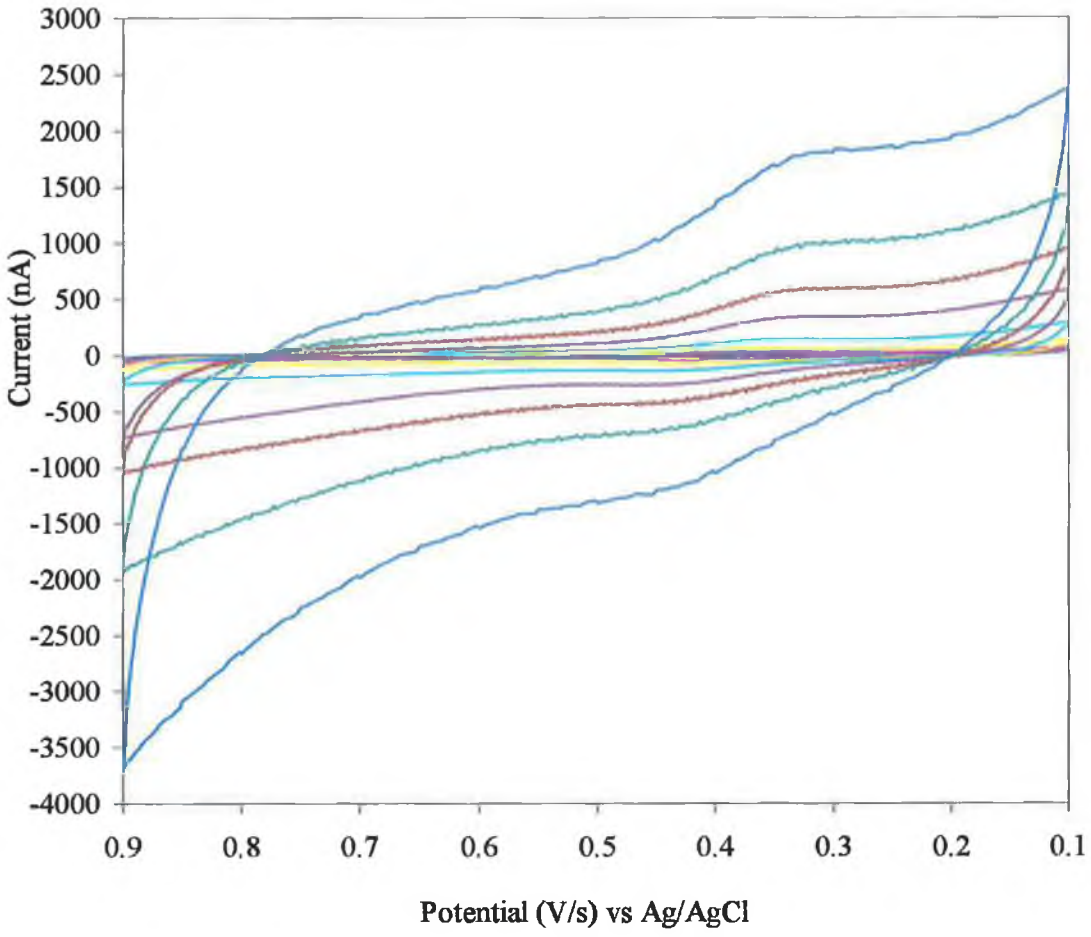

Figure 4.8: Cyclic voltammograms for the redox electron mediator $[Os(bpy)_2(PVP)_{10}Cl]^+$ and soybean peroxidase in 25mM MOPS/NaOH buffer, pH 7.0, showing the scan rate dependence on a 25μm platinum microelectrode. The inner most curve is 0.2V/s, the next 0.5, then 1.0, 2.0, and 5.0V/s respectively.

The peak current scaled linearly against the square root of the scan rate as illustrated in Figure 4.9. The slope of the line can be used to determine the diffusion coefficient for the mediator using the Randles-Sevçik relationship and it was calculated to be $2.49 \times 10^{-5}.cm^2.s^{-1}$.

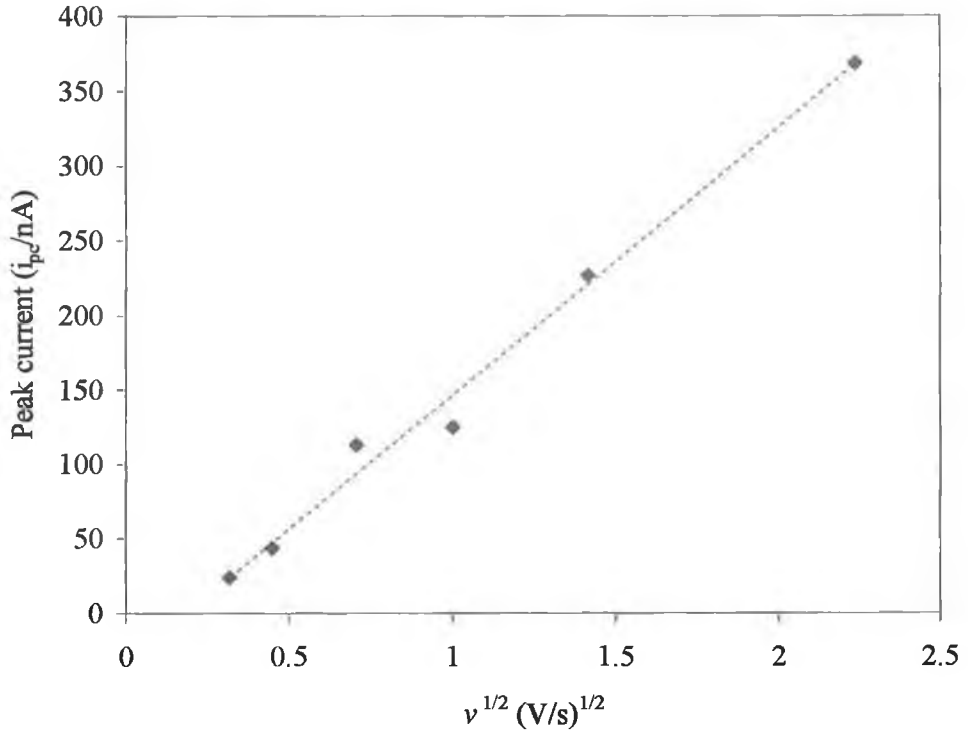

Figure 4.9: The plot of $v^{1/2}$ versus $-i_{pc}$ for reduction of $[Os(bpy)_2(PVP)_{10}Cl]^+$ and SBP in 25mM MOPS/NaOH buffer pH 7.0. The peak heights were obtained from data in Figure 4.8.

4.8: Comparison of electrode coverage by cyclic voltammetry:

Figure 4.10 shows the different CVs from the electrode with no mediator or enzyme adsorbed and with a mixture of enzyme and mediator. This indicates that there is a real difference between the three preparations and that the results recorded arise from the enzyme's being adsorbed to the electrode. The bare electrode gave a small background. The mediator immobilised alone gave a reduction and oxidation peaks, when the enzyme/mediator solution was immobilised onto the electrode surface the redox peaks shifted to more positive potentials than with the mediator alone.

4.9: Comparison of CVs of bare electrode, mediator and mediator-SBP immobilised onto the microelectrode:

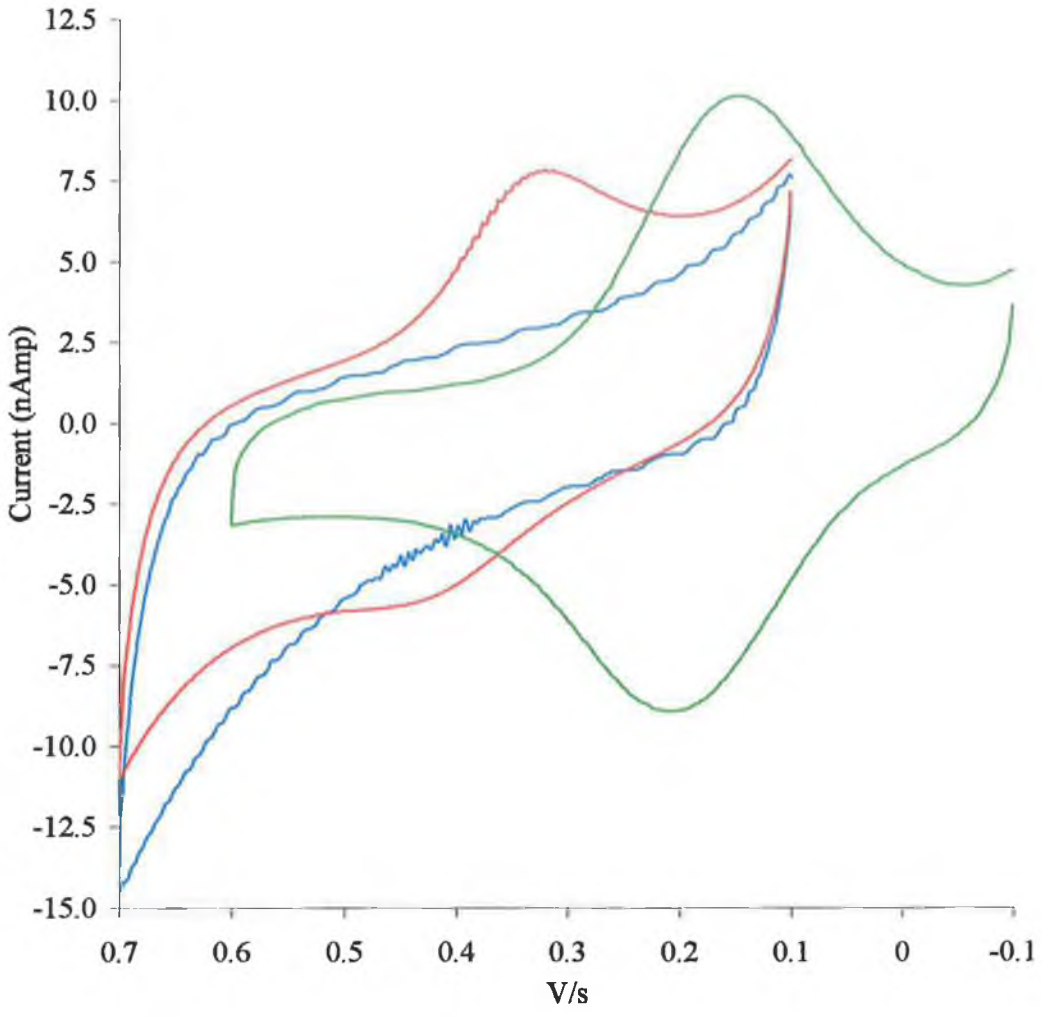

Figure 4.10: A cyclic voltammogram of the bare electrode (—), the enzyme (SBP) and mediator adsorbed onto the electrode surface (—) and the electrode surface with mediator immobilised alone (—).

4.10: Time-current response following the addition of hydrogen peroxide:

Figure 4.11 illustrates a typical steady state response current-time plot (- 0.2 V) of the SBP/mediator biosensor to hydrogen peroxide in 25 mM MOPS at pH 7.0. When an aliquot (20 µL, 5 µmol) of hydrogen peroxide was added into a stirring buffer solution the reduction current rose steeply to reach a stable value.

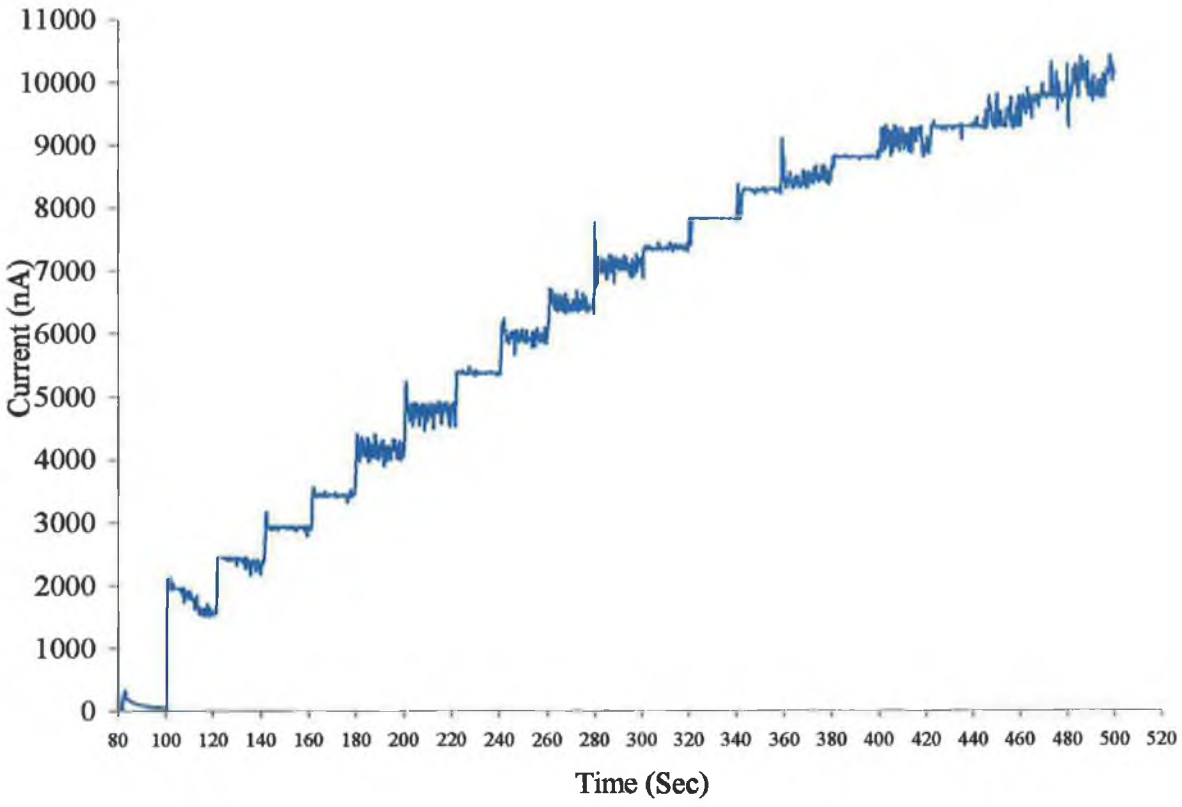

Figure 4.11 Steady-state current amperometric i-t analysis relationship of the SBP enzyme electrode's response to successive additions of hydrogen peroxide in 25 mM MOPS at pH 7.0. Each addition contained 5 µmol H_2O_2, and the potential was at -0.2V.

Figure 4.12 shows graph of the calibration plot for the SBP/mediator biosensor. The linear range of H_2O_2 is from 5 to 60μmol with a correlation coefficient of 0.99. The data for the graph was obtained from Figure 4.11.

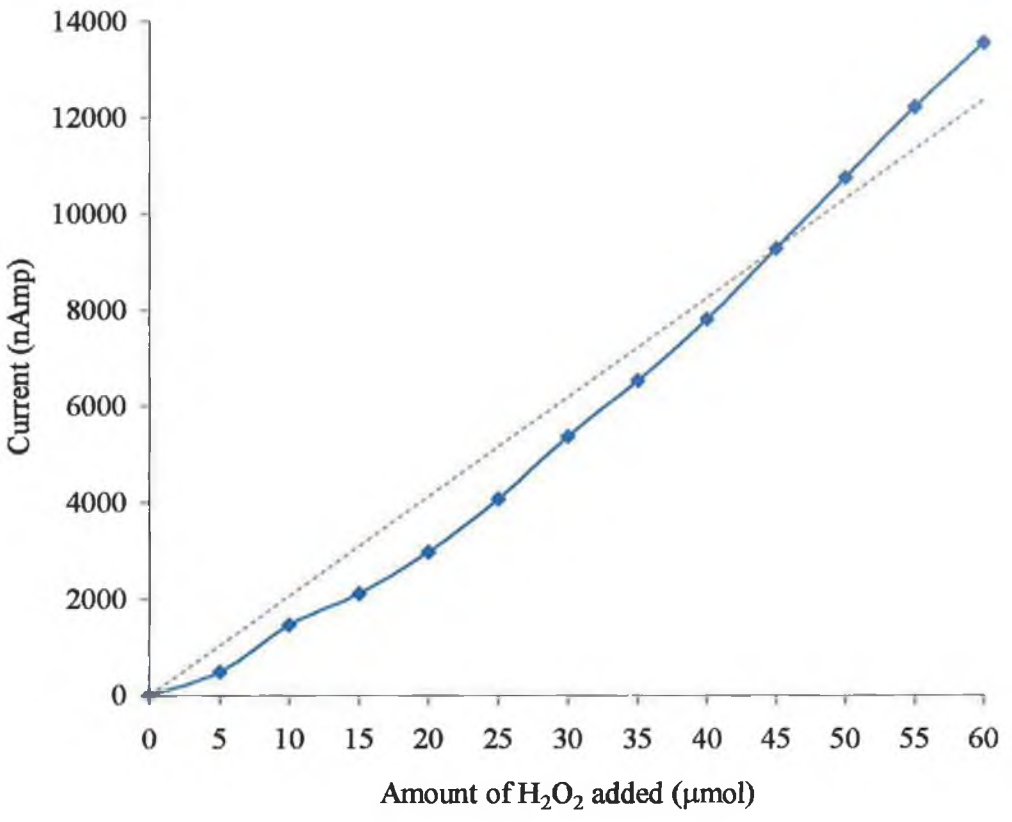

Figure 4.12: Calibration plot of the SBP-based biosensor to hydrogen peroxide.

4.11: Electrochemical Eadie-Hofstee plot:

There are several methods to determine the kinetic parameters of enzyme-catalysed reactions. However, as stated in the Chapter 1, it has been argued that the Eadie-Hofstee plot is the best suited to determining the kinetic properties of biosensors (Kamin and Wilson, 1980). Figure 4.13 replots the data of Figure 4.12. As can be seen, the curve has a roughly sigmoidal shape. The upward curvature has been

attributed to diffusional limitations within the enzyme-mediator film on the surface of the electrode. From the slope of the linear portion ($r^2 = 0.97$) of the graph (illustrated by the black line), the apparent K_m can be determined and this as calculated to be 6.49 x 10^{-3} M for H_2O_2.

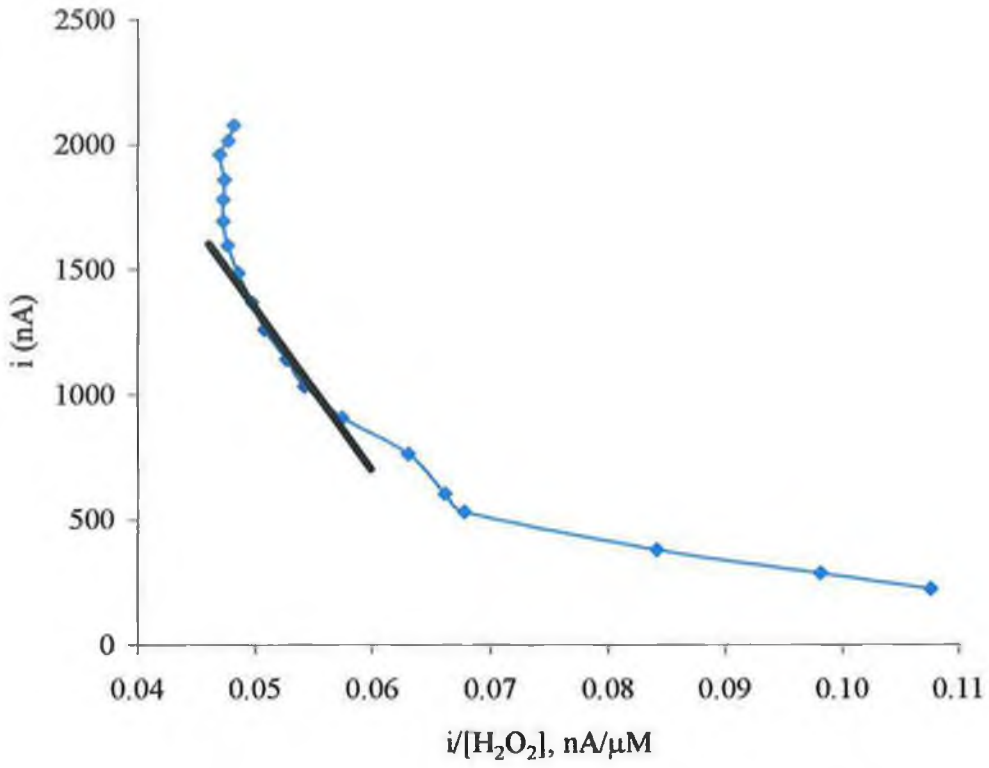

Figure 4.13: The electrochemical Eadie-Hofstee plot for the native SBP/$[Os(bpy)_2(PVP)_{10}Cl]^+$ biosensor. The slope of the linear portion of the curve was used to calculate the apparent K_m of the SBP (indicated by the black line).

4.12: Discussion:

Construction of the platinum microelectrode was detailed in Section 2.32, following which the electrode was extensively characterised. The surface roughness was calculated with the objective of achieving a value of approximately 2 through polishing. A CV (0.2 V/s; Figure 4.4) was performed in 25 mM MOPS, pH 7.0, to confirm that no electrochemical events occur over the potential range of interest, required for the analysis and detection of H_2O_2. A CV over a wide potential range (0.0 – 1.0 V) was performed in 25 mM MOPS, pH 7.0. A 20 μL aliquot of H_2O_2 was pipetted into the solution and a CV was recorded. At 0.95 V an anodic peak was observed. This was ascribed to the direct electrooxidation of H_2O_2 in the electrolyte solution. As a result of this experiment, when preparing for all other electrochemical assays, the upper limit of potential was known.

Following synthesis of the mediator, an aliquot (250 μL) was immobilised onto the surface of the electrode and the sensor placed in 25 mM MOPS, pH 7.0. A CV was carried out at 0.2 V/s to determine if the mediator was electroactive within the potential window that was to be used. Varying the scan rate altered the response of the redox potentials (Figure 4.6). As can be seen the peaks are not symmetrical. The formal potential ($E^{0'}$) of the mediator was determined to be 0.165 V. The peak cathodic currents were recorded and plotted (Figure 4.7) against the square root of the scan rate. A straight line was observed indicating semi-infinite linear diffusion. These assays proved that the Os containing mediator was redox active in the potential range that could be used to quantify the concentration of the important chemical, H_2O_2.

After demonstrating the redox activity of the mediator, a mixture of the mediator and SBP was immobilised onto the electrode surface. As before, a CV was carried out to determine if a redox event was occurring. Again, the redox potentials with varying scan rates are altered (Figure 4.8), but the peaks were not symmetrical. The formal potential ($E^{0'}$) of native SBP was determined to be 0.385 V. The peak cathodic currents were recorded and plotted against the square root of the scan rate (Figure 4.9). A straight line was observed, indicating that a reversible surface redox reaction was solution phase. A difference was observed between the formal potentials of the mediator and the mediator-SBP solution, indicating that the change in potential was caused by the immobilised SBP. There is a large difference (165mV) between the peak potentials of the mediator and the native SBP-mediator biosensor system. This is likely due to the response of the SBP in the mediator-SBP configuration. Figure 4.10 shows the difference in the CVs of the blank, mediator and SBP-mediator biosensor configurations. The blank, as expected, shows no activity.

A current – time response assay was performed (Figure 4.11) to access the response of the electrode to successive additions of H_2O_2. The potential was held at a value more negative than the formal potential. An aliquot (20μL, 5μmol) of H_2O_2 was added to the solution and the current was seen to increase as a consequence. The response time to H_2O_2 was better (approximately two times faster) than that recorded for a SBP biosensor by Wang and Dong (2000); their response time was approximately 50 seconds (from the graph). Comparing the results presented here to these of Wang *et al.* (1999) it can be seen that the present results are approximately 6 times greater in amplitude in response to the additions of H_2O_2, this indicates that the native biosensor results here are more sensitive to H_2O_2. Reports in the literature

(Wang *et al.,* 2001a, and Wang *et al.,* 1999) offer reasons why SBP has a greater sensitivity over HRP sensors. These include SBP's greater stability over a wider range of pH than HRP and the fact that the substrate access channel for SBP is larger allowing for greater movement of electrons from the active site to the surface of the electrode.

The sequential steps in current were linearised into a calibration curve and plotted against the concentration of H_2O_2 added. A straight line was recorded (Figure 4.12) with equation y = 231.45 x – 1052.8. The calibration plot was linear over the assay range of 5 – 60 μmol H_2O_2. SBP papers in the literature have recorded some i-t curves but comparison is difficult because of the biosensor designs employed. Wang *et al.* (1999) used a 4 mm glassy carbon macroelectrode. They immobilised the SBP into a sol-gel mixture. Wang *et al.* (2001b) again used a 4mm glassy carbon macroelectrode this time immobilising the SBP into a copolymer mixture of polyvinyl alcohol and 4-vinylpyridine. Both these reports, however, used macroelectrodes, which allow a greater quantity of enzyme sample to be immobilised onto the electrode surface. This in itself would cause the lifetime of their sensors to be greater than that developed here, the lifetime of which was no greater than 3 days. Due to the poor lifetime of the mediator-SBP biosensor no further investigations of its operational stability have been performed to date.

The calibration points were reconfigured as an electrochemical Eadie-Hofstee (Kamin and Wilson 1980) plot (Figure 4.13). The aim of this was to ascertain the K_m^{app} of the SBP-mediator biosensor and to determine if there were any diffusional limitations on substrate entry into the mediator-SBP layer on the electrode surface. The linear

portion of plot is used to determine the slope, which is equivalent to the - K_m^{app} of the enzyme system. The K_m^{app} was determined to be 6.5 mM for H_2O_2. Again, comparing this value it to the limited number of SBP biosensor papers is difficult because of the lack of published results. Wang *et al.* (2001b) published a K_m^{app} for their system of 12.8 mM, and Wang *et al.* (1999) published a value of 5.12mM. The value reported here for the K_m^{app} falls between these two reported values. The shape of the upper and lower portions of the plot indicate diffusional limitations affecting the entry (and, possibly, the release) of the substrate and the product respectively at the concentrations used (Goldstein, 1976).

CHAPTER 5

Chemical modifications of SBP by Ferrocene carboxylic acid for use in biosensors

5: Investigations into ferrocene carboxylic acid

5.1: Atomic absorption spectroscopy of iron:

The purpose of the following experiments was to covalently attach extra iron moieties (in the form of ferrocene carboxylic acid) to the surface of the enzyme with a view to increasing electron transfer from SBP's active site to the biosensor surface. The incorporation of ferrocene carboxylic acid into native SBP (Section 2.24) was measured by atomic absorption (Section 2.25). A standard curve was constructed using $FeCl_3.6H_2O$ in the range of 2.0 – 0.0625 mg/L (Figure 5.1). The absorbances of native and ferrocene-modified samples were read and their concentrations determined from this curve.

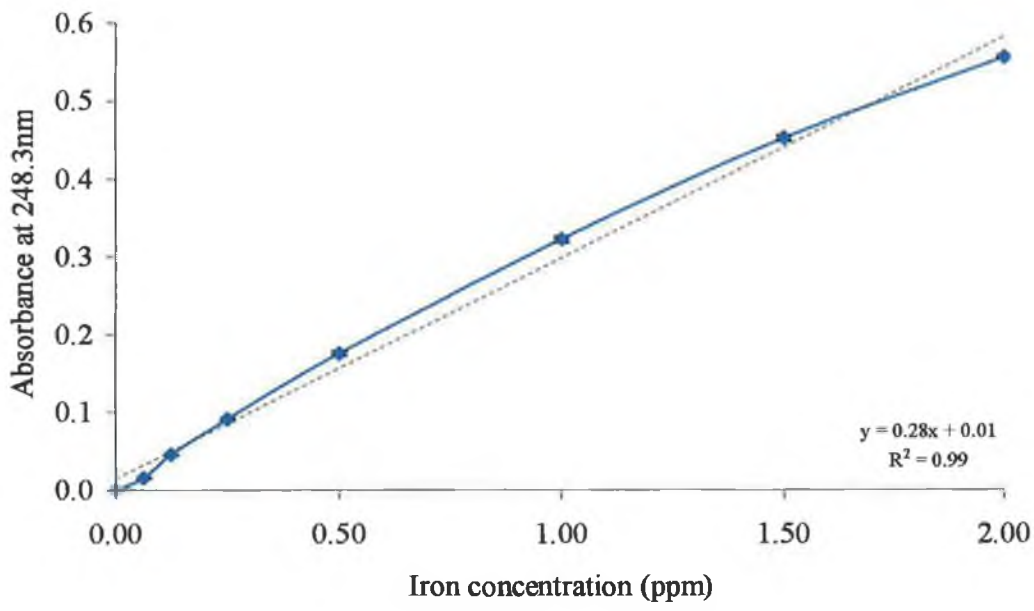

Figure 5.1: Standard curve for the determination of iron by atomic absorption analysis. Standards and samples were determined at 248.3 nm, in an oxy-acetylene flame using $FeCl_3.6H_2O$ as standard.

5.2: Proposed mechanism for the chemical modification of SBP by ferrocene carboxylic acid:

Figure 5. 2 depicts the steps involved in the ferrocene modification described in Section 2.30. After oxidation with $NaIO_4$, the ethylene diamine molecule is attached. It is possible that the second, unreacted free amine of ethylene diamine could bind to a free aldehyde of another oxidised sugar moiety on the same or on another SBP molecule, but ethylene diamine is very short and this is not very unlikely. This would prevent the ferrocene from binding to SBP, as free amine groups would not be available. To reduce the Schiff bases initially formed between the amines and the aldehyde functions of SBP glycans, $NaCNBH_3$ was used to convert the primary amines to secondary amines. The primary amines on the opposite end of the bifunctional ethylenediamine are unaffected by this treatment. The net result is the addition of new free amino groups onto the SBP molecule. The TNBS assay (Section 2.9) showed that there were additional free amines available for covalent attachment of ferrocene groups (Table 5.1). Ferrocene carboxylic acid was then added to the aminated SBP in the presence of EDC and NHS, resulting in the attachment of ferrocene units to the enzyme, as measured using atomic absorption spectroscopy (Section 2.25).

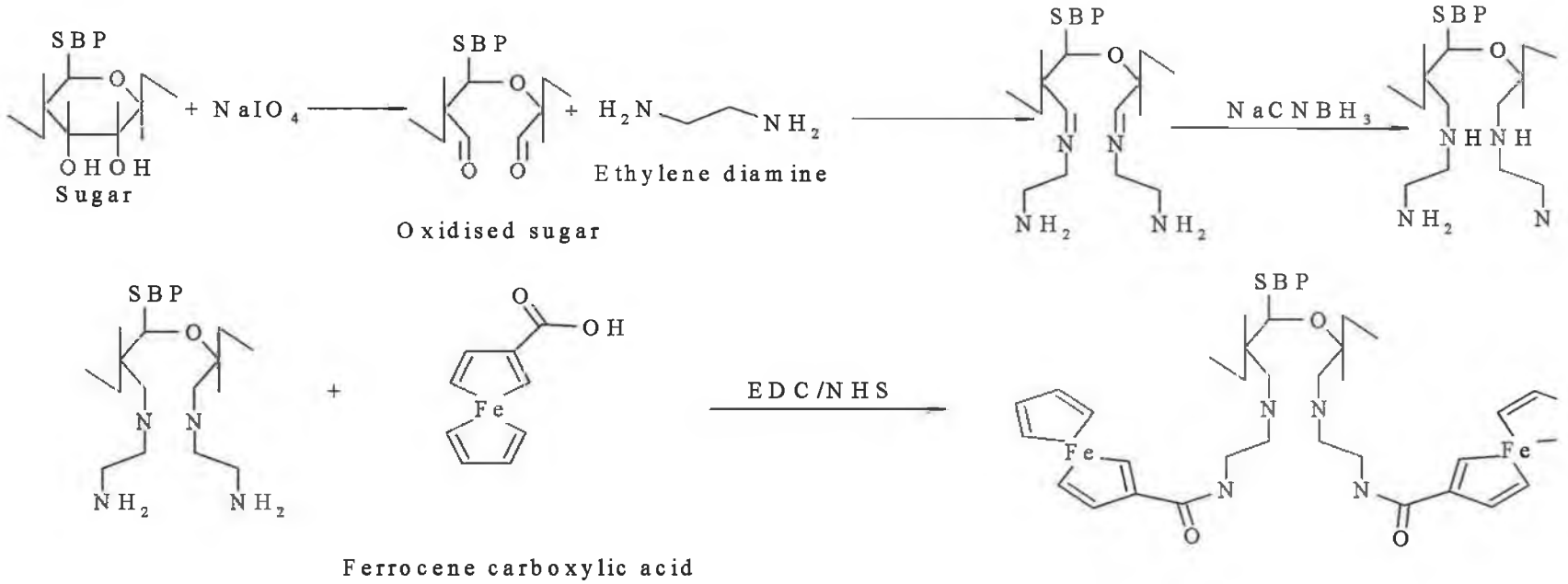

Figure 5.2: Proposed mechanism for the addition of ferrocene carboxylic acid to SBP. The sugars in the SBP glycans are oxidised to produce free aldehyde groups. Next, ethylene diamine is added to the oxidised SBP. $NaCNBH_3$ reduces the Schiff bases (formed between ethylene diamine and SBP) to secondary amines without affecting the primary amine on the opposite end of the bifunctional ethylenediamine. This results in the addition of new free amino groups onto the SBP. Ferrocene carboxylic acid is then added to the aminated SBP in the presence of EDC and NHS, resulting in attachment of ferrocene units to the enzyme.

5.3: Effect of modification:

Table 5.1 shows the results for the three steps involved in the modification of SBP by ferrocene carboxylic acid. The catalytic activity appeared to increase after the first modification even though the protein concentration decreased by approximately 50%. This was put down to the removal of inhibitory substances during the first dialysis step. Following the amination procedure, there was a 10-fold increase in the number of free amines on the SBP molecule. The iron content, as expected, showed no change in concentration at this stage. After the FCA-EDC-NHS modification step, the catalytic activity decreased to 77% of the initial value. The number of free amines also decreased but the iron concentration doubled; this indicated successful modification of SBP by ferrocene carboxylic acid.

Table 5.1: Results of the ferrocene carboxylic acid modification of SBP.

Enzyme	Catalytic activity (%)†	Protein BCA [μg/mL]	# of free amine groups ‡	Iron [ppb] ‡
Native SBP	100	478	3	55
Post amine modification	118	248	35	50
Post FeCOOH modification	77	270	3	127

† determined at 100μg/L protein,
‡ determined at 100μg/mL protein.

5.4: Effect of changing scan rate:

As described previously in Section 4.6, the redox peak currents change with the scan rate (Figure 5.3). Plotting $i_{pa}/_{pc}$ against the square root of the scan rate yields a straight line at scan rates between 0.2 and 5.0V/s, (Figure 5.4) indicating that the electron transport process is under semi-infinite linear diffusion. The formal potential ($E^{0'}$) of the osmium complex was determined as being 325 mV.

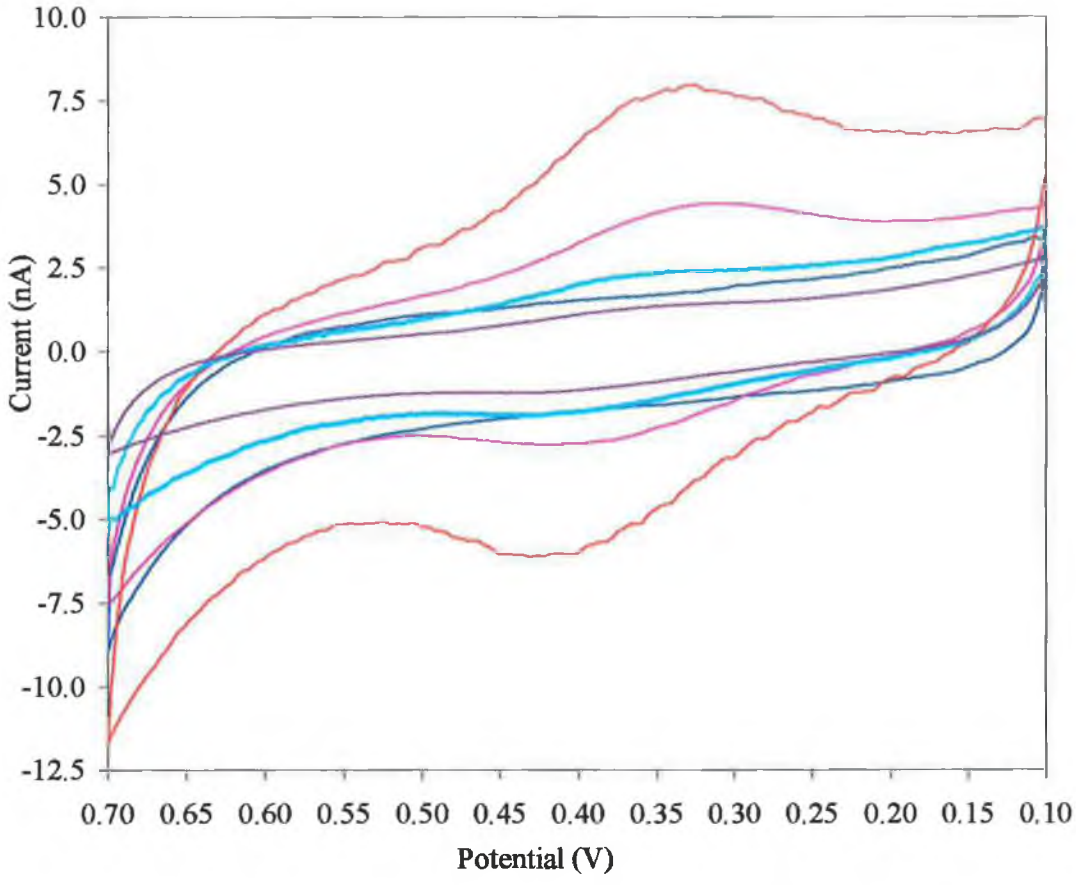

Figure 5.3: Cyclic voltammograms showing the scan rate dependence of $[Os(bpy)_2(PVP)_{10}Cl]^+$ mediator in 25 mM MOPS/NaOH buffer pH 7.0 with the ferrocene-modified soybean peroxidase on a 25 μm platinum microelectrode. The innermost curve is the background the next is at 0.05V/s, then 0.1, 0.2, and 0.5 V/s respectively.

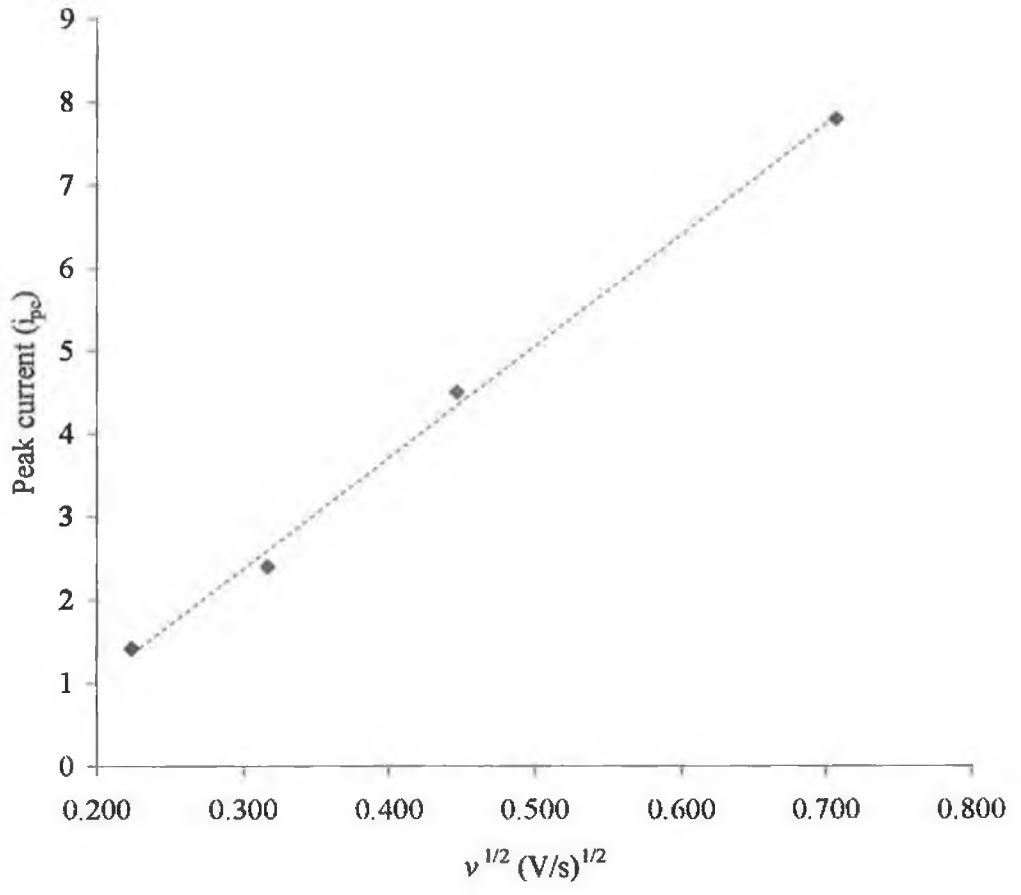

Figure 5.4: Plot of $\nu^{1/2}$ versus $-i_{pc}$ for cyclic voltammograms of $[Os(bpy)_2(PVP)_{10}Cl]^+$ with the ferrocene-modified SBP in 25 mM MOPS/NaOH buffer pH 7.0 on a 25 μm platinum microelectrode. The peak heights were measured from data in Figure 5.3.

5.5: Comparison of mediator and mediator-SBP immobilised onto the microelectrode:

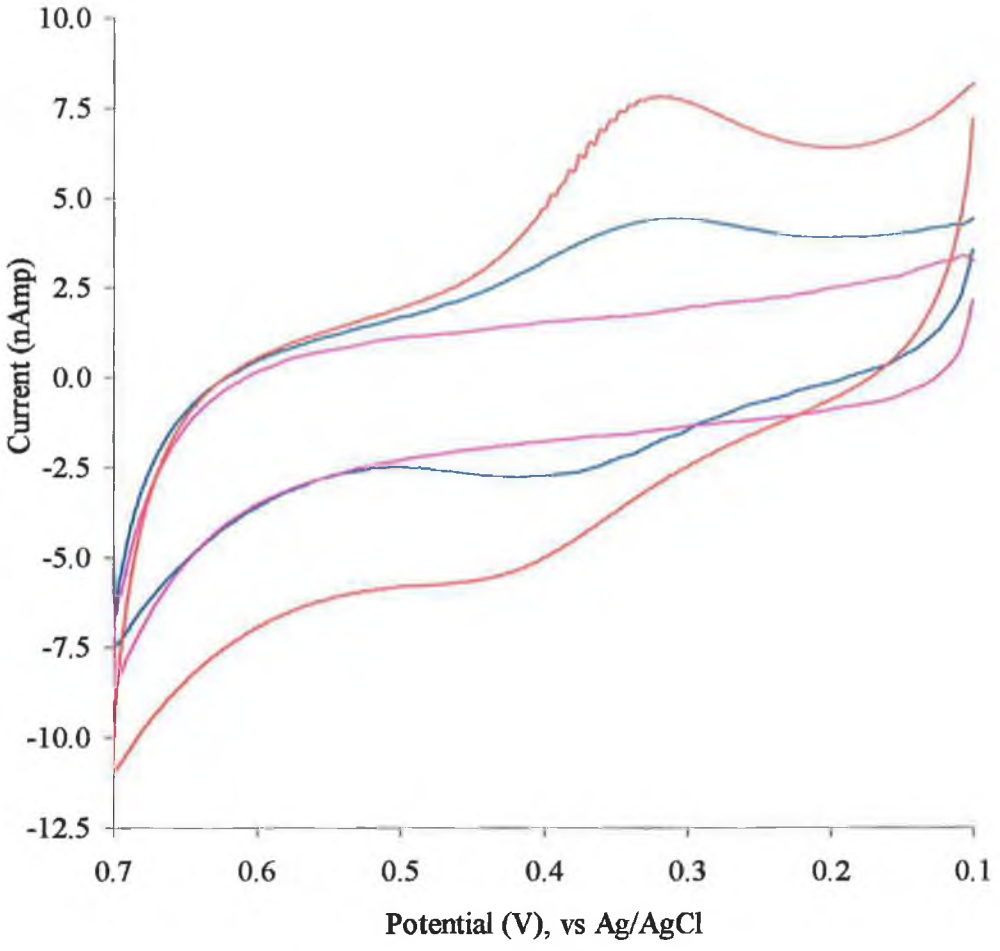

Figure 5.5: Comparison of the response to a potential sweep of a blank, SBP-$[Os(bpy)_2(PVP)_{10}Cl]^+$ mediator and a ferrocene-modified SBP-mediator biosensor. The change in the redox potentials of the SBP-mediator and a ferrocene-modified SBP can be seen. The bare electrode (—), SBP-mediator immobilised electrode (—), ferrocene-modified SBP-mediator electrode (—). The biological buffer the assays were performed in was 25 mM MOPS, pH 7.0.

Figure 5.6 illustrates a typical steady-state response current-time plot of the ferrocene-modified SBP/mediator biosensor to hydrogen peroxide in 25 mM MOPS at pH 7.0. When an aliquot (20 μL, 5 μmol) of hydrogen peroxide was added into the buffer solution the reduction current rose steeply to reach a stable value. As can be seen in Figure 5.5, the ferrocene-modified SBP has a greater response than native SBP, to successive additions of H_2O_2 made at 20-second intervals.

5.6: Current-time response to substrate addition:

Figure 5.6 shows the calibration plot for the ferrocene-modified and unmodified SBP/mediator biosensors. The linear range of H_2O_2 is from 5 to 55 mM with a correlation coefficient of 0.98 for native SBP and a correlation coefficient of 0.99 for ferrocene modified biosensor.

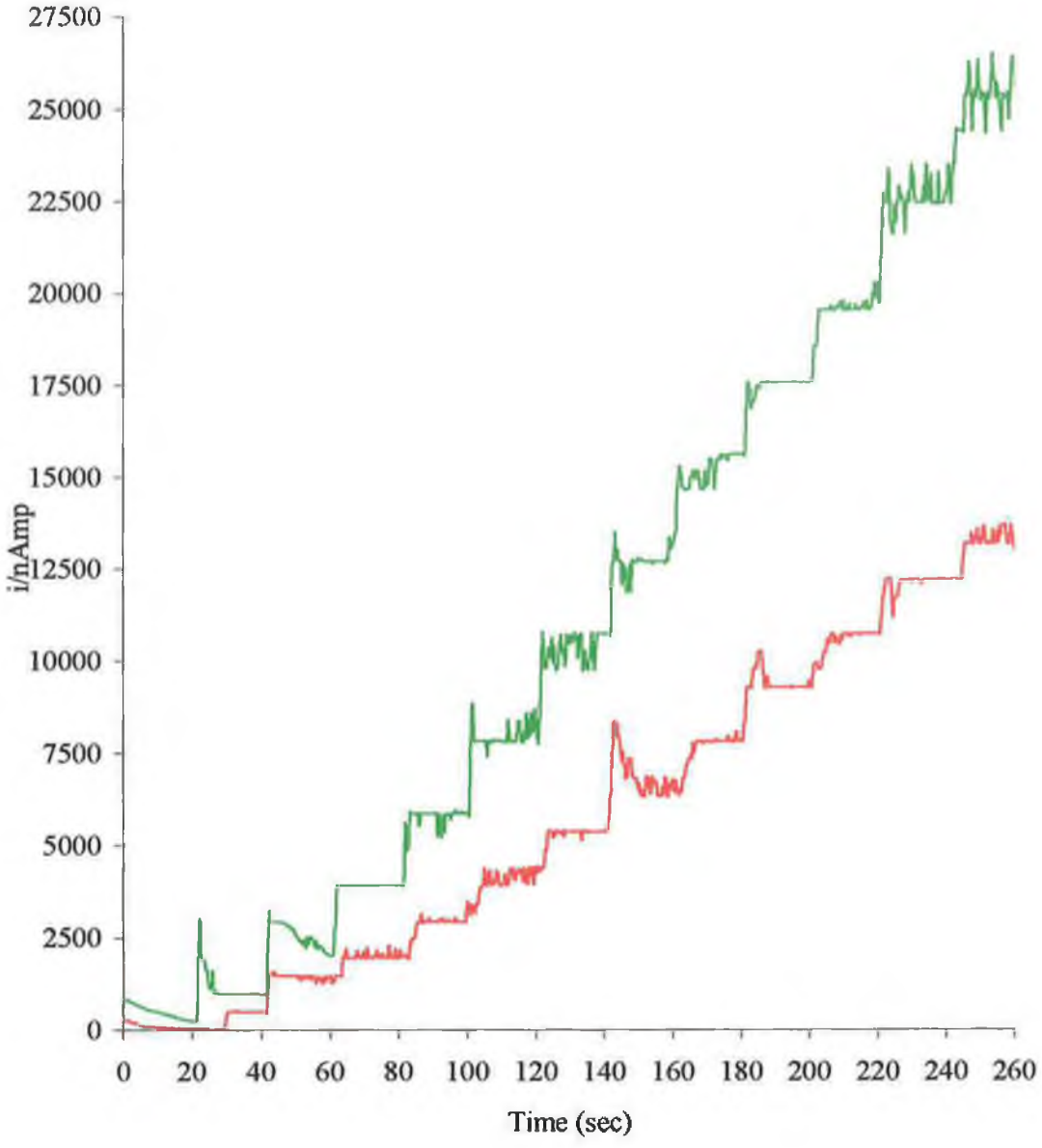

Figure 5.6: Steady-state current amperometric i-t analysis (Current-time relationship) of the SBP enzyme electrode's response to successive additions of hydrogen peroxide at pH 7.0 in MOPS. Native SBP (—), Ferrocene-modified SBP (—).

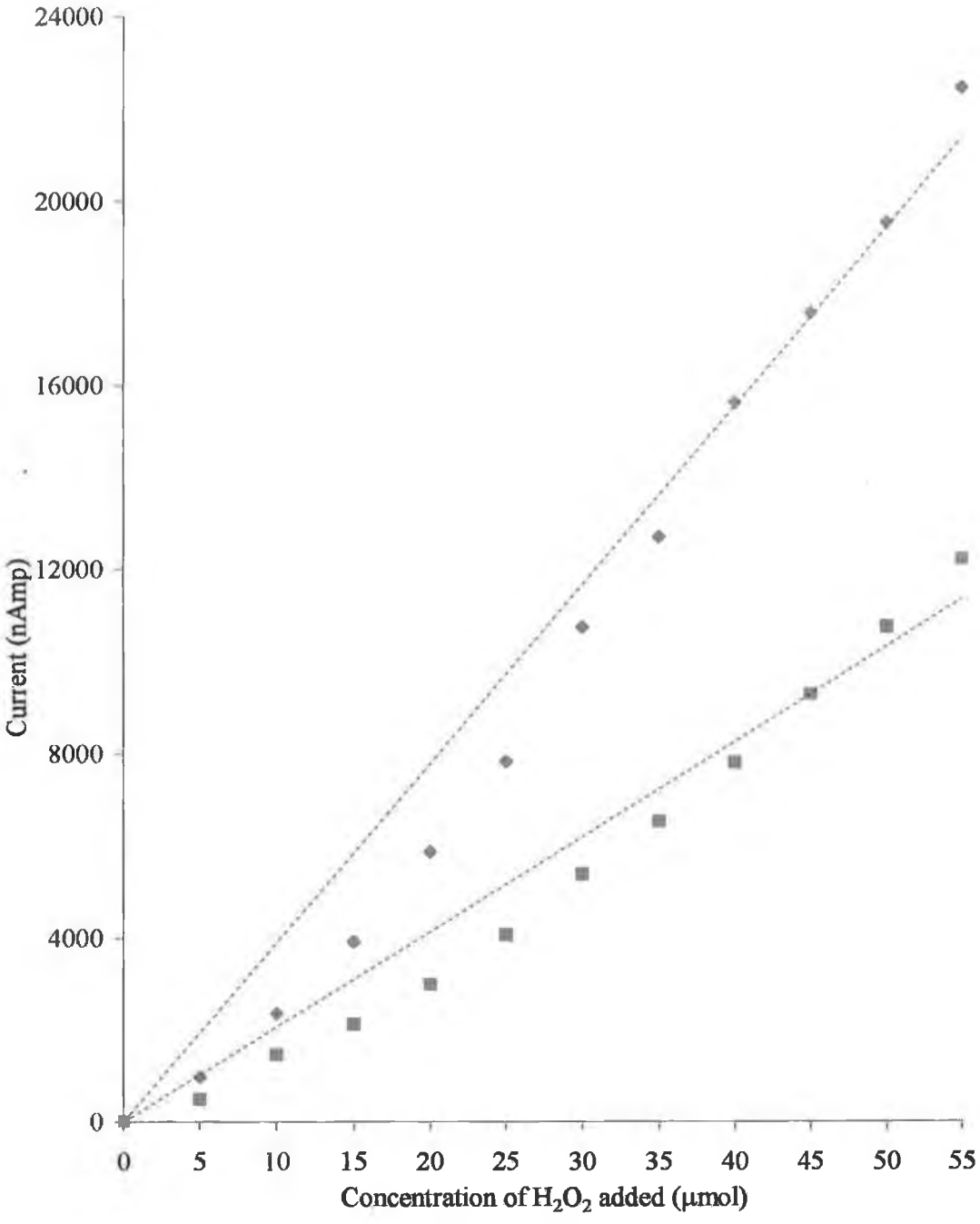

Figure 5.7: Calibration plots for native and ferrocene-modified SBP biosensors. Data points are taken from the heights of the steps in Figure 5.5. Native SBP (■), and Ferrocene modified SBP (♦).

As outlined in the introduction, the electrochemical Eadie-Hofstee plot can be used to determine the K_m^{app} of the immobilised enzyme in the biosensor configuration (Kamin and Wilson, 1980). Figure 5.7 illustrates the electrochemical Eadie-Hofstee plot of the native and the ferrocene-modified SBP, in the biosensor configuration with the electron transfer mediator. From the slopes the K_m^{app} can be determined. The K_m^{app} for native SBP was 5.6 μM, with a correlation coefficient of 0.99, the K_m^{app} for the ferrocene-modified SBP was 6.62 μM, with an r^2 value of 0.98.

5.7: Electrochemical Eadie-Hofstee plots:

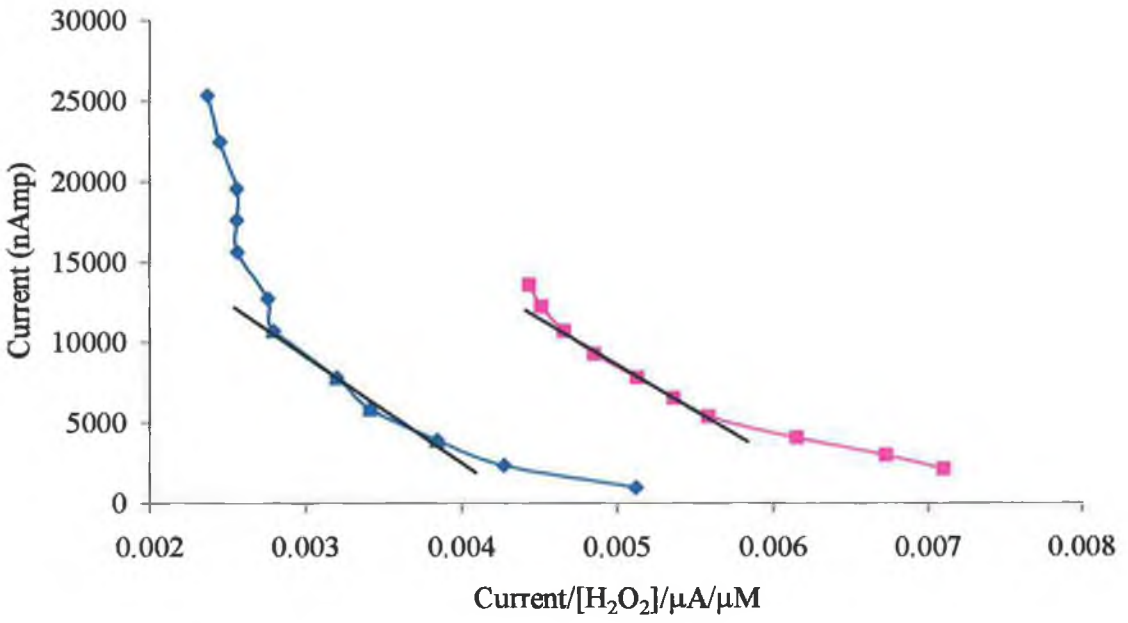

Figure 5.8: Electrochemical Eadie-Hofstee plot of native and ferrocene-modified SBP. The slope of the linear region of the plot is equal to the – K_m^{app} for the system. Native SBP (—), ferrocene-modified SBP (—).

5.8: Discussion:

As detailed by Lindgren *et al.* (2000) the higher the degree of enzyme glycosylation, the lower the percentage of molecules capable of direct transfer of electrons from the active site to the electrode surface. Glycosylation of enzymes hinders electron transfer due to greater bulk and, hence, distance to travel. Recombinant catalytically active forms of enzymes (from bacterial hosts) perform direct electron transfer better. Lindgren *et al.* (2000) showed that recombinant wild type HRP yielded a higher percentage of molecules properly orientated for successful electron transfer. Ferapontova *et al.* (2001c) showed that recombinant HRP immobilised onto gold electrodes gave very good direct electron transfer signals over native HRP preparations. The purpose of the present work was to design a procedure to modify a crude glycosylated native SBP enzyme preparation and to increase electron transfer from the enzyme to the electrode surface. Later, (Chapter 6) attempts were made to establish direct electron transfer between the modified SBP and the electrode surface.

Ever since Foulds and Lowe (1988) presented their research using ferrocene mediators, and as shown in Section 1.11, there have been multiple references to research into the use of ferrocene and its derivatives as electron transfer mediators in biosensors. However, most methods used to immobilise ferrocene to the enzyme in question are quite complex and time consuming. The method put forward here is based on that of Degani and Heller (1987) but with notable differences. As explained in the Introduction, Degani and Heller (1987) modified the amino acids of the GOx polypeptide directly. In the present work, the SBP carbohydrate moieties were used for covalent attachment of the

ferrocene carboxylic acid. Towards the end of their procedure Degani and Heller (1987) encountered problems. The polysaccharide envelope of GOx prevented the EDC intermediate O-acylisourea from reacting with the amino acids within. No such problem was encountered here, as all the reactions in the modification procedure occur on the surface of the SBP enzyme.

To ensure the modification was successful the iron content of the ferrocene-modified SBP was compared to native solutions by atomic absorption spectroscopy (AA). A standard curve (Figure 5.1) of Fe in $FeCl_3.6H_2O$ was constructed and the samples Fe contents were calculated from this. Following the attachment of Fe to aminated (the attachment of an amine groups to the enzyme) SBP, it was calculated from AA analysis that 2 ferrocene groups had been added to each SBP enzyme.

The protein concentration was observed to decrease by 50% after amination; this could be a result of the removal of low molecular weight proteins (observed in Figure 5.1) by the dialysis step (Section 2.4.1). The activity increased as a result of the removal of interfering agents. There is a discrepancy between the number of amines generated and the number of ferrocenes added to SBP. Ferrocene carboxylic acid is relatively insoluble in distilled water. Investigating this to see if it is possible to increase the solubility of it would increase the concentration of ferrocene in the water. This would then increase the possibility of adding more ferrocenes to the aminated SBP.

Gray *et al.* (1996) identified the glycans of SBP, which consist of Man (3.3mol), Xyl (0.7mol), Fuc (0.9mol), and GlcNAc (2.0mol). Except for GlcNAc, each of these sugars contain vicinal diols that can be exploited through periodate oxidation to produce aldehyde groups. As shown in Figure 5.2, ethylenediamine is attached to these, the Schiff bases are reduced to secondary amines and the ferrocene carboxylic acid is attached to the free primary amines. The success of the modification procedure is due to the fact that SBP is extensively glycosylated. The modification would not work with glycan-free recombinant SBP because of the lack of reactive Lys residues (SBP only has three lysines, and these seem to be unreactive under mild conditions (Henriksen *et al,* 2001; Welinder 2004; O'Brien, A., M. unpublished). Their locations in the tertiary structure of the enzyme, are shown later in Figure 7.1.

As in the previous Chapter (4), electrochemical assays were performed to determine the effect of modification on the enzyme. A mixture of mediator and ferrocene-modified SBP was immobilised onto the surface of the electrode and a CV carried out to determine if a redox event was occurring. Varying the scan rates led to altered voltammetric responses. The formal potential ($E^{0'}$) of the osmium in the ferrocene-modified SBP system was determined to be 325 mV, 60 mV less than the 385mV value for native SBP. This change in the $E^{0'}$ can be ascribed to the osmium and the addition of the ferrocene carboxylic acid units (Figure 5.3). The peak cathodic currents were recorded (Figure 5.4) and plotted against the square root of the scan rate. A straight line was observed with equation $y = 13.425\ x - 1.650$ and a correlation coefficient of 0.99.

The changes in current with scan rate shown in Figure 5.3 are less than those seen in Figure 4.8. One possible reason for this could be different concentrations of immobilised mediator or SBP. It was not possible to ensure uniform concentrations of mediator and SBP immobilised onto the electrode surface. Similar volumes and concentrations of mediator and SBP were prepared but there was no guarantee that reproducible amounts could be immobilised onto the surface. Addressing this lack of uniform dosage of the critical sensor components would be an item for future work.

A current-time response curve was constructed to compare the ferrocene-modified SBP to the native (Figure 5.6). The method was the same as discussed for Figure 4.11. The ferrocene-modified SBP shows an approximately two fold greater compared to SBP alone increase in current when a 20μL, (5μmol), aliquot of H_2O_2 is added to the solution.

The sequential steps in current (Figure 5.6) were linearised into a calibration curve and plotted against the concentration of H_2O_2 added, yielding a straight line (Figure 5.7). The equation for the native SBP was $y = 231.45 x - 1052.8$ (correlation coefficient 0.98) and the calibration plot was linear over the range 5 – 60 μmol H_2O_2. The equation for the ferrocene-modified SBP was $y = 432.46 x - 1830.98$ (correlation coefficient 0.99). The calibration plot again was linear over the range of 5 – 60 μmol H_2O_2. The response times for both biosensors were similar, at approximately 15 seconds. It can be seen that the ferrocene-modified SBP had a greater sensitivity (twice the sensitivity) towards the addition of H_2O_2, having a slope of 432 as compared to the native slope of 231.

The calibration points were used to plot an electrochemical Eadie-Hofstee plot (Kamin and Wilson 1980) (Figure 5.8). The linear portion of the plot was used to determine the slope, which is equivalent to the - K_m^{app} of the enzyme, the K_m^{app} was determined to be 6.5mM for native SBP while that for the ferrocene-modified SBP was 7.2 mM H_2O_2 a negligible difference.

Although there was little difference in the K_m^{app} for the two SBP preparations, there is a notable difference in the calibration curves, with the ferrocene-modified SBP showing a greater sensitivity to successive additions of H_2O_2 to the system. As stated by Kamin and Wilson (1980), that a non-linear electrochemical Eadie-Hofstee plot is a qualitative indicator of mass transport limitations. This is the case in Figure 5.8, indicating that there are limitations in the transport of the substrate and products through the enzyme mediator layer.

CHAPTER 6

Direct electrochemistry of native and ferrocene modified SBP

6.1: Introduction:

Schuhmann (2002) discuss the 3 generations of biosensors (first, second and third generations). In chapter four, the second-generation biosensor configuration was investigated using native SBP immobilised on the surface of the platinum microelectrode in the presence of the mediator $[Os(bpy)_2(PVP)_{10}Cl]^{+}$. That configuration has been further advanced by attaching ferrocene containing electron relays onto the surface of the SBP molecule, the preparation and characterisation of this second-generation biosensor configuration is described in Chapter 5.

6.2: SEM of etched microelectrode:

In this Chapter, the abilities of native and ferrocene modified SBP to transfer electrons directly from the active site to the surface of the electrode are investigated. To aid in the retention of SBP on the electrode surface a cavity was etched into the electrode using aqua regia, as described in Section 2.36. The electrode was etched over several hours and the cavity formed was imaged using a scanning electron microscope. Figure 6.1 shows the unetched electrode, while Figure 6.2 shows the same electrode after 8 hours etching with aqua regia. While it is clear that some etching has taken place, it was decided to etch further to deepen the cavity. This should enable the incorporation of enough SBP into the cavity to facilitate direct electron transfer from the active site to the electrode surface and prevent mechanical loss from the surface. In Figure 6.3, the platinum can be seen in the centre of the image and can be seen to be recessed into the glass surround. The dark ring around the wire is a result of charging: platinum conducts electricity but the glass does not; where the two meet, there is a difference in charge and the result is the darkened ring around the platinum. The roughness of the etched electrode surface was not

calculated, as the exact depth of the new electrode was undeterminable from the SEM images. When the cavity was deemed sufficiently deep, it was filled with the native or ferrocene-modified SBP as detailed in Section 2.38.

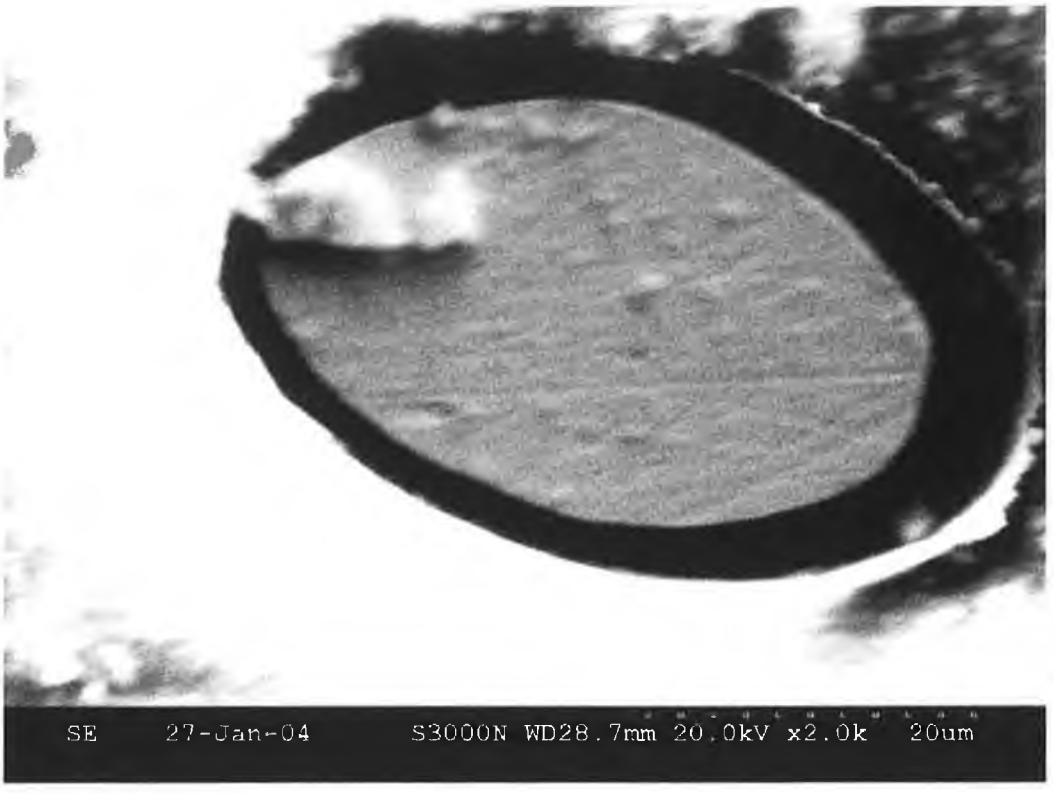

Figure 6.1: Scanning electron microscope image of the polished bare platinum microelectrode (magnification is at 2000X). The black ellipse surrounding the Pt wire is due to charging.

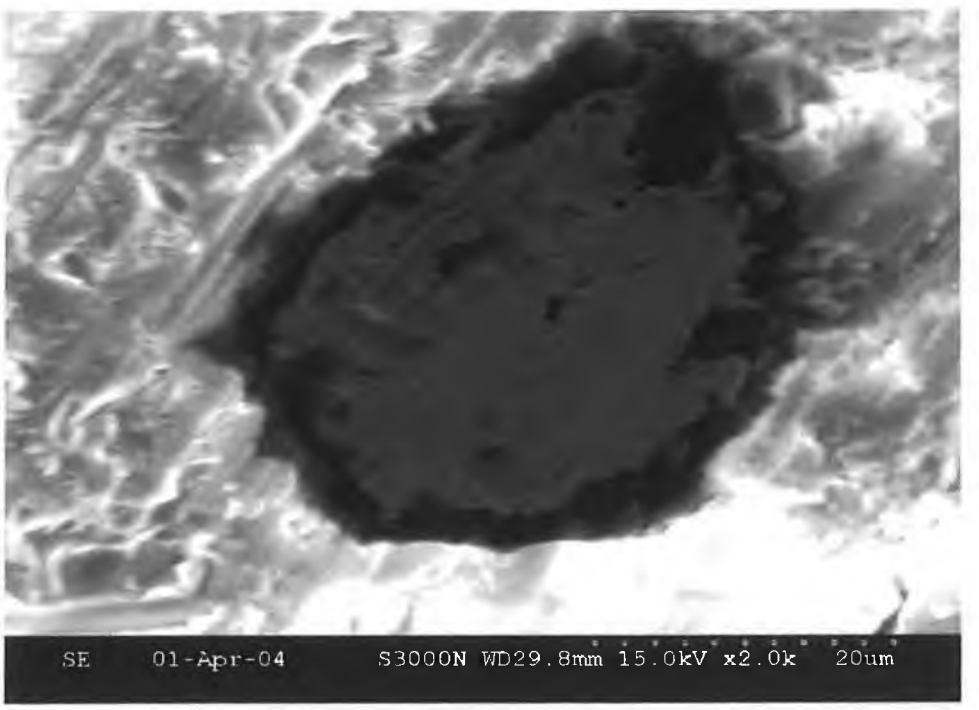

Figure 6.2: The effect of 2 hours etching on the electrode (magnification 2000X).

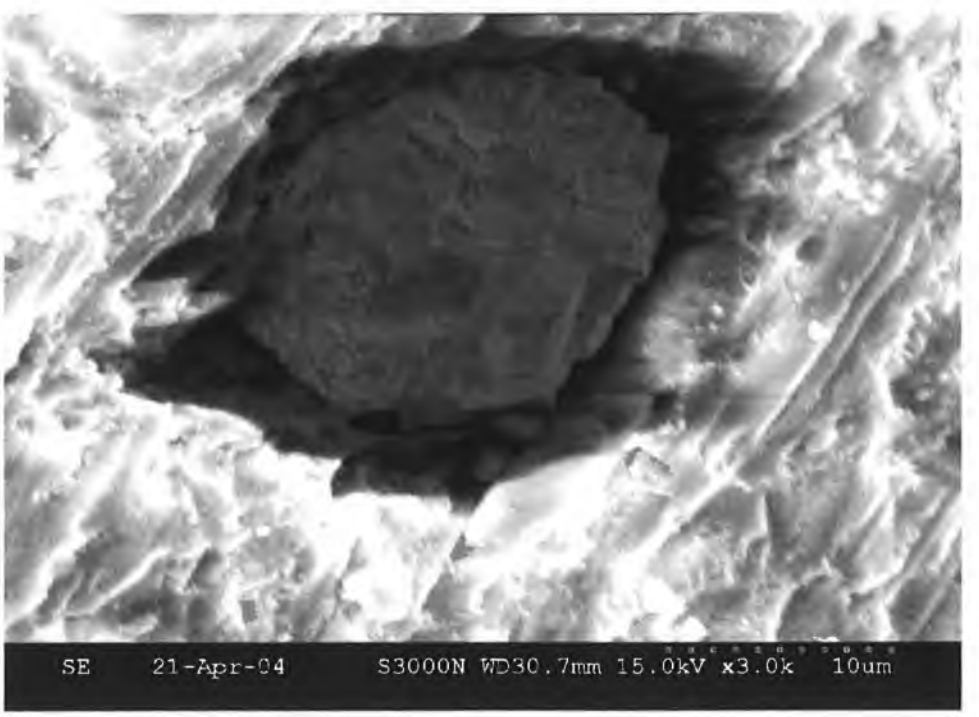

Figure 6.3: SEM image of the platinum microelectrode etched with aqua regia. The Pt wire is recessed into the glass surround (magnification 3000X).

6.3: Direct electrochemistry of immobilised native SBP:

Native SBP was immobilised in the etched cavity (Section 2.38). A CV was carried out at 0.2 $V.s^{-1}$ and the resulting scan recorded. The scan rate was varied, the voltammograms recorded (Figure 6.4) and peak heights were plotted against the square root of the scan rate. The resulting straight line (Figure 6.5) was obtained, (equation $y = 37.67x - 6.10$, correlation coefficient 0.98). The noise present in the scans was put down to instrumental noise rather than noise originating in the biosensor system.

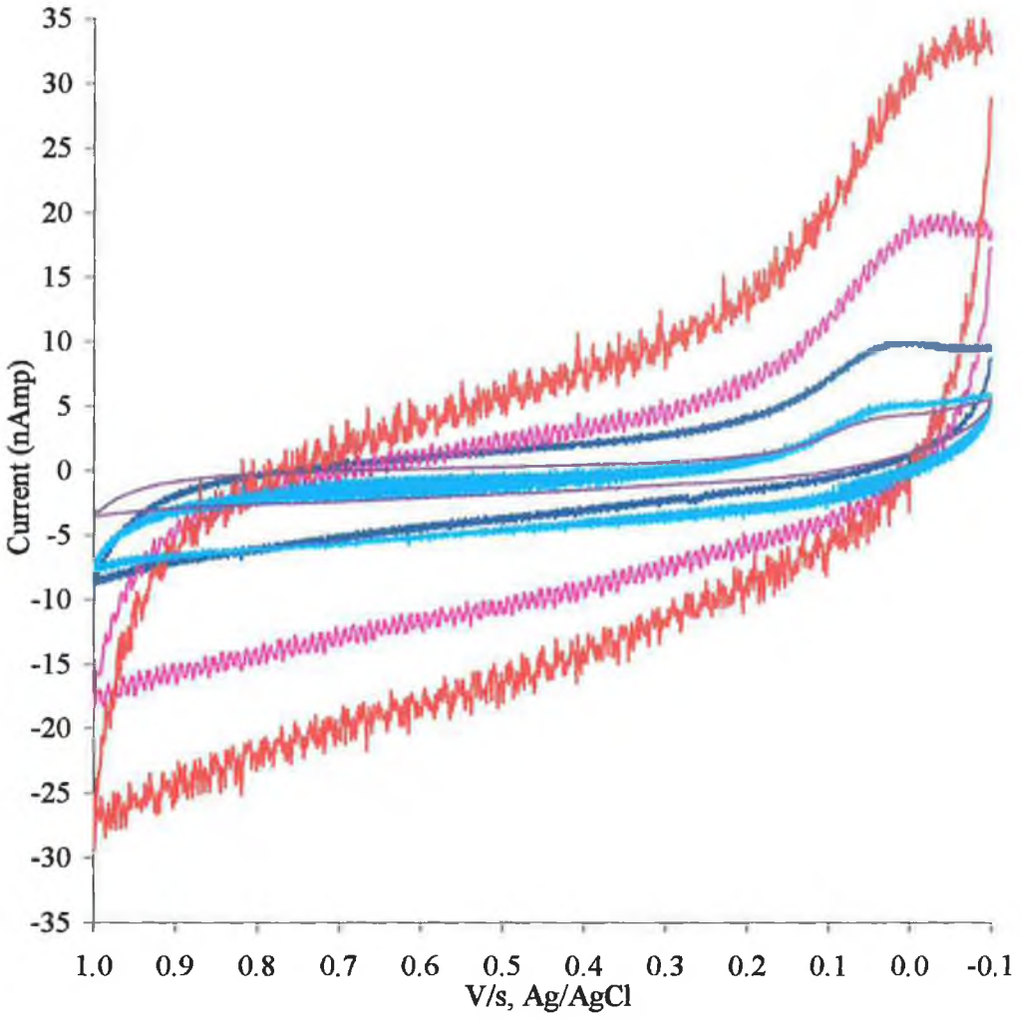

Figure 6.4: CVs for the direct electron transfer with native SBP in an etched platinum microelectrode. Where $0.05V.s^{-1}$ (—), $0.1V.s^{-1}$ (—), $0.2V.s^{-1}$ (—), $0.5V.s^{-1}$ (—) and $1.0V.s^{-1}$ (—).

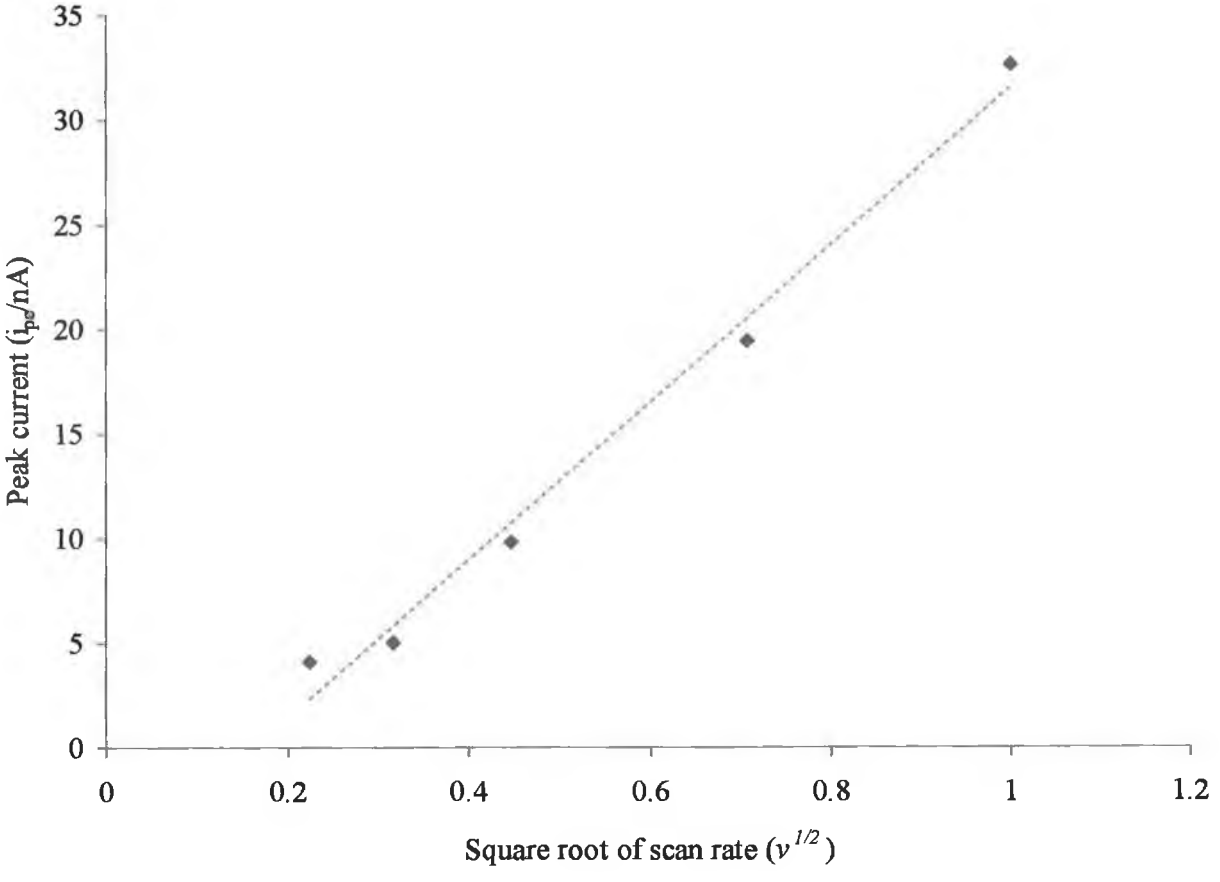

Figure 6.5: Plot of peak current versus the square root of scan rate of the data in Figure 6.4.

6.4: Direct electrochemistry of immobilised ferrocene-modified SBP:

Before any further electrochemical assays were performed on the etched electrode, the cavity was cleaned by sonication (Section 2.38). A CV with no peaks was obtained indicating a clean electrode. Next ferrocene-modified SBP was immobilised in the etched cavity (Section 2.38). A CV was carried out at $0.2V.s^{-1}$ and the resulting scan recorded. The scan rate was then varied, the voltammograms recorded (Figure 6.6) and their peak currents were plotted against the square root of the scan rate. The

resulting straight line (Figure 6.7, equation y = 66.59 x + 7.32, correlation coefficient 0.94) indicates that the species is semi-infinite linear diffusion.

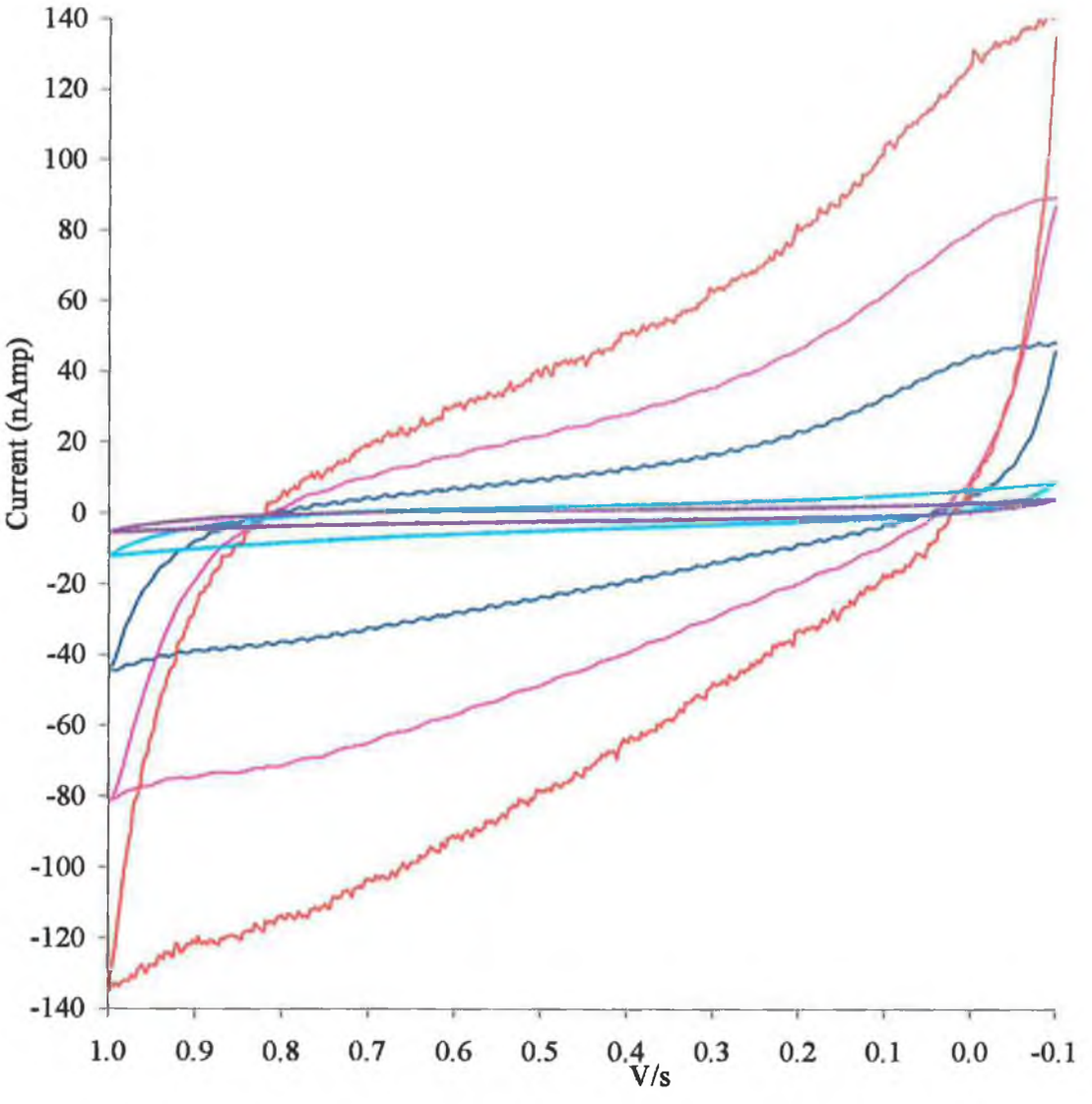

Figure 6.6: CVs for the direct electron transfer with ferrocene-modified SBP in an etched platinum microelectrode, where $0.1V.s^{-1}$ (—), $0.2V.s^{-1}$ (—), $1.0V.s^{-1}$ (—), $2.0V.s^{-1}$ (—), and $5.0V.s^{-1}$ (—).

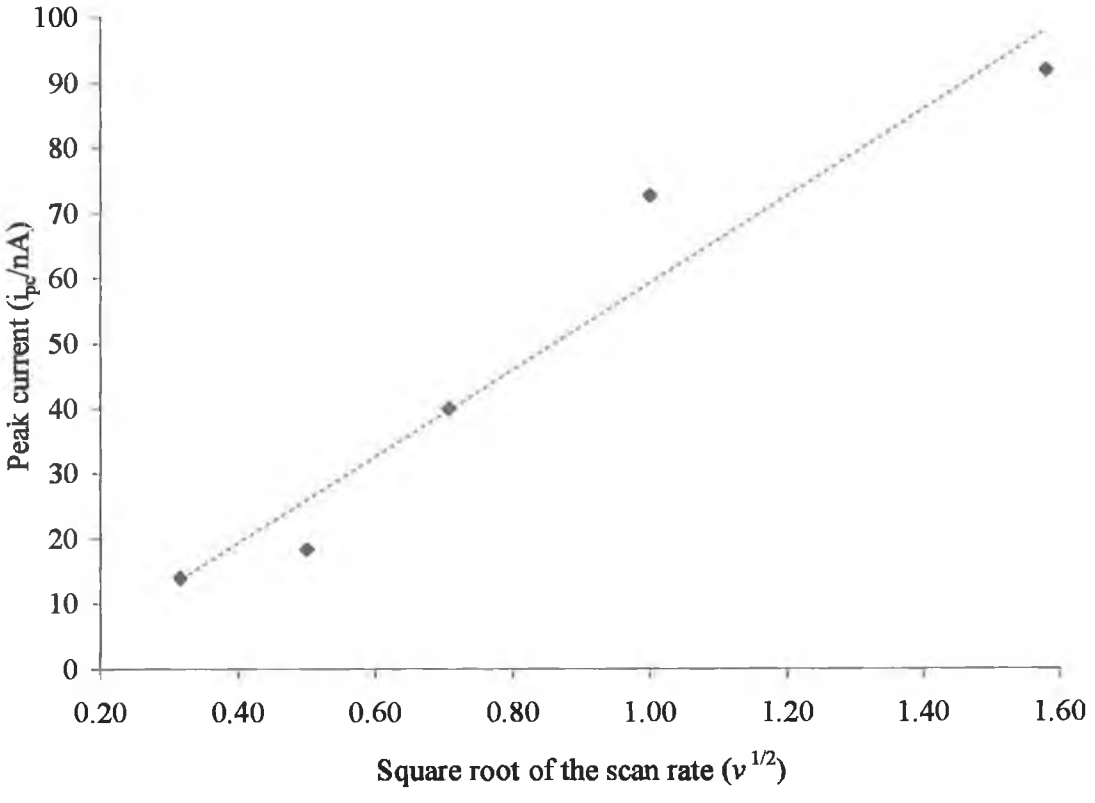

Figure 6.7: Plot of the peak currents to the square root of the scan rate from Figure 6.6. A straight line indicates a single-electron, reversible process.

6.5: Comparison of the different scans of directly immobilised SBP:

Figure 6.8 compares the CVs for the various configurations. The CV of the etched empty cavity acts as a background scan. The middle scan is that for immobilised native SBP, showing the reduction peak at 15 mV and a small oxidation peak at 36 mV. The final CV is that of ferrocene-modified SBP, where the reduction and oxidation peaks are less defined, but are present at 36 mV and 89 mV respectively.

6.6: Comparison of native and ferrocene modified SBP immobilised into the microelectrode etched cavity:

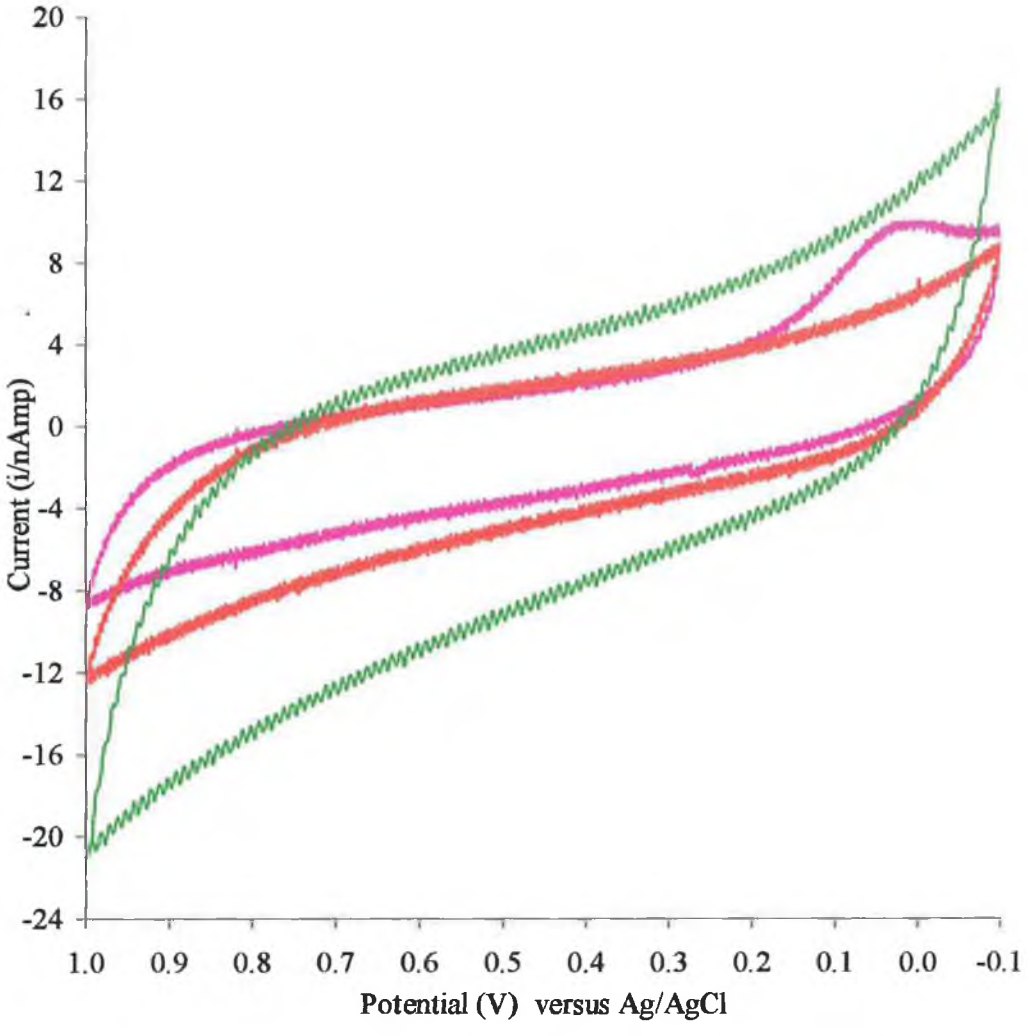

Figure 6.8: Graph illustrating the difference in signal generated from different biosensor configurations. The innermost curve is the background signal with no enzyme immobilised in the cavity of the electrode (—), the middle curve is native SBP (—), and the outer most curve is the ferrocene-modified SBP biosensor (—).

6.7: Current-time analysis of direct electrochemical set-up:

When a 20 μL (2.5 μmol) aliquot of H_2O_2 was added to the biosensor at constant potential, there was a sharp increase in the reduction current, which reached a steady-state constant current. Figure 6.9 shows the steady-state response of the native and ferrocene-modified SBP cavity-biosensors using 25 mM MOPS buffer, pH 7.0. From the graph it can be seen that the steady-state response is reached within 20 seconds of H_2O_2 addition.

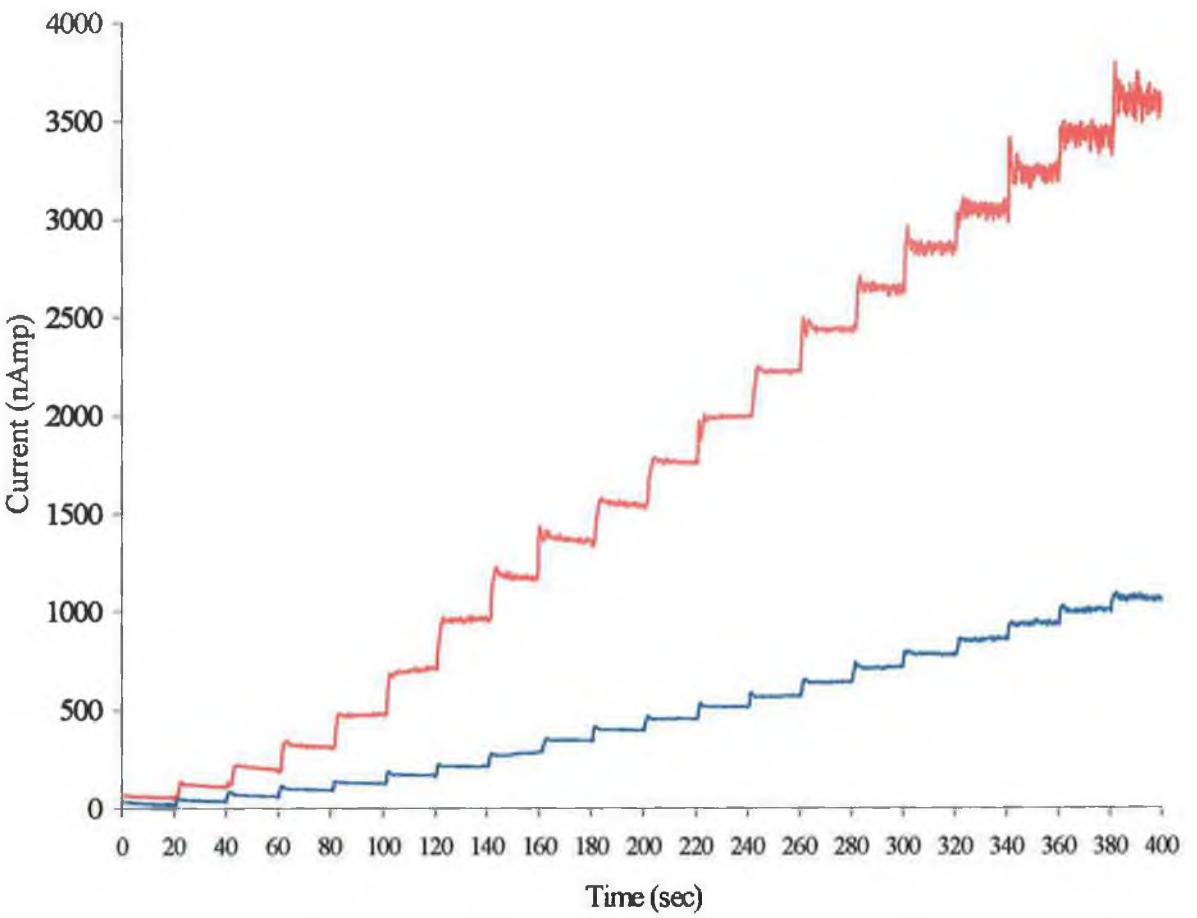

Figure 6.9: i-t analysis of native and ferrocene modified forms of SBP. Successive 20μL (2.5μmol) additions of H_2O_2 were made to the solution and the resulting change in current was measured. Where the native SBP signal is represented by (—), and is the ferrocene modified SBP signal (—).

6.8: Calibration curves for the hydrogen peroxide sensors:

From Figure 6.9, a calibration curve was constructed for the two SBP biosensor forms. The response with native SBP is linear within the range of H_2O_2 from 2.5 mM to 42.5 mM. The linear regression equation is $I(A) = 2.87\ \mu M[H_2O_2] - 13.56$, with a correlation coefficient of 0.98. The response for the ferrocene-modified SBP is linear within the range of H_2O_2 from 2.5 mM to 42.5 mM. The linear regression equation is $I(A) = 10.11\ \mu M[H_2O_2] - 22.73$ with a correlation coefficient of 0.99.

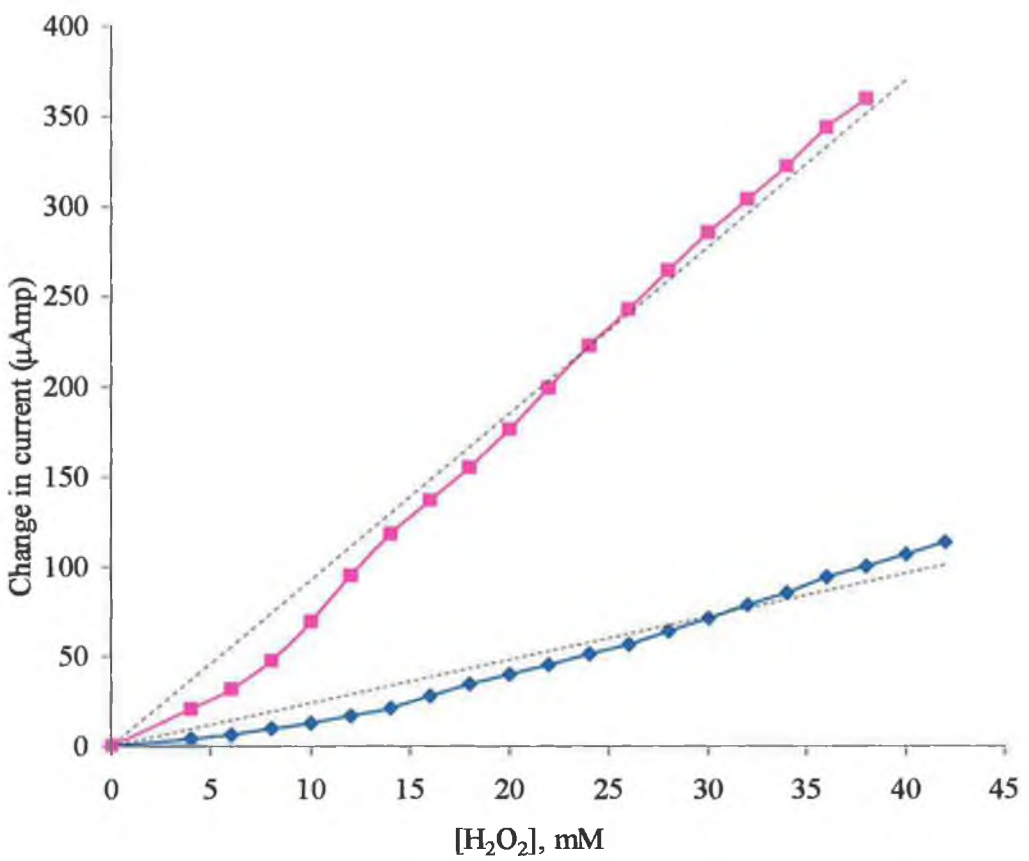

Figure 6.10: The results in Figure 6.9 are plotted linearly. Native SBP linearised signal (♦), Ferrocene modified SBP linearised signal (■).

6.9: Kinetic analysis of the third generation biosensors:

When the calibration data are plotted as an electrochemical Eadie-Hofstee plot (Kamin and Wilson, 1980) one can determine the K_m^{app} of the immobilised SBP in the etched cavity of the biosensor (from the slope native $r^2 = 0.99$ and ferrocene-modified $r^2 = 0.98$). K_m^{app} of the native and ferrocene-modified SBP were determined to be 0.18 and 4.01 μM respectively. As outlined in the introduction, the sigmoidal shape of the curve has been ascribed to diffusional limitations on the substrate entering the active site.

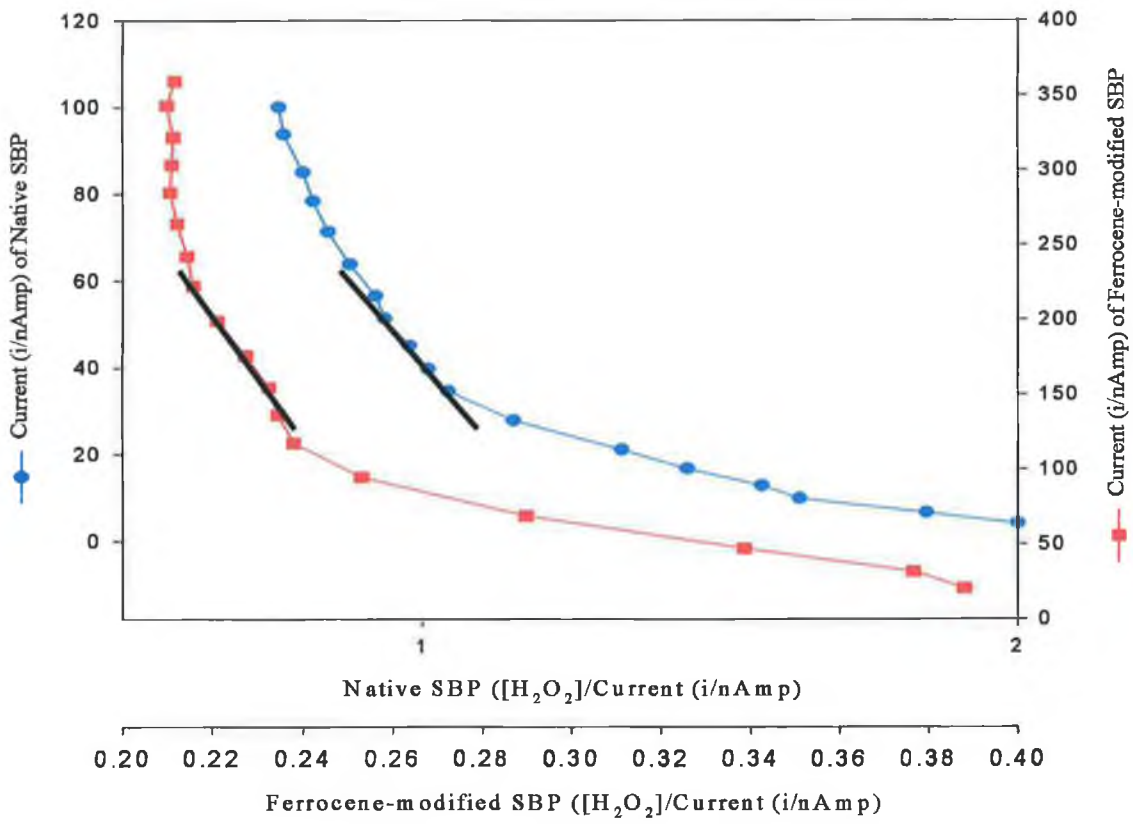

Figure 6.11: Modified electrochemical Eadie-Hofstee plots of native and ferrocene-modified SBP. The black lines represent the region where the K_m^{app} was calculated.

6.10: Discussion:

The distance and the orientation of the active site of an enzyme and the electrode surface influence direct electrochemical communication between an immobilised biological material and the electrode surface. Distance is dependent on the proper orientation of the enzyme before its immobilisation and the size of the enzyme is important in the success of direct electron transfer (Lötzbeyer *et al.* 1996). Horseradish peroxidase is a very slow electrochemical reactant, which is why mediators are used to speed up the reaction at gold and platinum electrodes (Dunford, 1999). Rarely has direct electron transfer of HRP been observed on metal electrodes such as platinum or gold electrodes, it is more usually obtained using carbon-based electrodes (Presnova, *et al.* 2000). It was found that the formation of compound I (defined in Chapter 1) was kinetically slow on a majority of electrode materials (Ferapontova *et al.* 2001c; Ferapontova and Puganova, 2002). Ferapontova *et al.*, (2001c) discovered that using phenol or *p*-cresol the rate of the reaction could be accelerated. This would lend the use of a biosensor to the detection of waste phenol based compounds in wastewater. There are two reasons for the slow direct electron transfer of peroxidase enzymes. First, the heme group and the active site are buried within the polypeptide, increasing the distance the electron has to travel. Secondly the glycosylation of peroxidases can act as an insulating cover, further increasing the distance for successful electron transfer (Presnova, *et al.* 2000). Both the SBP (native and ferrocene-modified) biosensors suffer from reduced rates of electron transfer. This can be seen in the small oxidation peaks seen in Figures 6.4 and 6.6. The lack of the reversible peaks would also be indicative of the reduced electron transfer from SBP to the electrode surface.

The purpose of direct electrochemistry is to reduce the distance of electron transport by bringing the enzyme's active site and the transducer surface into close proximity. In recent times recombinant enzymes from bacterial hosts have been used to enhance electron transfer (Ferapontova *et al.* 2001a; Ferapontova *et al.* 2001b; Lindgren, *et al.* 2000). This is because bacterial cultures do not glycosylate the enzymes post translationally, so there are no bulky glycans preventing close contact between enzyme and transducer. However, in the work presented in this Chapter, the enzyme preparation used was of plant origin. This means that the enzyme is glycosylated (18% of its 44KDa molecular weight is due to glycans). The fact that it was glycosylated was utilised and exploited, as illustrated in Chapter 5. The enzyme and mediator described in Chapter 4 were immobilised onto the electrode surface mainly through adsorption. Gross leaching was prevented by the charge interaction between the mediator and the SBP. However, there was some loss of enzyme activity, due to leaching from the cavity of the electrode.

To overcome these factors, and to eliminate the need for a mediator, it was decided to etch a cavity into the glass support. The etching was done using aqua regia (Section 2.38). By packing the newly formed cavity with SBP alone (in the absence of mediator) it was hoped that the enzyme would not leach from the electrode before analysis. Imaging of the electrode by SEM showed successful etching by the aqua regia. As can be seen in the three successive SEM images (Figures 6.1, 2 and 3) the effect of etching over time is apparent. The electrode was tested to ensure that it was still functioning after the etching procedure and performed with the characteristics of a bare electrode.

Both the native and ferrocene-modified SBP preparations were studied in the etched electrode for the possibility of direct electrochemical communication between SBP and the electrode surface. Unlike previous experiments with the platinum electrode, no polishing of the electrode could be performed. The electrode cavity was filled with native SBP as outlined in Section 2.38. To aid in immobilisation of SBP into the etched cavity the electrode was inverted and the SBP solution allowed to settle into the cavity overnight. To ensure that SBP was present in the cavity and that there were no air bubbles preventing electron transfer from the active sites to the electrode surface, a CV was carried out. The scan rate was varied and the resulting scans were recorded as Figure 6.4. As can be seen, the peaks are not symmetrical. The formal potential ($E^{0'}$) of native SBP-osmium system in the etched cavity was determined to be 459mV. The peak cathodic currents were recorded and plotted against the square root of the scan rate. A straight line was observed, indicating that the reversible surface redox reaction was solution phase. A current-time (i-t) assay was performed by adding successive aliquots of H_2O_2 into a stirred solution; after each addition a sharp increase in the reduction current, reaching a steady-state constant current, was observed.

To ensure the etched electrode was thoroughly clean and that the SBP had been removed, a CV was performed. The resulting scan indicated no redox reactions and this indicated that the electrode was clean. The ferrocene-modified SBP was immobilised into the cavity of the electrode as described above (Section 2.38) and characterised electrochemically. Figure 6.6 illustrates the effect of altering the scan rate. The formal potential ($E^{0'}$) of ferrocene-modified SBP system in the etched cavity was determined to be 465mV, scarcely different from native SBP. The slight

difference could be attributed to the addition of two ferrocene carboxylic acid groups to the SBP. An i-t assay was performed by adding successive aliquots of H_2O_2 into a stirred solution after each addition. A sharp increase in the reduction current was observed, which reached a steady-state constant current. The time taken to reach steady state was approximately 20 seconds for both the native and ferrocene-modified SBP preparations. This appears to be quicker by a factor of 2 compared to Wang *et al.* (2001b). Their SBP sensor was in a copolymer mix and the electrode used was a 4mm glassy carbon electrode. A reason for the improved time of analysis may be the use of a microelectrode, which exhibits short response times (Forster, 1994). The biosensor configuration compares well with other peroxidase sensors with respect to detection of substrate at micromole (μmol) concentrations. However, this seems to be the first report of a platinum microelectrode using SBP in direct electron transfer communication with the electrode surface.

A calibration curve was constructed from the i-t curves of the native and ferrocene-modified SBP (Figure 6.10). There is a noticeable difference in the calibration curves for the native and ferrocene-modified SBP biosensors. The native SBP biosensor plot had an equation: y = 2.87x - 13.56, (correlation coefficient 0.98), whereas the ferrocene-modified biosensor had an equation: y = 10.11x – 22.73 (correlation coefficient 0.99). The sensitivity of the ferrocene-modified biosensor is more responsive to the successive additions of H_2O_2 to the solution. This is reflected in the respective slope of the lines for the two calibration curves. The electrochemical Eadie-Hofstee plot can be used to demonstrate the effect of internal diffusion as well as to estimate the K_m^{app} of the system.

CHAPTER 7

Chemical modifications of SBP

7.1: Introduction:

In the course of fabricating a SBP-based biosensor, several methods of chemical modification were investigated to increase thermostability and to improve electron transfer from the active site of SBP and the electrode surface. The first method described here is the attachment of aminated SBP to dextran dialdehyde (Section 2.27). The intentions behind this modification were to attempt to increase the thermal stability of SBP and subsequently to incorporate this enzyme preparation into a biosensor that could be used at elevated temperatures for extended periods. The procedure was a multi step reaction with a 72-hour reaction time in the middle of the protocol. While the modification worked to a degree, it did not prove as successful as had been hoped. As will be expanded on in the discussion, the quality of the zero-length cross-linker EDC was to play an important part in the success of the procedure.

The second method undertaken to increase SBP's thermal and solvent stability in a biosensor configuration was chemical modification with the homobifunctional cross-linker adipic acid dihydrazide (Section 2.28). This procedure, like the ferrocene carboxylic acid method, exploited SBP's carbohydrate groups. The carbohydrate moieties were oxidised to functional aldehydes (Section 2.23) and the cross-linker was attached covalently to them.

One of the most popular methods of modifying proteins is through the ε-NH_2 group of lysine residues (Ugarova *et al.* 1979; Bagree, *et al.* 1980; Khajeh, *et al.* 2001 and Souppe, *et al.* 1988). It is possible to modify HRP Lys groups with the homo bifunctional cross-linker EG-NHS (Ryan *et al,* 1994b). Increases in stability of up to 20 minutes at 72°C have been reported and it was investigated if the Lys groups of SBP

could be similarly altered (A-M. O'Brien, unpublished). Review of the amino acid sequences (Figure 7.5) of SBP (Henriksen *et al.* 2001) show that there are three Lys residues (Lys84, 139 and 283). The distance between the residues has to be less than that between the reactive ends of any candidate cross-linker. The effective length of EG-NHS is 10.8Å. Looking at Figure 7.1, the distances between the lysines have been determined Lys139 to 283 is 14.41Å, the distance between Lys84 to 283 is 29.10Å and the distance between Lys84 to 139 is 38.11Å. All of these are too long for crosslink formation by EG-NHS. Despite publication of the revised SBP sequence by Welinder and Larsen (2004), the locations of the Lys residues have not altered

As a result of the limited number of lysine residues and the distances between them, the EG-NHS modification did not succeed. Another factor that could have prevented the cross-linker from binding was the possible steric hindrance of the sugar groups attached to Asn groups on the surface of the enzyme.

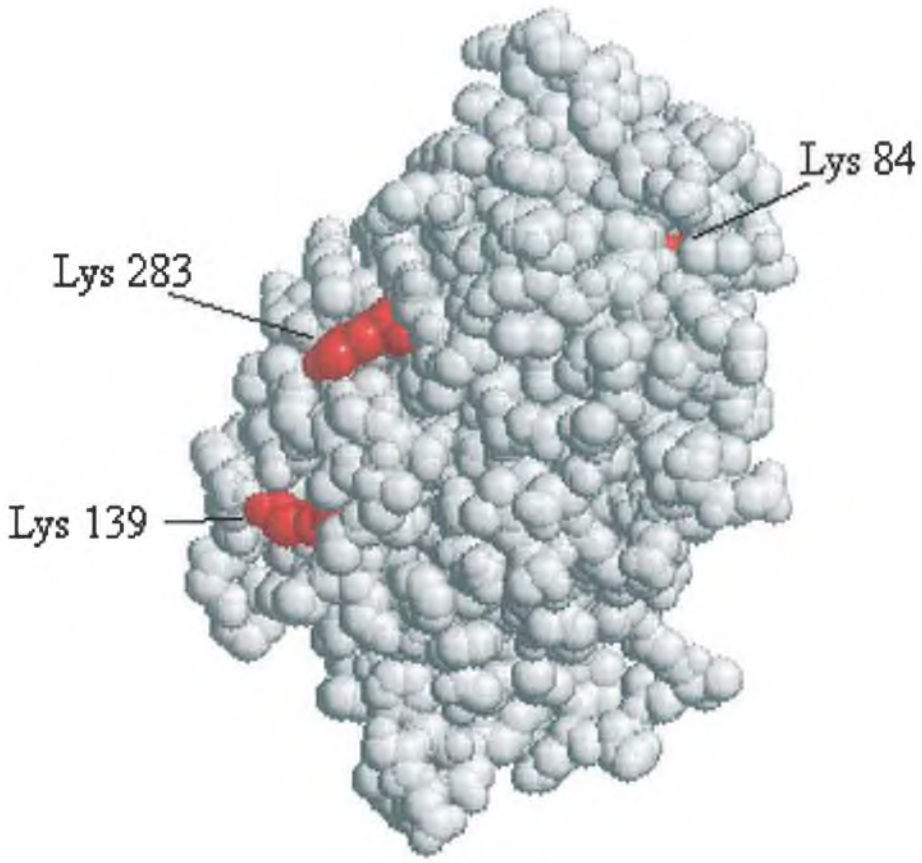

Figure 7.1: A schematic of SBP (1FHF, PDB accession number, Henriksen *et al.*, 2001) illustrating the locations of the lysine residues (coloured red). The distances between the lysine groups are too long for the attachment of the cross-linker EG-NHS. The SBP structure was constructed using the computer programme RasMol, (www.umass.edu/microbio/rasmol. 1998).

7.2: Chemical modifications:

7.2.1: Modification of peroxidase enzyme by the introduction of dextran dialdehyde:

This modification combines two widely used, separate modifications in an attempt to increase SBP stability. The amination is a two-step modification, firstly using 1-ethyl-3-(3-dimethylamino-propyl)carbodiimide (EDC) amination, and secondly covalently attaching dextran dialdehyde to the aminated SBP (D. O'Brien, 2000, Irish Patent application no: S2000/0860).

The first step is as outlined in Section 2.27 (Figure 7.2). SBP is exposed to the EDC and allowed to react for a given time. 1-ethyl-3-(3-dimethylaminopropyl)carbodiimide can react with biomolecules to form "zero-length" crosslinks, usually within a molecule or between subunits of a protein complex. Water-soluble carbodiimides catalyse the formation of amide bonds between carboxylic acids and amines to form an O-acylurea (Staros *et al.* 1986). The intermediate formed is a derivative of the carbodiimide (Sehgal and Vijay, 1994). Following the formation of this intermediate, it can be attacked by an amine directly. This stage is when the EDC-modified SBP is allowed to react with ethylediamine for 90 minutes. Amine attack is by the nucleophilic primary nitrogen of the amino compound, leading to about formation of the amide linkage with release of the soluble substituted urea. Sehgal and Vijay (1994) state that EDC is preferred over other carbodiimides such as *N,N'*-dicyclohexylcarbodiimide because of its solubility in water and the methods of removing unreacted reagent (by dialysis or gel filtration) and the urea product formed in the reaction.

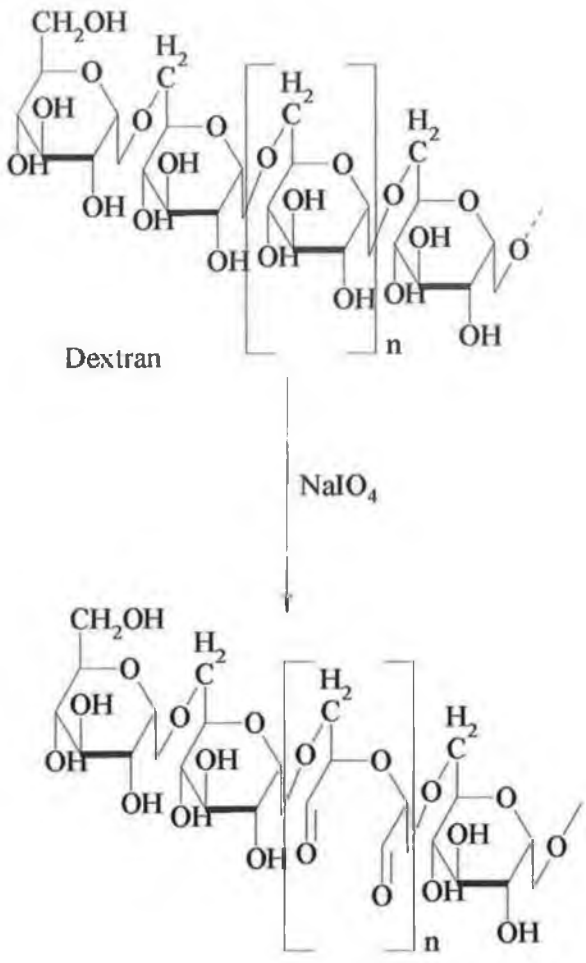

Figure 7.2: The introduction of dialdehyde groups into the glucose residues of dextran by sodium-*m*-periodate (Yamagata *et al., 1994*).

The second step involves chemical attachment of the dextran dialdehyde to the newly formed amine group. The dextran was of an average molecular weight of 66,900. Dextran, a carbohydrate polymer, can easily be oxidised by sodium-*m*-periodate ($NaIO_4$), to yield free aldehyde groups (Figure 7.2), at the C-2 and C-3 positions of its D-glucose residues.

Through Schiff base reactions, the aldehydes of dextran residues can attach to the primary amino groups of the aminated SBP (Figure 1.12 and 7.3). Yamagata *et al.*, (1994) showed that the aldehyde groups in the dextran dialdehyde have the ability to react with α-amino or ε- amino groups of amino acids, especially lysine.

The use of the two individual modifications has been widely used and reported. The procedure, however, involves the sequential use of two modifications to increase the stability of an enzyme has, to our knowledge, not been reported previously (O'Brien, D. 2000).

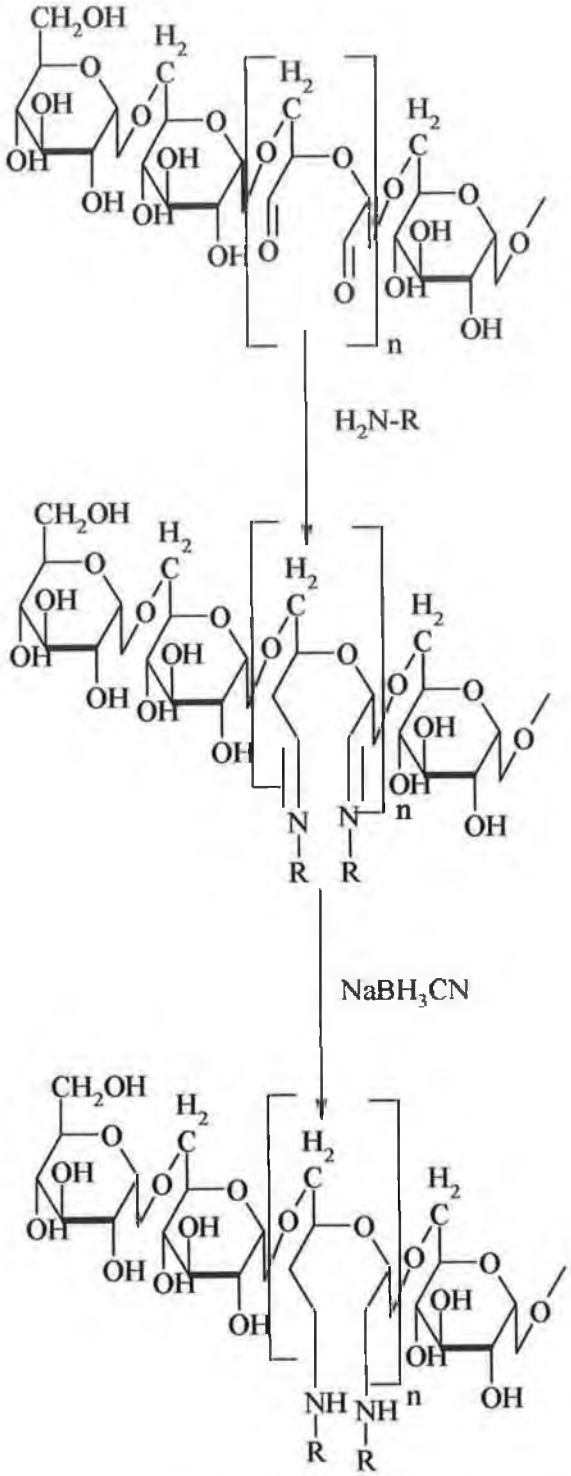

Figure 7.3: The attachment of dextran dialdehyde to the amine group of a previously modified enzyme (Yamagata *et al.*, 1994).

Figure 7.4 shows the thermal inactivation results of native and dextran dialdehyde-modified SBP. The $t_{1/2}$ of native SBP is approximately 19 minutes and that of dextran dialdehyde-modified SBP is seen to be 10 minutes. The modification was not considered successful and no further analysis of this particular preparation was carried out. This stage of the modification was not as effective as expected. One possible reason for this is the quality of the commercial EDC preparation. Another source of EDC was sought.

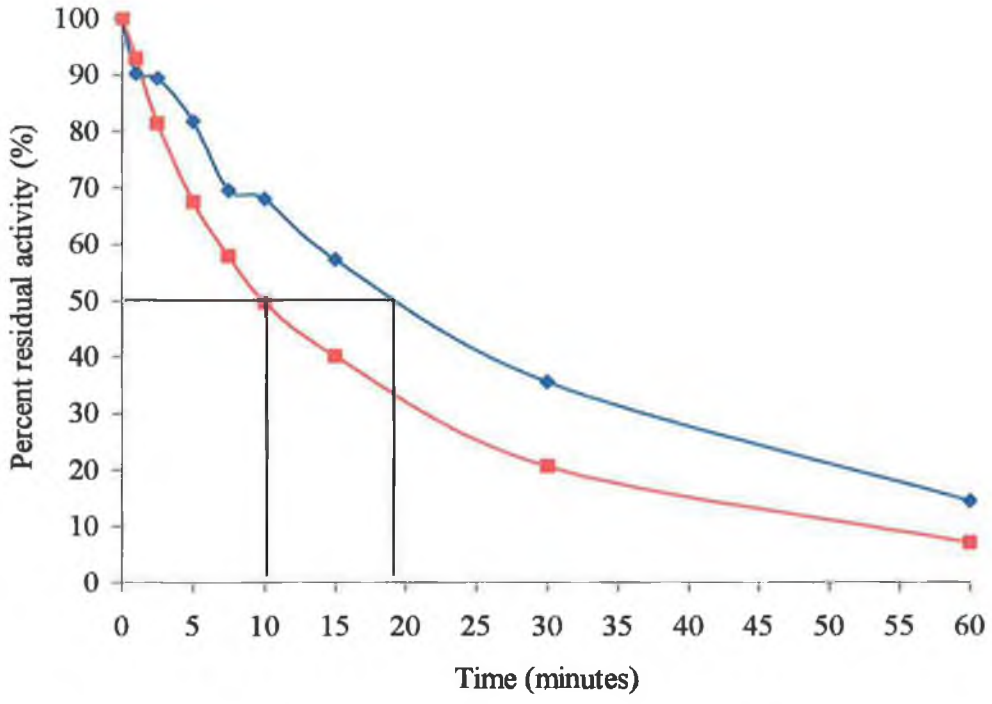

Figure 7.4: Thermal inactivation assay of native and dextran dialdehyde-modified SBP at 75°C. The $t_{1/2}$ of the native SBP is seen to be approximately 19 minutes and the $t_{1/2}$ of the dextran dialdehyde-modified SBP is 10 minutes native SBP — and dextran dialdehyde-modified SBP —.

7.2.2: Modification of peroxidase enzyme by the introduction of Adipic acid dihydrazide:

A thermal inactivation assay of native and AADH-modified SBP was carried out at 75°C. The $t_{1/2}$ for native SBP was estimated to be 16 minutes and that for AADH-modified SBP was 32 minutes. From this experiment, the kinetic stability of the modified SBP preparation was seen to double at 75°C.

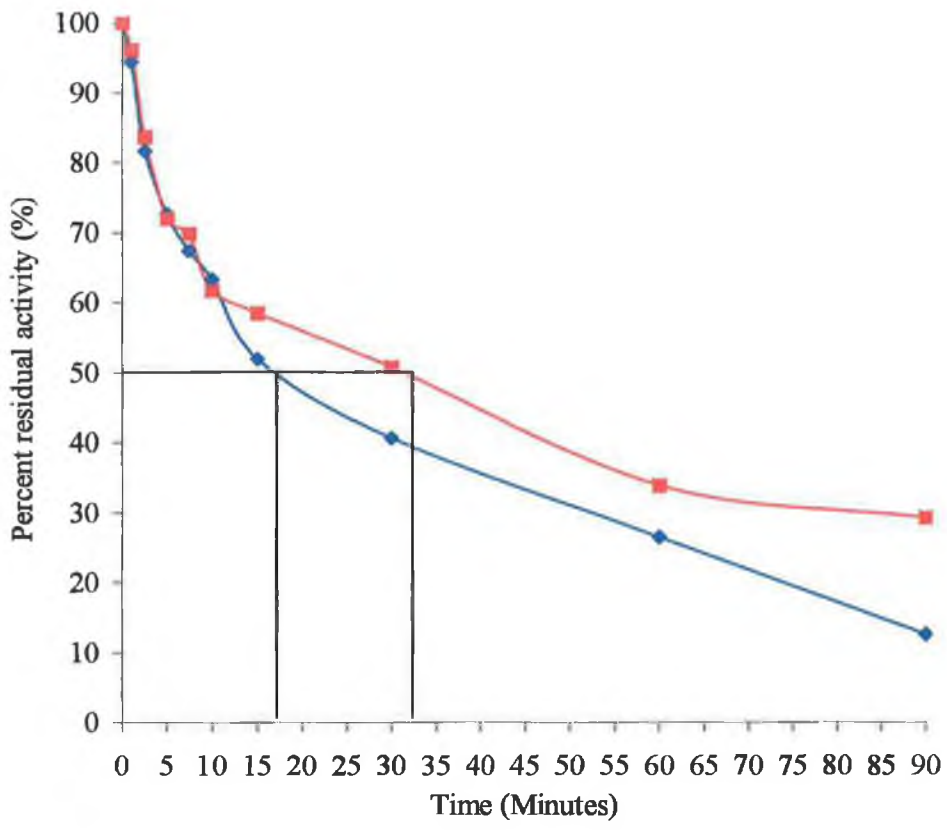

Figure 7.2.2.1: Thermal inactivation at 75°C of SBP chemically modified with AADH. The $t_{1/2}$ for the native SBP was determined graphically to be approximately 16 minutes while that of AADH modified SBP was 32 minutes. —◆— Native SBP, —■— AADH-modified SBP.

Table 7.1: A summary of the chemical modifications performed on SBP and their results as compared to the native form of the enzyme.

Enzyme preparation	Recovery of enzyme (%)	RZ value	Number of free amines †	Extent of stabilisation (Change in stability over native form)	Thermal inactivation ($t_{1/2}$, mins at 75°C)
Native SBP	100.0	2.9	3	-	16
SBP + amines	174.5	2.5	35	ND	ND
SBP dextran dialdehyde	87.5	1.9	-	38% decrease	10
SBP EG-NHS	77.3	2.5	-	No change	16
SBP AADH	65.3	2.0	-	200% increase	32

ND: not determined.
†: TNBS method (Section 2.9)

7.3: Discussion:

Covalent chemical modification is a powerful approach for tailoring proteins and enzymes to enhance their biocatalytic stability (DeSantis and Jones, 1999). The residues in HRP that are involved in a successful EG-NHS modification are Lys 232, 241, and 174 (O'Brien, *et al.* 2001). These lysine residues are not found in the SBP sequences as detailed by Welinder and Larsen (2004) and Henriksen *et al.* (2001) and, are replaced by Lys 232 → Arg, Lys 241 → Asn and Lys 174 → Arg, (Figure 7.5). In light of this, the EG-NHS method was not likely to return a highly modified SBP enzyme. Thus amine specific chemical modifiers are not likely to yield stabilised forms of SBP. Since SBP has no free Cys (all involved in it 4 – S – S - bridges), thiol specific reagents are unlikely to be successful either.

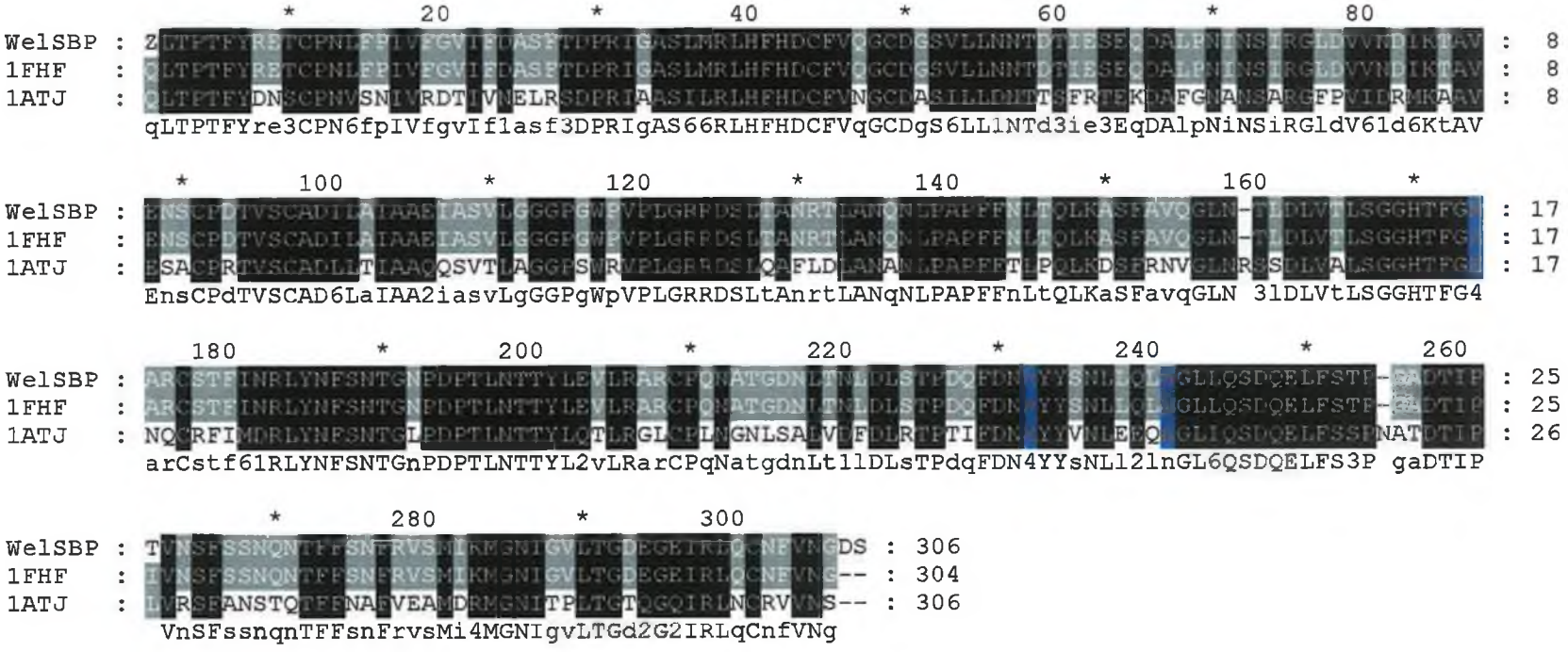

Figure 7.6: Sequence alignment of SBP (WelSBP, Welinder and Larsen, 2004 and 1FHF, Henriksen *et al.* 2001) and HRP (1ATJ, Gajhede *et al.* 1997). The residues coloured red indicate the lysine residues in HRP that bind EG-NHS as reported by O'Brien *et al.* (2001). The reactive Lys residues in HRP are replaced by Lys 232 → Arg, Lys 241 → Asn and Lys 174 → Arg in SBP.

Several problems arose with the dextran dialdehyde modification. The method was a multi-step modification with dialysis steps involved, as a result of multiple dialysis steps sample was lost over time. The most problematic area with the was with the use of the zero length cross-linker [1-(3-dimethylaminoproypl)-3-ethylcarbodiimide hydrochloride] (EDC). The first supplier was Sigma-Aldrich and successive batches of EDC failed repeatedly. The company (while unwilling to admit there was a problem with the product) offered to replace preparations that didn't work for no charge. Following successive failures however, the offer was not taken up. Since the EDC step was one of the last steps the modification protocol had to be completed before it was possible to detect if the modification had been a success. This meant that the assay could have failed at the EDC method and it would not be detected until the last step. When, after repeated attempts, the method failed to produce an improved enzyme, it was abandoned. It was only at a later stage when preparing for the ferrocene carboxylic acid modification (Section 2.24) that another source of EDC was utilised available namely Pierce. It was hoped to reproduce the dextran dialdehyde modification with the new source of EDC, but due to time constraints this was not possible.

Successful oxidation of the sugar moieties of carbohydrate groups followed by amination results in an increased absorbance at 420nm in the TNBS assay. After a successful AADH modification the free aldehyde groups should have been modified by one of the hydrazine groups from AADH, the other end can bind to another free aldehyde group. This results in the decrease in the absorbance in the TNBS assay (Bystrický, *et al.* 1999).

The $t_{1/2}$ of AADH-modified SBP shows a two-fold increase from 16 to 33 minutes. Kozulić *et al.* (1987) showed increases in thermostability following successful AADH modification of glucose oxidase, invertase and especially of acid phosphatase At pH 11, AADH-modified alkaline phosphatase had a $t_{1/2}$ of approximately 24 hours over the native $t_{1/2}$ of approximately 45 minutes. The present result was fitted to second order plot (Enzfitter software), indicating that there were at least two events contributing to the inactivation of the enzyme. Up to 10 minutes as seen in Figure 7.2.2.1 there is no difference between native and modified; the process of thermal inactivation is seen to be biphasic; this would indicate that, in the modified solution, there is a mixture of the native and modified enzyme preparations. One reason why the modification was only moderately successful is that hydrazine is an inhibitor for haem-containing proteins, showing a high specificity for the δ meso-haem edge of the prosthetic group of peroxidase enzymes (Zhu *et al.* 1997). To overcome this problem the concentration of AADH was significantly decreased to 5mM AADH from 500mM (Brugger *et al.* 2001). As a result of decreasing the concentration of the cross-linker the extent of modification will be reduced. It may be possible to overcome the adverse effect of AADH on the haem group by using a competitive inhibitor. One of the best studied is the aromatic benzhydroxamic acid (BHA), which binds in a competitive fashion to the aromatic donor-binding site of the haem group (Smith *et al,* 1992). This would prevent the AADH from attacking the haem group and a higher concentration of AADH could be used to yield a higher degree of modification of SBP.

A number of chemical modifications have been illustrated in this Chapter; however, due to one reason or another they failed to produce the desired effect of stabilisation of SBP.

CHAPTER 8

CONCLUSION

8: Conclusion:

SBP (a class III peroxidase that has been used in research and industrial applications only recently) is found in the hulls of the soybean. It is cheap to source and relatively easy to purify. SBP is a heme peroxidase that has been shown to have a high tolerance against temperature, pH and solvents (M^{c}Eldoon and Dordick, 1996). The enzyme used in this study was obtained as a food grade preparation. It was shown to have no contaminating proteolytic activity. Assays for activity were optimised for this SBP source, with respect to time of assay and concentrations of enzyme and substrates to be used. It was shown that SBP has a T_{50} of 75°C (greater than that of HRP (~ 65°C), the archetypal peroxidase of biochemical and biosensor research) and a $t_{1/2}$ of 14 minutes at 75°C. Of the studied solvents DMSO, was the only one to have a significant effect on the catalytic activity of SBP, which lost approximately 90% activity at 80% v/v DMSO. SBP is active in the pH range from 2-10, much greater than HRP, which is active from approximately pH 6-9. SDS-PAGE analysis showed that SBP had a molecular weight of approximately 44kDa, and IEF analysis showed it having an isoelectric point of 4.3, while native PAGE gels showed a single band for the purified enzyme (the enzyme was purified according to the protocol of Nissum *et al* (2001)). The TNBS assay showed that it had three available lysine residues as reported by Henriksen *et al.* (2001) and Welinder and Larsen (2004). Certain lysine residues in the amino acid of HRP have been used to cross-link the protein modifier EG-NHS to the polypeptide. However, SBP is lacking the required lysine residues (O'Brien *et al.* 2001) for successful cross-linking with EG-NHS.

The aim of this work was to make and characterise a biosensor for the detection of H_2O_2. Since Vreeke *et al.* (1995) reported the first SBP biosensor, there has been a

increasing number of reports in the literature of the use of SBP in a biosensor configuration. SBP is a highly glycosylated plant enzyme (18% of its 44kDa weight). As a result of its sugar moieties, the distance the electrons have to travel from the active site to the transducer is large, causing a decreased signal. An $[Os(bpy)_2(PVP)_{10}Cl]^+$ mediator polymer was synthesized to aid electron transfer from the SBP active site to the surface of the electrode. Amperometric time current assays showed that the mediator-SBP biosensor could detect 5μmol additions of H_2O_2 to the system. A standard curve for H_2O_2 was constructed for H_2O_2.

A derivative of the mediator ferrocene (ferrocene carboxylic acid) was covalently attached to the oxidised glycans of SBP. The purpose of this modification was to improve electron transfer by reducing the distance the electrons have to migrate before coming in contact with the electrode surface. Successful attachment of the ferrocene carboxylic acid was confirmed by atomic absorption spectroscopy. This was followed by electrochemical characterisation of the modified SBP with mediator$[Os(bpy)_2(PVP)_{10}Cl]^+$ on a 25μm platinum microelectrode. It was shown (by i-t analysis) that the ferrocene-modified SBP performed better than the native SBP and mediator biosensor in response to the presence of H_2O_2 in this system.

Further investigations into the ferrocene-modified SBP explored the possibilities of direct communication between SBP and the electrode surface in the absence of mediator. In an effort to prevent leaching of SBP from the electrode surface, a cavity was etched in the electrode using aqua regia. SEM image analysis showed that a cavity had been formed. The newly etched electrode had an electrochemical signal and the etching had no deleterious effects on the electrode. Initially native SBP was

immobilised into the cavity of the microelectrode without any mediator. Electrochemical studies showed that a signal was obtained and direct electron transfer was occurring. The ferrocene-modified SBP was re-immobilised into the cleaned cavity and, as before, direct electron transfer was shown to occur. Amperometric i-t analysis showed a greater current response to H_2O_2 for ferrocene-modified SBP over native SBP. This was shown in the slopes (2.87 for the native and 10.11 for the ferrocene-modified SBP) of the standard curve constructed from the i-t results. There is nearly a four times increase between the two biosensor configurations.

Comparison of these results with the literature show that the ferrocene-modified SBP has a greater response than other biosensors using SBP as the biological sensing material. The use of a platinum microelectrode was shown to be successful as well as the co-immobilisation of an Os based mediator and native and/or ferrocene-modified SBP. Further investigations should focus on trying to increase the degree of covalent attachment of ferrocene carboxylic acid to the aminated SBP.

Other chemical modifications were carried out on SBP aimed at improving its stability still further, but due to one problem or another as explained (in Chapter 7) they failed to return the beneficial results anticipated. The dextran dialdehyde procedure showed promise but due to circumstances beyond experimental control the modification didn't perform to the extent anticipated. The AADH modification, even with reduced cross-linker concentrations resulted in significant loss of catalytic activity. Reducing the concentration of the cross-linker will also reduce the extent of any chemical modification as compared to the published results of Brugger *et al.* (2001), who achieved very good increases in thermostability of a fungal phytase.

In summary, the experiments described in this thesis have achieved the following successes. The use of SBP with and Os based mediator in a Pt microelectrode based biosensor. The covalent attachment of ferrocene units to the glycans of SBP, leading to and improved electrochemical responses to the analyte H_2O_2. The method of attachment appears to be easier to perform than the other modification using ferrocene units to glycans of an enzyme as reported by Schuhmann (2002). Direct mediator free electrochemical coupling between SBP and an etched Pt microelectrode has been shown to occur. Once again the ferrocene-modified SBP gave notably improved responses in this electrode configuration than native SBP. An improved understanding of the scope and limitations of chemical modification as a strategy for the manipulation/modulation of SBP properties such as stability has been investigated. Together these results demonstrate the flexibility of a number of novel biosensor configurations, indicate numerous avenues for further study and provide a fuller understanding of the potential role of SBP in amperometric electrochemical biosensors.

REFERENCES

References:

Aebi, H., E. (1974). Catalase. Methods in Enzymatic Analysis, Third edition. H., Ù Bergmeyer (ed). Verlag Chemie Weinheim. pp 627-628.

Alfonta, L. Singh, A., K. and Wilner, I. (2001). Liposomes labelled with biotin and horseradish peroxidase: a probe for the enhanced amplification of antigen-antibody or oligonucleotides-DNA sensing processes by the precipitation of an insoluble product on electrodes. *Analytical Chemistry.* **73.** 91-102.

Alegret, S. Alonso, J. Bartrolí, J. Céspedes, F. Martínez-Fàbergas, E. and del Valle, M. (1996). Amperometric biosensors based on bulk-modified epoxy graphite biocomposites. *Sensors and Materials.* **8** (3)**.** 147-153.

Amisha Kamal, J., K. and Behere, D., V. (2002a). Thermal and conformational stability of seed coat soybean peroxidase. *Biochemistry.* **41.** 9034-9042.

Amisha Kamal, J., K. and Behere, D., V. (2002b). Thermal unfolding of soybean peroxidase. Appropriate high denaturant concentrations induce cooperativity allowing the correct measurement of thermodynamic parameters. *The Journal of Biological Chemistry.* **27** (43). 40717-40721.

Amisha Kamal, J., K. and Behere, D., V. (2003). Activity, stability and conformational flexibility of seed coat soybean peroxidase. *Journal of Inorganic Biochemistry.* **94.** 236-242.

Bagree, A. Sharma, I., K. Gupta, K., C. Narang, C., K. Saund, A., K. and Mathur, N., K. (1980). Modification of ε-amino group of lysine in proteins by acylation with pyromellitic dianhydride and *o*-sulphobenzoic anhydride. *FEBS Letters.* **120** (2). 275-277.

Bairoch A. (1993). The ENZYME data bank. *Nucleic acid research.* **21**, 3155-3156

Bartlett, P., N. and Pratt, K., F., E. (1995). Theoretical treatment of diffusion and kinetics in amperometric immobilized enzyme electrodes Part I: Redox mediator entrapped within the film. *Journal of Electroanalytical Chemistry.* **397.** 61-78.

Bartlett, P., N. Whitaker, R., G. Green, M., J. and Frew, J. (1987). Covalent binding of electron relays to glucose oxidase. *Journal of the Chemical Society, Chemistry Communications.* 1603-1604.

Bedard P, and Mabrouk P., A. (1997) Resonance Raman Spectroscopy of Soybean peroxidase. *Biochemical and Biophysical Research Communications.* **240** 65-67.

Berkowitz, D., B. and Webert, D., W. (1981). The inactivation of horseradish peroxidase by a polystyrene surface. *Journal of Immunological Methods.* **47**, 121-124.

Berman, H. M., Westbrook, J., Feng, Z., Gilliland, G., Bhat, T, N., Weissig H., Shindyalov, I. N., Bourne, P. E., (2000). The Protein Data Bank. *Nucleic Acids Research*, **28** 235-242.

Bickerstaff G., F. and Zhou H. (1993). Protease activity and autodigestion (autolysis) assays using Coomassie blue dye binding. *Analytical Biochemistry.* **210**, 155-158.

Boguslavsky, L., Hale, P., D. Geng, L. Skotheim, T., A. and Lee, H-S. (1993). Applications of redox polymers in biosensors. *Solid State Ionics.* **60.** 189-197.

Bradford, M., M. (1976). A rapid and sensitive method for the quantitation of microgram quantities of protein utilizing the principles of protein-dye binding. *Analytical Biochemistry.* **72**, 248-254.

Brugger, R. Kronenberger, A. Bischoff, A, Hug, D. Lehmann, M, van Loon, A., P., G., M, and Wyss, M. (2001). Thermostability engineering of fungal phytases using low-M_r-additives and chemical crosslinking. *Biocatalysis and Biotransformations.* **19.** 505-516.

Bucke, C. (1987). Cell immobilisation in calcium alginate. *IN:* K. Mosbach (ed.). *Methods in Enzymology.* **135** (B). New York: Academic Press. pp175-189

Bystrický, S. Machová, E. Malovíková, A. and Kogan, G. (1999). Determination of the cross-linking effect of adipic acid dihydrazide on glycoconjugate preparation. *Glycoconjugate Journal.* **16.** 691-695.

Carraway, K., L. and Koshland, Jr. D., E. (1972). Carbodiimide modification of proteins. *IN:* K., L. Carraway, and D., E. Koshland, Jr. (eds.). *Methods in Enzymology.* **25.** New York: Academic Press. pp616-623.

Calvo, E., J. and Danilowicz, C. (1997). Amperometric enzyme electrodes. *Journal of the Brazilian Chemical Society.* **8** (6). 563-574.

Carbodiimide coupling using EDC. Available from http://chem.ch.huji.ac.il/~eugeniik/edc.htm. [Accessed 17-May-2002].

Cass, A., E., G. Davis, G. Francis, G., D. Hill, H., A., O. Aston, W., J. Higgins, I., J. Plotkin, E., V. Scott, L., D., L. and Turner, A., P., F. (1984). Ferrocene-mediated enzyme electrode for amperometric determination of glucose. *Analytical Chemistry.* **56.** 667-671.

Cass, A., E., G. Davis, G. Green, M., J. and Hill, H., A., O. (1985). Ferricinium ion as an electron acceptor for oxido-reductases. *Journal of Electroanalytical Chemistry.* **190.** 117-127.

Cassidy, J., F. Doherty, A., P. and Vos, J., G. (1998). Amperometric methods of detection. *IN:* Diamond, D. *Principles of chemical and biological sensors.* New York John Wiley and Sons Inc. 73-132.

Caza, N. Bewtra, J., K. Biswas, N. and Etaylok, K. (1999). Removal of phenolic compounds from synthetic wastewater using soybean peroxidase. *Water Research.* **33** (13). 3012-2018.

Česi, V. Kozulić, B. and Barbarić, S. (1993). A process for stabilisation of glycoproteins. *IN:* W., J., J. van den Tweel, A. Harder, and R., M. Buitelaar, (eds.). *Stability and Stabilisation of Enzymes.* Maastricht. Elsevier Science Publishers B., V. pp247-253.

Chattopadhyay, K. and Mazumdar, S. (2000). Direct electrochemistry of heme proteins: effect of electrode surface modification by neutral surfactants. *Bioelectrochemistry.* **53** 17-24.

Chen H. B, and Vierling R. A. (2000) Molecular cloning characterisation of soybean peroxidase gene families. *Plant Science.* **150** 129-137.

Chibata, I. Tosa, T. Sato, T. and Takata, I. (1987). Immobilisation of cells in carrageenan. *IN:*K. Mosbach. *Methods in Enzymology.* **135 (B).** New York: Academic Press. pp189-198.

Childs, R., E. and Bardsley, W., G. (1975). The steady state kinetics of peroxidase with 2,2'-Azino-di-(3-ethyl-benthiazoline-6-sulphonic acid) as chromogen. *Biochemical Journal.* **145**. 93-103.

Choi, J-W. Lim, I., H. Kim, H., H. Min, J. and Lee, W., H. (2001). Optical peroxide biosensor using the electrically controlled-release technique. *Biosensors and Bioelectronics.* **16.** 141-146.

Chuang, C., L. Wang, Y., J. and Lan, H., L. (1997). Amperometric glucose sensors based on ferrocene-containing B-polyethylenimine and immobilised glucose oxidase. *Analytica Chimica Acta.* **353.** 37-44.

Clark, D., S. (1994). Can immobilisation be exploited to modify enzyme activity? *Trends in Biotechnology.* **12.** 439-443.

Clark, L., C. and Lyons, C. (1962). *Annals of the New York Academy of Science.* **102.** 29-45.

Classification and nomenclature of enzyme catalysis reactions. www.chem.qmw.ac.uk/iubmb/enzym.e/rules.html [First accessed: 28-May-2000].

Cleland, W., W. (1970). Steady state kinetics *IN:* P., D. Boyer (ed.), *The Enzymes, kinetics and mechanism. Volume II.* 3rd edition. New York. Academic Press. 1-64.

Cosnier, S. Le Pellec, A. Marks, R., S. Périé, K. and Lellouche, J-P. (2003). A permselective biotinylated polydicarbazole film for the fabrication of amperometric enzyme electrodes. *Electrochemistry Communications.* **5.** 973-977.

Creighton, T., E. (1990). Disulphide bonds between cysteine residues. *IN:* T., E. Creighton (ed.). *Protein structure, a practical approach.* Oxford. IRL Press at Oxford University Press. pp155-168.

Crumbliss, A., L. Stonehuerner, J., G. and Henkens, R., W. (1993). A carrageenan hydrogel stabilised colloidal gold multi-enzyme biosensor electrode utilising immobilised horseradish peroxidase and cholesterol oxidase/ cholesterol esterase to detect cholesterol in serum and whole blood. *Biosensors and Bioelectronics.* **8.** 331-337.

Csöregi, E. Jönsson-Pettersson, G. and Gorton, L. (1993). Mediatorless electrocatalytic reduction of hydrogen peroxide at graphite electrodes chemically modified with peroxidases. *Journal of Biotechnology.* **30**. 315-337.

Davis, G. (1985). Electrochemical techniques for the development of amperometric biosensors. *Biosensors.* **1.** 161-178.

da Silva M. E, and Franco T., T. (2000) Purification of soybean peroxidase (*Glycine max*) by metal affinity partitioning in aqueous two-phase systems. *Journal of Chromatography B.* **743** 287-294.

Degani, Y., and Heller, A. (1987). Direct electrical communications between chemically modified enzymes and metal electrodes. 1 Electron transfer from glucose oxidase to metal electrodes via electron relays, bound covalently to the enzyme. *Journal of Physical Chemistry.* **91** (6). 1286-1289.

DeSantis, G. and Jones, J., B (1999). Chemical modification of enzymes for enhanced functionality. *Current Opinion in Biotechnology.* **10.** 324-340.

Dunford, H., B. (1998). Catalytic mechanisms of plant peroxidases: with emphasis on reactions of compounds I and II. *IN:* H. Greppin, Penel, C, and Gaspar, T. *Molecular and Physiological aspects of plant peroxidases.* Genève: University of Genève Press. pp15-24.

Dunford, H., B. (1999). Horseradish peroxidase. *IN:* J. Everse and K. Everse. *Peroxidases in chemistry and biology.* Boca Raton: CRC Press. pp2-24.

Dunford, H., B. (1999). *Heme Peroxidases.* Toronto, Wiley VCH.

Ferapontova, E., E. Grigorenko, V., G. Egorov, A. (2001a). P-chip and P-chip bienzyme electrodes based on recombinant forms of horseradish peroxidase immobilised on gold electrodes. *Biochemistry (Moscow).* **66** (8). 1026-1035.

Ferapontova, E., E. Grigorenko, V., G. Egorov, A., M. Börchers, T., Ruzgas, T., and Gorton, L., (2001b). Mediatorless biosensor for H_2O_2 based on recombinant forms of horseradish peroxidase directly adsorbed on polycrystalline gold. *Biosensors and Bioelectronics.* **16**, 147-157.

Ferapontova, E., E. Grigorenko, V., G. Egorov, A., M. Börchers, T., Ruzgas, T., and Gorton, L., (2001c). Direct electron transfer in the system gold electrode-

recombinant horseradish peroxidase. *Journal of Electroanalytical Chemistry.* **509.** 19-26.

Ferapontova, E., and Puganova, E. (2002). Effect of pH on direct electron transfer between graphite and horseradish peroxidase. *Journal of Electroanalytical Chemistry.* **518.** 20-26.

Fersht, A. (2002). *Structure and mechanism in protein science. A guide to enzyme catalysis and protein folding.* New York: W., H. Freeman and Company.

Fields, R. (1971). The measurement of amino groups in proteins and peptides. *Biochemical Journal.* **124**, 581-590.

Findl, E. Strope, E., R. and Conti, J., C. (1985). Electrochemical techniques in the biological sciences. *IN:* Srinivasan, S. Chizmadzhev, Y., A. Bockris, J., O'M.

Forster, R. (1994). Microelectrodes: new dimensions in electrochemistry. *Chemical Society Reviews.* 289-297.

Forster, R. (1998). Miniaturised chemical sensors IN: Diamond, D. *Principles of Chemical and Biological Sensors.* New York. John Wiley and Sons, Inc. 235-261.

Foulds, N., C. and Lowe, C., R. (1988). Immobilisation of glucose oxidase in ferrocene modified pyrrole polymers. *Analytical Chemistry.* **60.** 2473-2478.

Franks, F. (1993). Conformational stability of proteins. *IN:* F. Franks. *Protein Biotechnology, Isolation, characterisation and stabilization.* New Jersey. The Humana Press. pp395-436.

Frew, J., E. and Hill, H., A., O. (1987). Electron-transfer biosensors. *Philosophical Transactions of the Royal Society of London, Series B.* **316.** 95-106.

Frew, J., E. and Hill, H., A., O. (1988). Direct and indirect electron transfer between electrodes and redox proteins. *European Journal of Biochemistry.* **172.** 261-269.

Gajhede M, Schuller D, Henriksen A, Smith A, Poulos T. (1997). Crystal structure of Horseradish peroxidase C at 2.15Å resolution. *Nature Structural Biology.* **4** (12). 1032-1038

García Armada, M., P. Losada, J. Cuadrado, I. Alonso, B. González, B. Ramírez-Oliva, E. and Casado, C., M. (2003). Electrodes modified with a siloxane copolymer containing interacting ferrocenes for determination of hydrogen peroxide and glucose. *Sensors and Actuators B.* **88.** 190-197.

Gaspar, S. Habermüller, K. Csöregi, E. and Schuhmann, W. (2001). Hydrogen peroxide sensitive biosensor based on plant peroxidases entrapped in Os-modified polypyrrole films. *Sensors and Actuators B.* **72.** 63-68.

Gaspar S, Popescu I. C, Gazaryan I. G, Bautista A. G, Sakharov I. Y, Mattiasson B, and Csöregi E. (2000). Biosensors based on novel plant peroxidase: a comparative study. *Electrochimica Acta.* **46** 255-264.

Ghindilis, A., L. Atanasov, P. and Wilkins, E. (1996). Potentiometric immunoelectrode for fast assay based on direct electron transfer catalysed by peroxidase. *Sensors and Actuators B.* **34.** 528-532.

Ghosh (Hazra), S. Sarker, D. and Misra, T., N. (1998). Development of an amperometric enzyme electrode biosensor for fish freshness detection. *Sensors and Actuators B.* **53.** 58-62.

Gianfreda, L. and Scarfi, M., R. (1991). Enzyme stabilisation: state of the art. *Molecular and Cellular Biochemistry.* **100.** 97-128.

Gilfoyle, D., J. Rodriguez-Lopez, J., N. and Smith A., T. (1996). Probing the aromatic-donor-binding site of horseradish peroxidase using site-directed mutagenesis and the suicide substrate phenylhydrazine. *European Journal of Biochemistry.* **236**. 714-722.

Goldstein, L. (1976). Kinetic behaviour of immobilized enzyme systems *IN:* Mosbach. K. *Methods in Enzymology.* **44**. New York. Academic Press. 397-450.

Goodwin, D. C., Yamazaki, I., Aust, S. D., and Grover, T. A., (1995). Determination of rate constants for rapid peroxidase reactions. *Analytical Biochemistry.* **231**. 333-338.

Gray J. S. S, and Montgomery R. (1997). The *N*-glycosylation sites of soybean seed coat peroxidase. *Glycobiology.* 7 (5) 679-685.

Gray J. S. S, Yang B. Y, Hull S. R, Venzke D. P, and Montgomery R. (1996) The glycans of soybean peroxidase. *Glycobiology.* **6** (1). 23-32.

Gregg, B., A. and Heller, A. (1990). Cross-linked redox gels containing glucose oxidase for amperometric biosensor applications. *Analytical Chemistry.* **62.** 258-263.

Gülce, H., Aktas, Y., S. Gülce, A. and Yildiz, A. (2003). Polyvinylferrocenium enzyme electrode for choline analysis. *Enzyme and Microbial Technology.* **32.** 895-899.

Habermüller, K. Mosbach, M. and Schuhmann, W. (2000). Electron-transfer mechanisms in amperometric biosensors. *Fresenius Journal of Analytical Chemistry.* **366.** 560-568.

Haughland, R., P. (2001). Introduction to Crosslinking Reagents. *Handbook of fluorescent probes and research products.* Eighth edition. [CD-ROM]. Available from: Molecular Probes. Eugene, Oregon [Accessed 03-May-2004].

Heller, A. (1992). Electrical connection of enzyme redox centres to electrodes. *Journal of Physical Chemistry.* **23.** 128-.

Heller, A. (1996). Amperometric biosensors. *Current Opinion in Biotechnology.* **7.** 50-54.

Heller, A. and Degani, Y. (1988). Direct electrical communication between chemically modified enzymes and metal electrodes: III electron-transfer relay modified glucose and D-amino-acid oxidase. *IN:* G. Dryhurst and K. Niki (eds) *Redox chemistry and interfacial behaviour of biological molecules. Procedures of the 3rd international symposium on redox mechanisms and interfacial properties of molecules of biological importance.* New York: Plenum Press. pp151-171.

Heller A, and Vreeke M. S. (1997). E. Heller and Company. *Soybean peroxidase electrochemical sensor.* United States Patent. US. 5665222.

Helmerhorst, E. and Stokes, G., B. (1980). Microcentrifuge desalting: a rapid, quantitative method for desalting small amounts of protein. *Analytical Biochemistry.* **104.** 130-135.

Henriksen A, Mirza O, Indiani C, Teilum K, Smulevich G, Welinder K. G, and Gajhede M. (2001) Structure of soybean seed coat peroxidase: A plant peroxidase with unusual stability and haem-apoprotein interactions. *Protein Science.* **10**. 108-115.

Henriksen A., Smith A., and Gajhede M. (1999) The structures of the horseradish peroxidase C-ferulic acid complex and the ternary complex with cyanide suggest how peroxidases oxidise small phenolic substrates. *Journal of Biological Chemistry.* **274**, (49), 35005-35011.

Hermanson, G., T. (1996). *Bioconjugate Techniques.* Toronto. Academic Press. 39, 140, 169-170

Hertzberg, S. Kvittingen, L. Anthonsen, T. and Skjak-Braek, G. (1992). Alginate as immobilisation matrix and stabilising agent in a two-phase liquid system: Application in lipase-catalysed reactions. *Enzyme Microbial Technology.* **14.** 42-47.

Hoare, D., G. and Koshland, Jr. D., E. (1966). A procedure for the selective modification of carboxyl groups in proteins. *Journal of American Chemical Society.* **88** (9). 2057-2058

Hodgson, A., J. Spencer, M., J. and Wallace, G., G. (1992). Incorporation of proteins into conducting electroactive polymers. *Reactive Polymers.* **18.** 77-85.

Hogan C., F., (1999). *Electrochemiluminescent sensing based on ruthenium poly(pyridyl) systems.* Ph. D. Thesis. Dublin City University.

Horvath, C. and Engasser, J-M. (1974). External and internal diffusion in heterogeneous enzyme systems. *Biotechnology and Bioengineering.* **16**. 909-923.

Isgrove, F., H. Williams, R., J., H. Niven, G., W. and Andrews, A., T. (2001). Enzyme immobilisation on nylon optimisation and the steps used to prevent enzyme leakage from the support. *Enzyme and Microbial Technology.* **28.** 225-232.

Ivanova, E., V. Sergeeva, V., S. Oni, J. Kurzawa, C. Ryabov, A., D. and Schuhmann, W. (2003). Evaluation of redox mediators for amperometric biosensors: Ru-complex modified carbon-paste/enzyme electrodes. *Bioelectrochemistry.* **60.** 65-71.

Iwuoha, E. I. Smyth, M. R. and Vos, J. G. (1994). Amperometric glucose sensor containing nondiffusional osmium centers: analysis of organic-phase responses. *Electroanalysis.* **6** 982-989.

Jiang, H. Zou, H. Wang, H, Ni, J. Zhang, Q. and Zhang, Y. (2000). On-line characterisation of the activity and reaction kinetics of immobilised enzymes by high-performance frontal analysis. *Journal of Chromatography A.* **903.** 77-84.

Josephy, P., D. Eling, T. and Mason, R., P. (1982). The horseradish peroxidase-catalysed oxidation of 3,5,3',5'-tetramethylbenzidine. Free radical and charge-transfer complex intermediates. *The Journal of Biological Chemistry.* **257** (7). 3669-3675.

Kamin, R., A. and Wilson, G., S. (1980). Rotating ring-disk enzyme electrode for biocatalysis kinetic studies and characterisation of an immobilised enzyme layer. *Analytical Chemistry.* **52** (8). 1198-1205

Kataky, R. Dell, R. and Senanayake, P., K. (2003). Cyclodextrin-modified biosensors: comparison of cyclodextrin-linker ferrocenes as mediators in sol-gel and screen-printed formats for sensing acetylcholine. *The Analyst.* **126.** 2015-2019.

Katz, E. (2002). Mediated electron-transfer between redox-enzymes and electrode supports. *IN.* A. Bard and J. Stratmann. *Encyclopaedia of Electrochemistry, Bioelectrochemistry.* **9.** New York. John Wiley and Sons Inc. 561-626.

Katz, E. Heleg-Shabati, V. Willner, B. Willner, I. and Bückmann, A., F. (1997). Electrical contact of redox enzymes with electrodes: novel approaches for amperometric biosensors. *Bioelectrochemistry and Bioenergetics.* **42.** 95-104.

Kenausis G, Chen Q, and Heller A. (1997). Electrochemical glucose and lactate sensors based on "wired" thermostable soybean peroxidase operating continuously and stably at 37°C. *Analytical Chemistry.* **69** 1054-1060.

Khajeh, K. Naderi-Manesh, H. Ranjibar, B. Moosavi-Movahedi, A., A. and Nemat-Gorgan, M. (2001). Chemical modification of lysine residues in *Bacillus α-amylases*: effect on activity and stability. *Enzyme and Microbial Technology.* **28.** 543-549.

Kim, Y., H. An, E., S. Song, B., K. Kim, D., S. and Chelikani, R. (2003). Polymerisation of cardonal using soybean peroxidase and its potential application as anti-biofilm coating material. *Biotechnology Letters.* **25** (18). 1521-1524.

Kinsley, C and Nicell, J., A. (2000). Treatment of aqueous phenol with soybean peroxidase in the presence of polyethylene glycol. *Bioresource Technology.* **73.** 139-146.

Kissinger, P., T. and Heineman, W, R. (1983). Cyclic voltammetry. *Journal of Chemical Education.* **60** (9), 702-706.

Klibanov, A., M. (1986). Enzymes that work in organic solvents. *Chemtech.* 354-359.

Kong, Y-T. Boopathi, M. and Shim, Y-B. (2003). Direct electrochemistry of horseradish peroxidase bonded on a conducting polymer modified glassy carbon electrode. *Biosensors and Bioelectronics.* **19.** 227-232.

Kozulić, B. Leuštek, I. Pavlović, B. Mildner, P. and Barbarić, S. (1987). Preparation of the stabilised glycoenzymes by cross-linking their carbohydrate chains. *Applied Biochemistry and Biotechnology.* **15.** 265-278.

Krajewska, B. (1991). Chitin and its derivatives as supports for immobilisation of enzymes. *Acta Biotechnologica.* **3.** 269-277.

Kulys, J., J. and Samalius, A., S. (1983). Kinetics of biocatalytic current generation. *Bioelectrochemistry and Bioenergetics.* **10.** 385-393.

Kulys, J. and Schmid, R., D. (1990). Mediatorless peroxidase electrode and preparation of bienzyme sensors. *Bioelectrochemistry and Bioenergetics.* **24.** 305-311.

Lambrechts, W. and Sansen, W. (1996). *Biosensors: Microelectrochemical devices.* Philadelphia. Institute of Physics Publishing.

Laemmli, U., K. (1970). Cleavage of structural proteins during the assembly of the head of bacteriophage T4. *Nature.* **227.** 680-685.

Lange, M., A. and Chambers, J., Q. (1985). Amperometric determination of glucose with a ferrocene-mediated glucose oxidase/polyacrylamide gel electrode. *Journal.* **B.** 89-97.

Lei, C. and Deng, J. (1996). Hydrogen peroxide sensor based on coimmobilized methylene green and horseradish peroxidase in the same Montmorillonite-modified bovine serum albumin-glutaraldehyde matrix on a glassy carbon electrode surface. *Analytical Chemistry.* **68** 3344-3349.

Li, W. Wang, Z. Sun, C. Xian, M. and Zhao. (2000). Fabrication of multilayer films containing horseradish peroxidase and polycation-bearing Os complex by means of

electrostatic layer-by-layer adsorption and its applications as a hydrogen peroxide sensor. *Analytica Chimica Acta.* **418.** 225-232.

Liem, H., H. Cardenas, F. Tavassoli, M. Poh-Fitzpatrick, M., B. and Muller-Eberhard, U. (1971). Quantitative determination of hemoglobin and cytochemical staining for peroxidase using 3,3',5,5'-Tetramethylbenzidine dihydrochloride, a safe substitute for benzidine. *Analytical Biological Chemistry.* **98**, 388-393.

Limoges, B. and Savéant, J-M. (2003). Cyclic voltammetry of immobilized redox enzymes. Interference of steady state and non-steady-state Michaelis-Menten kinetics of the enzyme-redox cosubstrate system. *Journal of Electroanalytical Chemistry.* **549.** 61-70.

Lindgren, A. Ruzgas, T. Gorton, L. Csöregi, E. Bautista Ardila, G. Sakharov, I., Y. and Gazaryan, I., G. (2000). Biosensors based on novel peroxidases with improved properties in direct and mediated electron transfer. *Biosensors and Bioelectronics.* **15.** 491-497.

Liu, H. Ying, T. Sun, K. Li, H. and Qi, D. (1997). Reagentless amperometric biosensors highly sensitive to hydrogen peroxide, glucose and lactose based on *N*-methyl phenazine methosulfate incorporated in a Nafion film as an electron transfer mediator between horseradish peroxidase and an electrode. *Analytica Chimicia Acta.* **344,** 187-199.

Löfås, S. Johnsson, B. Edström, A. Hansson, A. Lindquist, G. Muller Hillgren, R-M. and Stigh, L. (1995). Methods for site controlled coupling to carboxymethyldextran surfaces in surface plasmon resonance sensors. *Biosensors and Bioelectronics.* **10.** 813-822.

Lötzbeyer, T. Schuhmann, W. and Schmidt, H-L. (1996). Electron transfer principles in amperometric biosensors: direct electron transfer between enzymes and electrode surfaces. *Sensors and Actuators B.* **33.** 50-54.

Loughman J. P., (2001). *Voltammetry of absorbed monolayers: Computer simulation and experimental.* Ph. D. Thesis. Dublin City University.

Lumry R., and Eyring H. (1954). Conformational changes of proteins. *Journal of Physical Chemistry.* **58**. 110-120.

Luong, J., H., T. Brown, R., S. Male, K., B. Cattaneo, M., V. and Zhao, S. (1995). Enzyme reactions in the presence of cyclodextrins: biosensors and enzyme assays. *Trends in Biotechnology.* **13.** 457-463.

Magner, E. (1998). Trends in electrochemical biosensors. *The Analyst.* **123.** 1967-1970.

Marcinkeviciene, J. and Kulys, J. (1993). Bienzyme strip-type glucose sensor. *Biosensors and Bioelectronics.* **8.** 209-212.

Marcus, R., A. and Sutin, N. (1985). Electron transfers in chemistry and biology. *Biochimica et Biophysica Acta.* **811.** 265-322.

Martin, S., P. Lynch, J., M. and Reddy, S., M. (2002). Optimisation of the enzyme-based determination of hydrogen peroxide using the quartz crystal microbalance. *Biosensors and Bioelectronics.* **17.** 735-739.

Mayo, S. L. Ellis, W., R. Jr. Crutchley, R., J. and Gray, H., B. (1986). Long-range electron transfer in heme proteins. *Science.* **233,** 948-952.

M^{c}Cormack, T. Keating, G. Killard, A. Manning, B., M. and O'Kennedy, R. (1998). Biomaterials for biosensors. *IN:* D. Diamond (ed.). *Principles of chemical and biological sensors.* New York: John Wiley and Sons. pp133-194.

M^{c}Eldoon J. P, and Dordick J. S. (1996) Unusual thermal stability of soybean peroxidase. *Biotechnology Progress.* **12** 555-558.

M^{c}Eldoon J. P, Pokora A. R, and Dordick J. S. (1995) Lignin peroxidase-type activity of soybean peroxidase. *Enzyme and Microbial Technology.* **37** 359-365.

Miyakawa, H. Nagasue, H. and Shiraishi, F. (1999a). A highly accurate numerical method for calculating apparent kinetic parameters of immobilised enzyme reactions: 1. Theory. *Biochemical Engineering Journal.* **3**. 91-101.

Miyakawa, H. Nagasue, H. and Shiraishi, F. (1999b). A highly accurate numerical method for calculating apparent kinetic parameters of immobilised enzyme reactions: 2. Accuracies of calculated values. *Biochemical Engineering Journal.* **3**. 103-111.

Mizutani, F. Sato, Y. Yabuki, S. Sawaguchi, T. and Iijima, S. (1999). Enzyme electrodes based on self-assembled monolayers of thiol compounds on gold. *Electrochimica Acta.* **44.** 3833-3838.

Molecular probes website (Homepage): www.probes.com/ [First accessed 7th-Feburary-2001].

Molecular visualisation freeware; Protein explorer, Chime and RasMol. www.umass.edu/microbio/rasmol (2001). First accessed: 15-Feb-2001

Mozhaev, V., V. (1992). Stabilisation of proteins by chemical methods. *IN:* W., J., J. van den Tweel, A. Harder, R., M. Buitelaar (eds.). *Stability and Stabilisation of Enzymes.* Maastricht. Elsevier Science Publishers B. V.

Munir I. Z, and Dordick J. S. (2000) Soybean peroxidase as an effective bromination catalyst. *Enzyme and Microbial Technology.* **26** 337-341.

Murray, R., W. Ewing, A., G. and Durst, R., A. (1987). Chemically modified electrodes. Molecular design for Electroanalysis. *Analytical Chemistry.* **59** (5). 379A-390A.

Nakanishi, K. Sakiyama, T. and Imamura, K. (2001). On the adsorption of proteins on solid surfaces, a common but very complicated phenomenon. *Journal of Bioscience and Bioengineering.* **91** (3). 233-244.

Nissum M, Feis A, and Smulevich G. (1998) Characterization of soybean seed coat peroxidase: Resonance Raman evidence for a structure-based classification of plant peroxidases. *Biospectroscopy.* **4.** 355-364.

Nissum M, Schiødt C. B, and Welinder K. G. (2001) Reactions of soybean peroxidase and hydrogen peroxide pH 2.4-12.0, and veratryl alcohol at pH 2.4. *Biochimica et Biophysica Acta.* **1545.** 339-348.

O'Brien, D. (1999). *Characterisation of chemical modified horseradish peroxidase and their potential uses in sensor technology.* Ph. D. Transfer report. Dublin City University.

O'Brien, D. Ó Fágáin, C. (2000). Dublin City University. *A chemical method for stabilising proteins.* S2000/0860.

O'Brien, A-M. Ó Fágáin, C. Nielsen, P., F. and Welinder, K., G. (2001). Location of crosslinks in chemically stabilised horseradish peroxidase: implications for design of crosslinks. *Biotechnology and Bioengineering.* **76** (4). 277-284.

Ó Fágáin, C. (1997). Immobilisation. *IN:* C. Ó Fágáin, *Stabilising protein function.* Berlin: Springer. pp115-128.

Ó Fágáin, C. (2003). Enzyme stability – recent experimental progress. *Enzyme and Microbial Technology.* **33.** 137-149.

Oungpipat, W. Alexander, P., W. and Southwell-Keely, P. (1995). A reagentless amperometric biosensor for hydrogen peroxide determination based on asparagus tissue and ferrocene mediation. *Analytica Chimica Acta.* **309.** 35-45.

Pal, P., S. and Sarkar, P. (2002). Polymers in biosensors – a review. *Journal of the Indian Chemical Society.* **79.** 211-218.

Patel, H. Li, X. and Karan, H., I. (2003). Amperometric glucose sensors based on ferrocene containing polymeric electron transfer systems – a preliminary report. *Biosensors and Bioelectronics.* **18.** 1073-1076

Presnova, G. Grigorenko, V. Egorov, A. Ruzgas, T. Lindgren, A. Gorton, L. and Börchers, T. (2000). Direct heterogeneous electron transfer of recombinant horseradish peroxidases on gold. *Faraday Discussions.* **116.** 281-289.

Pierce. (2000). *Protein assay technical handbook.* Pierce chemicals, Rockford, Il, USA.

Pokora A. R, and Johnson M. A. (1993). The Mead Corporation. *Soybean peroxidase treatment of contaminated substances.* United States Patent. US. 5178762.

Poulos, T., L. and Kraut, J. (1980). The stereochemistry of peroxidase catalysis. *Journal of Biological Chemistry.* **255** (17). 8199-8205.

Price, J., F. and Baldwin, R., P. (1980). Preconcentration and determination of ferrocenecarboxaldehyde at a chemically modified platinum electrode. *Analytical Chemistry.* **52.** 1940-1944.

Razumiene, J. Vilkanauskyte, A. Gureviciene, V. Laurinavicius, V. Roznyatovskaya, N., V. Ageeva, Y., V. Reshetova, M., D. and Ryabov, A., D. (2003). New bioorganometallic ferrocene derivatives as efficient mediators for glucose and ethanol biosensors based on PQQ-dependent dehydrogenases. *Journal of Organometallic Chemistry.* **668.** 83-90.

RCSB protein data bank. www.rcsb.org/pdb/index.html (2002). Accessed 19-May-2002.

Rich, D., H. and Singh, J. (1979). The carbodiimide method. *IN:* E. Gross, and J. Meienhofer (eds). *The Peptides, Analysis, Synthesis, Biology. Major Methods of Peptide Bond Formation.* Volume 1. New York. Academic Press. pp241-261.

Riklin, A. Katz, E. Willner, I. Stocker, A. and Bückmann, A., F. (1995). Improving enzyme-electrode contacts by redox modification of cofactors. *Nature.* **376.** 672-675.

Rosatto, S., S. Sotomayor, P., T. Kubota, L., T. and Gushikem, Y. (2002). SiO_2/Nb_2O_5 sol-gel as a support for HRP immobilisation in biosensor preparation for phenol detection. *Electrochimica Acta.* **47.** 4451-4458.

Rubtsova, M., Y. Kovba, G., V. and Egorov, A., M. (1998). Chemiluminescent biosensors based on porous supports with immobilised peroxidase. *Biosensors and Bioelectronics.* **13 (1).** 75-85.

Ryan, O. Smyth, M., R. and Ó Fágáin, C. (1994a). Horseradish peroxidase: the analyst's friend. *IN:* K., F. Tipton (ed.). *Essays in Biochemistry.* London, Portland Press. 129-146.

Ryan, O. Smyth, M., R. and Ó Fágáin, C. (1994b). Thermostabilized chemical derivatives of horseradish peroxidase. *Enzyme and Microbial Technology.* **16.** 501-505.

Sánchez, P., D. and Ordieres, A., J., M. Costa Garcia, A. and Tuñón Blanco, P. (1991). Peroxidase–ferrocene modified carbon paste electrode as a amperometric sensor for the hydrogen peroxide assay. *Electroanalysis.* **3.** 281-285.

Santucci, R. Laurenti, E. Sinibaldi, F. and Ferrari, R., P. (2002). Effect of dimethyl sulfoxide on the structure and the functional properties of horseradish peroxidase as observed by spectroscopy and cyclic voltammetry. *Biochimica et Biophysica Acta.* **1596.** 225-233.

Scheller, F. and Schubert, F. (1992). Physicochemical, biochemical, and technological fundamentals of biosensors *IN: Biosensors, techniques and instrumentation in analytical chemistry* **11.** Amsterdam: Elsevier. 7-84.

Schmidt, H-L. Schuhmann, W. Scheller, F. and Schubert, F. (1992). Specific features of biosensors. *IN:* Göpel, W. Hesse, J. Zemel, J., N. (eds.). *Sensors, A comprehensive survey.* **3.** Weinheim: VCH. pp717-818.

Schmitz N, Gijzen M, and van Huystee R. (1997) Characterization of anionic soybean (*Glycine max)* seed coat peroxidase. *Canadian Journal of Botany.* **75** 1336-1341.

Schreurs, J. and Barendrecht, E. (1984). Surface-modified electrodes (SME). *Journal of the Royal Netherlands Chemical Society.* **103** *(7-8).* 205-219.

Schuhmann, W. (1993). Non-leaking amperometric biosensors based on high-molecular ferrocene derivatives. *Biosensors and Bioelectronics.* **8**. 191-196.

Schuhmann, W. (1995). Electron-transfer pathways in amperometric biosensors. Ferrocene-modified enzymes entrapped in conducting-polymer layers. *Biosensors and Bioelectronics.* **10**. 181-193

Schuhmann, W. (2002). Amperometric enzyme biosensor based on optimised electron-transfer pathways and non-manual immobilisation procedures. *Reviews in Molecular Biotechnology.* **82.** 425-441.

Sehgal, D. and Vijay, I., K. (1994). A method for the high efficiency of water-soluble carbodiimide-mediated amidation. *Analytical Biochemistry.* **218.** 87-91.

Smit, M. ,H. and Cass, A., E., G. (1990). Cyanide detection using a substrate-regenerating peroxidase-based biosensor. *Analytical Chemistry.* **62.** 2429-2436.

Smith, A., T. Sanders, S., A. Thorneley, R., N., F. Burke, J., F. and Bray, R., R., C. (1992). Characterisation of a haem active-site mutant of horseradish peroxidase, Phe41 → Val, with altered reactivity towards hydrogen peroxide and reducing substrates. *European Journal of Biochemistry.* **207**. 507-519.

Smith, A., T. Santama, N. Dacey, S. Edwards, M. Bray, R., C. Thorneley, R., N., F. and Burke, J., F. (1990). Expression of a synthetic gene for horseradish peroxidase C in *Escherichia coli* and folding and activation of the recombinant enzyme with Ca^{2+} and heme. *Journal of Biological Chemistry.* **265** (22). 13335-13343.

Smith, K. Silvernail, N., J. Rodgers, K., R. Elgren, T., E. Castro, M. and Praker, R., M. (2002). Sol-gel encapsulated horseradish peroxidase: A catalytic material for peroxidation. *Journal of the American Chemical Society.* **124.** 4247-4252.

Smith, P., K. Krohn, R., I. Hermanson, G., T. Mallia, A., K. Gartner, F., H. Provenzano, M., D. Fujimoto, E., K. Goeke, N., M. Olson, B., J. and Klenk, D., C. (1985). Measurement of protein using bicinchoninic acid. *Analytical Biochemistry.* **150** 76-85.

Smolander, M. Livio, H.-L. and Räsänen, L. (1992). Mediated amperometric determination of xylose and glucose with an immobilised aldose dehydrogenase electrode. *Biosensors and Bioelectronics.* **7**. 637-643.

Somasundun. M. Aoki, K. (2002). The steady-state current at microcyclinder electrodes modified by enzymes immobilised in conducting or non-conducting material. *Journal of Electroanalytical Chemistry.* **530.** 40-46.

Souppe, J. Urrrtigoity, M. and Levesque, G. (1988). Application of the reaction of dithioesters in lysine to the chemical modification of proteins. *Biochimica et Biophysica Acta.* **957.** 254-257.

Southampton Research Group. Pletcher, D. Greef, R. Peat, R. Peter, L., M. and Robinson, J. (2001). *Instrumental Methods in Electrochemistry.* Chichester, UK. Horwood Publishing. pp26-30

Sowdhamini, R., and Balaram, P. (1992). Protein structure and stability. *IN:* Gupta, M., N. *Thermostability of Enzymes.* Narosa. Springer Verlag. pp2-21.

Staros, J., V. Wright R, W. and Swingle, D, M. (1986). Enhancement by *N*-hydroxysulfosuccinimide of water-soluble carbodiimide-mediated coupling reactions. *Analytical Biochemistry.* **156**. 220-222.

Sun, D. Cai, C. Li, X, Xing, W. Lu, T. (2004). Direct electrochemistry and bioelectrocatalysis of horseradish peroxidase immobilised on active carbon. *Journal of Electroanalytical chemistry.* **566.** 415-421.

Sun, Y. Sun, J. Zhang, X. Sun, C. Wang, Y. and Shen, J. (1998). Chemically modified electrode via layer-by-layer deposition of glucose oxidase (GOD) and polycation-bearing Os complex. *Thin Solid Films.* **327-329.** 730-733.

Tang, J. Wang, B. Wu, Z. Han, X. Dong, S. and Wang, E. (2003). Lipid membrane immobilised horseradish peroxidase biosensor for amperometric determination of hydrogen peroxide. *Biosensors and Bioelectronics.* **18.** 867-872.

Tkac, J. Vostair, I. Gemeiner, P. and Sturdik, E. (2002). Indirect evidence of direct electron communication between the active site of galactose oxidase and a graphite electrode. *Bioelectrochemistry.* **56.** 23-25.

Tijssen, P. (1985). Properties and preparations of enzymes used in enzyme-immunoassays. *Practice and theory of enzyme immunoassays, Laboratory techniques in biochemistry and molecular biology.* **15.** Amsterdam, Elsevier. pp173-189.

Tyagi, R. and Gupta, M., N. (1992a). Chemical modification and chemical crosslinking for enhancing thermostability of enzymes. *IN:* Gupta, M., N. *Thermostability of Enzymes.* Narosa. Springer Verlag. pp2-21.

Tyagi, R. and Gupta, M., N. (1998b). Chemical modification and chemical cross-linking for protein/enzyme stabilisation. *Biochemistry (Moscow).* **63** (3). 334-407.

Tyagi, R. and Gupta, M., N. (1998). Chemical modification and chemical cross-linking for enhancing thermostability of enzymes. *IN:* Gupta, M., N. *Thermostability of Enzymes.* Narosa. Springer Verlag. pp146-160.

Uang, Y-M. and Chou, T-C. (2003). Fabrication of glucose oxidase/polypyrrole biosensor by galvanostatic method in various pH aqueous solutions. *Biosensors and Bioelectronics.* **19.** 141-147.

Ugarova, N., N. Rozhkova, G., D. and Berezin, I., V. (1979). Chemical modification of the ε-amino groups of lysine residues in horseradish peroxidase and its effect on the catalytic properties and thermostability of the enzyme. *Biochimica et Biophysica Acta.* **570.** 31-42.

van de Velde F, Lourenço N. D, Bakker M, and van Rantwijk F. (2000) Improved operational stability of peroxidases by coimmobilization with glucose oxidase. *Biotechnology and Bioengineering.* **69** (3) 286-291.

Veitch, N., C. and Smith A., T. (2001). Horseradish peroxidase. *Advances in Inorganic Chemistry.* **51.** 107-162.

Vishwanath, S. Bhattacharyya, D. Huang, W. and Bachas, L., G. (1995). Site-directed and random enzyme immobilization on functionalised membranes: kinetic studies and models. *Journal of Membrane Science*. **108.** 1-13.

Vreeke, M., S. Yong, K., T. and Heller, A. (1995). A thermostable hydrogen peroxide sensor based on "wiring" of soybean peroxidase. *Analytical Chemistry*. **67**. 4247-4249.

Wang, B. and Dong, S. (2000). Sol-gel-derived amperometric biosensor for hydrogen peroxidase based on methylene green in Nafion film. *Talanta*. **51.** 565-572.

Wang B. Q, Li B, Cheng G. J, and Dong S. J. (2001a) Acid-stable amperometric soybean peroxidase biosensor based on a self-gelatinizable grafting copolymer of polyvinyl alcohol and 4-vinyl pyridine. *Electroanalysis*. **13** (7) 555-558.

Wang, X., Q. Li, L., S. van der Meer, B., W. Jin, J. Tang, D. Hui, Z. Li, Y-Z. and Li, T., J. (2001b). Comparison of photovoltaic behaviours for horseradish peroxidase and its mimicry by surface photovoltage spectroscopy. *Biochimica et Biophysica Acta*. **1544.** 333-340.

Wang B. Q, Li B, Wang Z. X, Xu G. B, Wang Q, and Dong S. J. (1999) Sol-Gel thin film immobilized soybean peroxidase biosensor for the amperometric determination of hydrogen peroxide in acid medium. *Analytical Chemistry*. **71**, 1935-1939.

Welinder K. G. (1992) Superfamily of plant, fungal, and bacterial peroxidases. *Current Opinion in Structural Biology.* **2**, 388-393.

Welinder, K., G. and Larsen, Y., B. (2004). Covalent structure of soybean coat peroxidase. *Biochimica et Biophysica Acta.* **1698.** 121-126.

Wong, T., S. and Schwaneberg, U. (2003). Protein engineering in bioelectrocatalysis. *Current Opinion in Biotechnology.* **14.** 590-596.

Wright, H. and Nicell, J., A. (1999). Characterisation of soybean peroxidase for the treatment of aqueous phenols. *Bioresource Technology.* **70.** 69-79.

Yamagata, Y. Arakawa K. Yamaguichi M. Kobayashi M, and Ichishima E. (1994). Functional changes of dextran-modified alkaline proteinase from alkalophilic Bacillus sp. *Enzyme Microbial Technology.* **16.** 99-103.

Yamamoto, K. Shi, G. Zhou, T. Xu, F. Xu, J. Kato, T. Jin, J-Y. and Jin, L. (2003). Study of carbon nanotubes-HRP modified electrode and its applications for novel on-line biosensors. *The Analyst.* **128.** 249-254.

Yi, X. Huang-Xian, J. Hong-Yuan, C. (2000). Direct electrochemistry of horseradish peroxidase immobilised on a colloidal/cysteamine-modified gold electrode. *Analytical Biochemistry.* **278.** 22-28.

Yu, X. Chattopadhyay, D. Galeska, I. Papadimitrakopoulos, F. and Rusling, J., F. (2003). Peroxidase activity of enzymes bound to the ends of single-walled carbon nanotubes forest electrodes. *Electrochemistry Communications.* **5.** 408-411.

Zhang, Z. Chouchane, S. Magliozzo, R., S. and Rusling, J., F. (2002). Direct voltammetry and catalysis with *Mycobacterium tuberculosis* catalysis – peroxidase, peroxidases, and catalase in lipid films. *Analytical Chemistry.* **74.** 163-170.

Zhou, G-J. Wang, G. Xu, J-J. Chen, H-Y. (2002). Reagentless chemiluminescent biosensor for determination of hydrogen peroxide based on the immobilisation of horseradish peroxidase on biocompatible chitosan membrane. *Sensors and Actuators B.* **81.** 334-339.

Zhu, Y. Zhang, J. and Dong, S. (1997). Hydrazines probe of interaction of horseradish peroxidase with cryo-hydrogel. *Analytica Chimica Acta.* **353.** 45-52.